



UNIVERSITÀ
POLITECNICA
DELLE MARCHE

FACOLTÀ DI MEDICINA E CHIRURGIA

Dipartimento di Eccellenza di Scienze Biomediche e Sanità Pubblica

PhD Course in Biomedical Sciences

XXXV cycle

Coordinator: Prof. Carlo Catassi

**METABOLISM AND ANALYSIS OF NEW PSYCHOACTIVE
TRYPTAMINES**

PhD Student:

Dott.ssa Sara Patrícia Romão Malaca

Tutor:

Prof. Raffaele Giorgetti

Co-Tutor:

Prof. Francesco Paolo Busardò

a.a. 2022-2023

Index

Introduction	4
1. New Psychoactive Substances.....	4
2. Tryptamines.....	4
2.1. Tryptamines of Natural Origin.....	13
2.2. Tryptamines of Synthetic Origin	16
2.2.1. Ring Substituted Tryptamines	16
2.2.2. 4-Substituted Tryptamines	20
2.2.3. 5-Substituted Tryptamines	21
2.3. Analytical Methods to Determine Tryptamines and/or Metabolites in Conventional and Non-Conventional Biological Matrices	24
Aims	37
Part I: Tryptamines' Metabolite Profiling	38
1.4-AcO-DiPT Metabolic Profiling in Human Hepatocyte Incubations	38
Material and Methods.....	39
1.2. Results	41
1.3. Discussion	49
1.4. Conclusion.....	50
2.4-OH-MPT Metabolite Profiling in Human Hepatocyte Incubations	51
2.1. Materials and Methods	51
2.2. Results	54
2.3. Discussion	67
2.4. Conclusion.....	69
3. α -MT Metabolite Profiling in Human Hepatocyte Incubations and Urine	69
3.1. Materials and Methods	70
3.2. Results	74
3.3. α -MT Metabolites in <i>Postmortem</i> Blood	81
3.4. Discussion	82

3.5. Conclusion.....	88
Part II: Tryptamines' Detection In Urine Using LC-HRMS/MS.....	90
1. Materials and Methods.....	92
2. Results.....	99
3. Discussion.....	101
4. Conclusion.....	104
Conclusions.....	105
References.....	107
Acknowledgements.....	124

Introduction

1. New Psychoactive Substances

New psychoactive substances (NPS) are "substances of abuse, whether in a pure form or a preparation, that are not prohibited by the 1961 Single Convention on Narcotic Drugs or the 1971 Convention on Psychoactive Substances"; the term "new" indicates the recent commercialization of the substances on the drug market and does not refer to newly manufactured drugs. NPS are intended to mimic the recreational effects of conventional drugs of abuse while evading legislation and analytical detection and can be found on the drug market as "legal highs", "bath salts" and "research chemicals". The quick spread of NPS poses a serious risk to public health as they have been involved in many cases of intoxication and fatalities throughout the world. Moreover, the emergence of different substances every year poses a problem for drug regulation [1].

2. Tryptamines

Psychedelic tryptamines are a diverse group of naturally occurring and synthetic NPS that induce distorted states of consciousness, perception, thinking and feeling [2]. Tryptamines share their core structure with the neurotransmitter serotonin, also named 5-hydroxytryptamine (5-HT). The effects of tryptamines, are mediated by the 5-HT_{2A} receptor [3–7] but may also be modulated by interactions with other 5-HT receptors, monoamine transporters, and trace amine-associated receptors [7–15]. Furthermore, Luethi et al. presented a brief report based on correlations between *in vitro* human 5-HT receptor affinities and their dose estimates [13], reporting that human doses for psychedelics were significantly correlated with 5-HT_{2A} and 5-HT_{2C} receptor binding but not with 5-HT_{1A} receptor binding. 5-HT_{2A} receptors expressed on neocortical pyramidal cells are involved in the psychedelic effects of tryptamines [4]. The activation of 5-HT_{2A} receptors increases cortical glutamate levels by a presynaptic receptor-mediated release from thalamic afferents. As serotonin receptor agonists, psychedelics can produce synesthesia and altered perceptions of reality, where senses usually experienced separately are combined. The status of control for different psychedelics varies, many are controlled under the Convention on Psychotropic Substances of 1971 (e.g. diethyltryptamine (DET), DMT, α -ethyltryptamine (α -ET)), although some synthetic psychedelics are not currently under international control.

Many countries report the use of psilocybin or magic mushrooms to the United Nations Office on Drugs and Crime (UNODC) [2]. The ranking of drugs by Member States, based on prevalence data from 123 countries, including 78 countries providing psychedelic data, suggests that the use of this drug class is currently ranked on average 5.3 from 2013–2017, being less of a threat than the use of cannabis, sedatives and tranquillizers, opioids and cocaine. From the available data on trends in the use of different substances from 2001-2017, the majority of countries reported no significant change in psychedelic use over time. Nonetheless, there are signs of an increase in the overall use of psychedelics in recent years, particularly from 2012 to 2016, with the number of countries reporting increases in the use of psychedelics greater than the number of countries reporting decreases. Furthermore, according to the 2019 Global Drug Survey (GDS) [16], psychedelics were consumed by 40% of drug users, with tryptamines the psychedelic class with the greatest increase in use. The psychedelics with the greatest prevalence of use were lysergic acid diethylamide (LSD) (17.5%), psilocybin or magic mushrooms (14.8%), DMT (4.2%), magic truffles (3.3%) and ayahuasca (1.1%) [17].

Several tryptamines occur naturally in a variety of plants, fungi and animals [2]. Some tryptamines are also chemically synthesized, with several DMT analogs, such as alpha-methyltryptamine (α -MT) and 5-methoxy-diisopropyltryptamine (5-MeO-DiPT), currently popular. Several reviews report the toxicology of different NPS [18–24]; however, only two focused on tryptamines [25,26]. In 2015, Tittarelli et al. [25] presented a summary of all the currently available information on tryptamines and their derivatives, including pharmacology, chemical structures, and effects related to routes of administration, and toxicities. Data were provided for twelve tryptamines and/or derivatives and some intoxication reports. In the same year, Araújo et al. [26] provided an overview for the same classic tryptamines plus other derivatives, providing additional detail on the drugs' toxicodynamics, preclinical physiological studies and adverse effects in humans. NPS and tryptamines are constantly evolving, with new drugs appearing rapidly onto the market. The morbidity associated with tryptamine intake is considerable, and it is important for toxicologists to be informed of the latest data on this public health threat. The aim is to present the latest tryptamine intoxication cases and new analytical methods to identify and quantify tryptamines in conventional and non-conventional biological matrices over the last five years.

Tryptamines are psychedelic drugs derived from decarboxylation of the amino acid tryptophan, which produces the typical indole ring [27], giving these compounds the name “indolealkylamines”. A compound's chemical structure determines which receptors it can bind and activate, its absorption, distribution, metabolism and elimination, and its effects.

In fact, minor additions and modifications to the indolealkylamine backbone provide an endless supply of novel tryptamine structures, each with a unique pharmacology. Table 1 presents the most common and newest tryptamines and metabolites, with their common backbone structure and numerous ring substitutions.

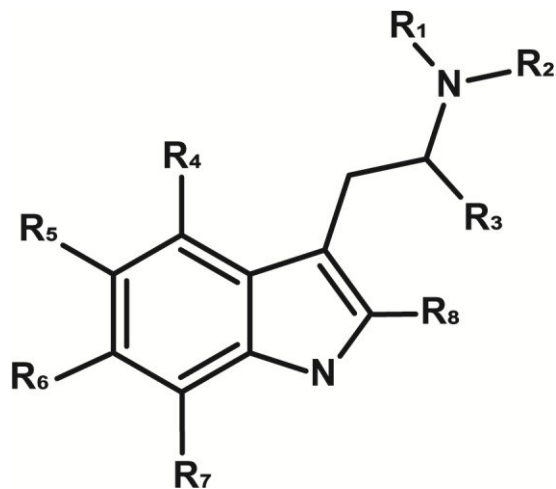
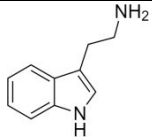
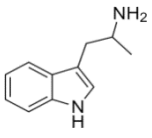
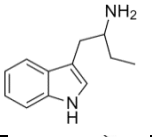
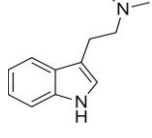
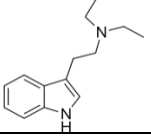
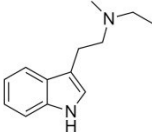
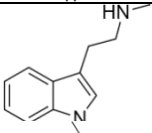
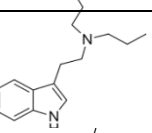
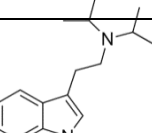
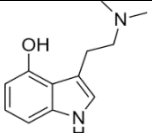
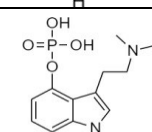
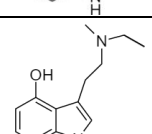
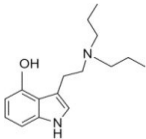
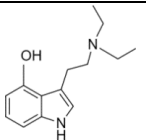
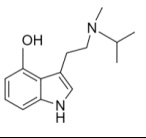
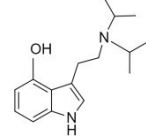
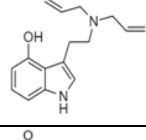
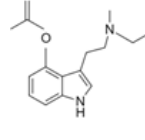


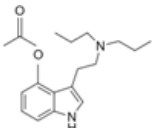
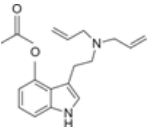
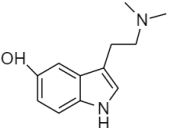
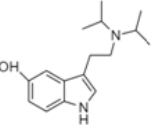
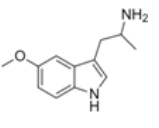
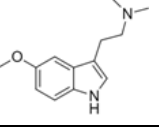
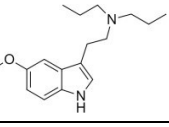
Figure 1. Tryptamines base structure.

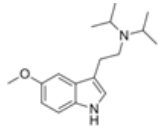
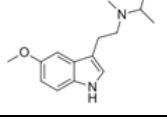
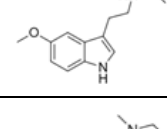
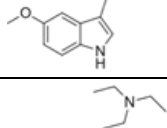
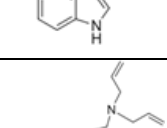
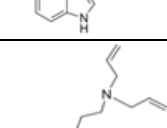
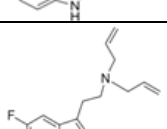

Table 1. Chemical structures of tryptamines.

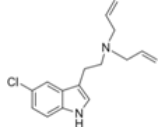
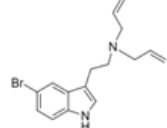
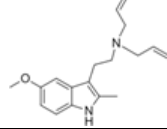
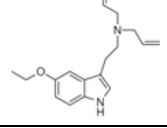
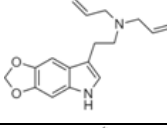
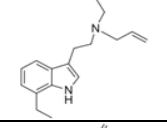
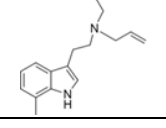
Abbreviation	Chemical name	Molecular formula	Chemical structure	Molecular weight (g/mol)	R1	R2	R3	R4	R5	R6	R7	R8
Tryptamine	Tryptamine	C ₁₀ H ₁₂ N ₂		160.2	H	H	H	H	H	H	H	H
Ring unsubstituted tryptamines												
α -MT	α -methyltryptamine	C ₁₁ H ₁₄ N ₂		174.2	H	H	CH ₃	H	H	H	H	H
α -ET	α -ethyltryptamine	C ₁₂ H ₁₆ N ₂		188.3	H	H	CH ₂ CH ₃	H	H	H	H	H
DMT	N,N-dimethyltryptamine	C ₁₂ H ₁₆ N ₂		188.3	CH ₃	CH ₃	H	H	H	H	H	H
DET	N,N-diethyltryptamine	C ₁₄ H ₂₀ N ₂		216.3	CH ₂ CH ₃	CH ₂ CH ₃	H	H	H	H	H	H

MET	N-methyl-N-ethyltryptamine	$C_{13}H_{18}N_2$		202.3	CH_3	CH_2CH_3	H	H	H	H	H	H
NMT	N-methyltryptamine	$C_{11}H_{14}N_2$		174.2	H	CH_3	H	H	H	H	H	H
DPT	N,N-dipropyltryptamine	$C_{16}H_{24}N_2$		244.4	$CH_2CH_2CH_3$	$CH_2CH_2CH_3$	H	H	H	H	H	H
DiPT	N,N-diisopropyltryptamine	$C_{16}H_{24}N_2$		244.4	$CH(CH_3)_2$	$CH(CH_3)_2$	H	H	H	H	H	H
4-Substituted tryptamines												
Psilocin	4-Hydroxy-N,N-dimethyltryptamine	$C_{12}H_{16}N_2O$		204.3	CH_3	CH_3	H	OH	H	H	H	H
Psilocybin	4-Phosphoryloxy-N,N-dimethyltryptamine	$C_{12}H_{17}N_2O_4P$		284.3	CH_3	CH_3	H	OPO_3H_2	H	H	H	H
4-OH-MET	4-Hydroxy-N-methyl-N-ethyltryptamine	$C_{13}H_{18}N_2O$		218.3	CH_3	CH_2CH_3	H	OH	H	H	H	H

4-OH-DPT	4-Hydroxy-N,N-dipropyltryptamine	$C_{16}H_{24}N_2O$		260.4	$CH_2CH_2CH_3$	$CH_2CH_2CH_3$	H	OH	H	H	H	
4-OH-DET	4-Hydroxy-N,N-diethyltryptamine	$C_{14}H_{20}N_2O$		232.3	CH_2CH_3	CH_2CH_3	H	OH	H	H	H	H
4-OH-MiPT	4-Hydroxy-N-methyl-N-isopropyltryptamine	$C_{14}H_{20}N_2O$		232.3	CH_3	$CH(CH_3)_2$	H	OH	H	H	H	H
4-OH-DiPT	4-Hydroxy-N,N-diisopropyltryptamine	$C_{16}H_{24}N_2O$		260.4	$CH(CH_3)_2$	$CH(CH_3)_2$	H	OH	H	H	H	H
4-OH-DALT	4-Hydroxy-N,N-diallyltryptamine	$C_{16}H_{20}N_2O$		256.3	CH_2CHCH_2	CH_2CHCH_2	H	OH	H	H	H	H
4-AcO-MET	4-Acetoxy-N-methyl-N-ethyltryptamine	$C_{15}H_{20}N_2O_2$		260.3	CH_3	CH_2CH_3	H	$OCOCH_3$	H	H	H	H

4-AcO-DPT	4-Acetoxy-N,N-dipropyltryptamine	C ₁₈ H ₂₆ N ₂ O ₂		302.4	CH ₂ CH ₂ CH ₃	CH ₂ CH ₂ CH ₃	H	OCOCH ₃	H	H	H	H
4-AcO-DALT	4-Acetoxy-N,N-diallyltryptamine	C ₁₈ H ₂₂ N ₂ O ₂		298.4	CH ₂ CHCH ₂	CH ₂ CHCH ₂	H	OCOCH ₃	H	H	H	H
5-Substituted tryptamines												
Bufotenine	5-Hydroxy-N,N-dimethyltryptamine	C ₁₂ H ₁₆ N ₂ O		204.3	CH ₃	CH ₃	H	H	OH	H	H	H
5-OH-DiPT	5-Hydroxy-N,N-diisopropyltryptamine	C ₁₆ H ₂₄ N ₂ O		260.4	CH(CH ₃) ₂	CH(CH ₃) ₂	H	H	OH	H	H	H
5-MeO- α -MT	5-Methoxy-alpha-methyltryptamine	C ₁₂ H ₁₆ N ₂ O		204.3	H	H	CH ₃	H	OCH ₃	H	H	H
5-MeO-DMT	5-Methoxy-N,N-dimethyltryptamine	C ₁₃ H ₁₈ N ₂ O		218.3	CH ₃	CH ₃	H	H	OCH ₃	H	H	H
5-MeO-DPT	5-Methoxy-N,N-dipropyltryptamine	C ₁₇ H ₂₆ N ₂ O		274.4	CH ₂ CH ₂ CH ₃	CH ₂ CH ₂ CH ₃	H	H	OCH ₃	H	H	H

5-MeO-DiPT	5-Methoxy-N,N-diisopropyltryptamine	C ₁₇ H ₂₆ N ₂ O		274.4	CH(CH ₃) ₂	CH(CH ₃) ₂	H	H	OCH ₃	H	H	H
5-MeO-MiPT	5-Methoxy-N-methyl-N-isopropyltryptamine	C ₁₅ H ₂₂ N ₂ O		246.4	CH ₃	CH(CH ₃) ₂	H	H	OCH ₃	H	H	H
5-MeO-IPT	5-Methoxy-N-isopropyltryptamine	C ₁₄ H ₂₀ N ₂ O		232.3	H	CH(CH ₃) ₂	H	H	OCH ₃	H	H	H
5-MeO-MET	5-Methoxy-N-methyl-N-ethyltryptamine	C ₁₄ H ₂₀ N ₂ O		232.3	CH ₃	CH ₂ CH ₃	H	H	OCH ₃	H	H	H
5-MeO-DET	5-Methoxy-N,N-diethyltryptamine	C ₁₅ H ₂₂ N ₂ O		246.4	CH ₂ CH ₃	CH ₂ CH ₃	H	H	OCH ₃	H	H	H
5-MeO-DALT	5-Methoxy-N,N-diallyltryptamine	C ₁₇ H ₂₂ N ₂ O		270.4	CH ₂ CHCH ₂	CH ₂ CHCH ₂	H	H	OCH ₃	H	H	H
5-Me-DALT	5-Methyl-N,N-diallyltryptamine	C ₁₇ H ₂₂ N ₂		254.4	CH ₂ CHCH ₂	CH ₂ CHCH ₂	H	H	CH ₃	H	H	H
5-F-DALT	5-Fluoro-N,N-diallyltryptamine	C ₁₆ H ₁₉ N ₂ F		258.3	CH ₂ CHCH ₂	CH ₂ CHCH ₂	H	H	F	H	H	H

5-Cl-DALT	5-Chloro-N,N-diallyltryptamine	C ₁₆ H ₁₉ N ₂ Cl		274.8	CH ₂ CHCH ₂	CH ₂ CHCH ₂	H	H	Cl	H	H	H
5-Br-DALT	5-Bromo-N,N-diallyltryptamine	C ₁₆ H ₁₉ N ₂ Br		319.2	CH ₂ CHCH ₂	CH ₂ CHCH ₂	H	H	Br	H	H	H
5-MeO-2-Me-DALT	5-Methoxy-2-methyl-N,N-diallyltryptamine	C ₁₈ H ₂₄ N ₂ O		284.4	CH ₂ CHCH ₂	CH ₂ CHCH ₂	H	H	OCH ₃	H	H	CH ₃
5-EtO-DALT	5-Ethoxy-N,N-diallyltryptamine	C ₁₈ H ₂₄ N ₂ O		284.4	CH ₂ CHCH ₂	CH ₂ CHCH ₂	H	H	OCH ₂ CH ₃	H	H	H
Others												
5,6-MD-DALT	5,6-Methylenedioxy-N,N-diallyltryptamine	C ₁₇ H ₂₀ N ₂ O ₂		284.4	CH ₂ CH	CH ₂ CH	H	H	OCH ₂ O *	H	H	
7-Et-DALT	7-Ethyl-N,N-diallyltryptamine	C ₁₈ H ₂₄ N ₂		268.4	CH ₂ CHCH ₂	CH ₂ CHCH ₂	H	H	H	H	CH ₂ CH ₃	H
7-Me-DALT	7-Methyl-N,N-diallyltryptamine	C ₁₇ H ₂₂ N ₂		254.4	CH ₂ CHCH ₂	CH ₂ CHCH ₂	H	H	H	H	CH ₃	H

*Both R₅ and R₆ groups take part of the methylenedioxy ring.

Some tryptamine structures facilitate crossing the blood brain barrier, with a rapid onset of highly potent effects, and other structures prevent rapid metabolic degradation, increasing the duration of effects [28]. Some tryptamines and derivatives are potent and short-acting psychedelics, whose total duration of action is less than thirty min [28]. Such compounds must be taken parenterally or enterally to experience the psychedelic effects. MAO is a mitochondrial flavin-dependent enzyme that oxidatively deaminates serotonin and other biogenic and neuroactive amines and is present in the liver, gut and brain of humans and other mammals. If tryptamines are orally ingested, protection from peripheral degradation by a monoamine oxidase inhibitor (MAOI) may be necessary for activity. Consequently, MAOI generally increases the pharmacological effects of such bioactive amines.

2.1. Tryptamines of Natural Origin

- Dimethyltryptamine (DMT)

DMT shares psychedelic and hallucinogenic activity with lysergic acid diethylamide (LSD) and mescaline in terms of intensity and characteristics [25]. Common routes of DMT administration are oral, insufflation, intravenous (IV) and smoking [27]. The time course of DMT administered via inhalation of vaporized freebase or IV injection of a water-soluble salt is brief. The onset is rapid, with full effects noted within 2 min of administration and subjective effects fully resolving within 20–30 min [28]. Szára et al. also reported a rapid onset (2–5 min) of effects and a duration of action of 30–60 min following intramuscular (IM) administration of 0.2–1 mg/kg DMT [29]. These authors reported that 0.7 mg/kg IM DMT resulted in diarrhea, nausea and vomiting. Additionally, elevated heart rate, blood pressure, and rectal temperature were reported by others following DMT administration [30]. Psychologically, DMT can cause short-term emotional distress, and in some cases precipitate long-lasting psychosis. DMT is an agonist at the 5-HT_{1A}, 5-HT_{2A}, and 5-HT_{2C} serotonin receptors, and at the sigma-1 receptor. DMT's broad agonist activity includes modulation of physiological processes and regulation of inflammation through the sigma-1 and 5-HT receptors, and changing immune responses through the sigma-1 receptor. IM effects are usually less intense than those following IV or inhalation. Oxidative deamination of DMT by monoamine oxidase (MAO) produces indole-3-acetic acid (3-IAA) and 3-indole-acetic acid [31]. Other metabolic pathways include *N*-oxidation, *N*-demethylation and cyclization. DMT-*N*-oxide (DMT-NO), *N*-methyltryptamine (NMT), 2-methyl-1,2,3,4-tetrahydro-beta-carboline (2-MTHβC) were also identified as minor DMT metabolites [31].

DMT was first isolated from *Mimosa hostiles*, *Mimosa tenuiflora*, and *Mimosa* root bark and is also present in *Psychotria viridis* leaves and *Virola* plants, all parts of the beverage Ayahuasca [28]. Ayahuasca is produced by mixing different plants by native populations of the basin of the Amazon river, suggested to be a drink with magic and curative powers. For the decoction preparation, the natives boil the bark or crushed stems of *Banisteriopsis caapi* together with other plants, including the leaves of *Psychotria viridis*, a member of the Rubiaceae family. The two plants are distinguished by the content of active compounds. *Psychotria viridis* contains DMT and *Banisteriopsis caapi* contains harmala alkaloids (*Peganum harmala* or Syrian Rue) harmine, tetrahydroharmine, and harmaline [32]. DMT is a hallucinogen and the harmala alkaloids are MAO inhibitors that enhance DMT's effects. Ayahuasca is used to treat depression, anxiety, and alcohol, tobacco [33] and drug addiction [34]. DMT is also found as a minor alkaloid in the bark, pods, and beans of *Anadenanthera peregrina* and *Anadenanthera colubrina* [35].

In 2015, Paterson et al. [36] reported an acute intoxication in Los Angeles, California of an unknown amount of smoked DMT by a 42-year-old male with no psychiatric history other than multiple substance use disorders. He was on an involuntary legal hold for bizarre and disorganized behavior that ultimately led to his hospitalization. During the interview in the emergency department (ED), he reported smoking cannabis and three weeks before hospitalization, he began smoking DMT. The subject was agitated, underweight and exhibited a marked disorientation to time. The patient received supportive therapy, including sedation with benzodiazepines. After 21 days hospitalization, he was discharged without complications. The urine toxicology analysis was performed 5 days after ED admission and resulted positive only for benzodiazepines and negative for DMT.

In 2017, Bilhimer et al. [37] reported an acute intoxication involving DMT in the U.S. A 25-year-old male with a history of mental illness had strong hallucinations and suicidal thoughts after injecting DMT intravenously. The subject had dilated pupils, tachycardia (88 bpm) and systolic and diastolic blood pressure of 116/71 mm Hg. His urine was immunoassay positive for amphetamines and DMT at a concentration greater than 2000 ng/mL.

- **Psilocybin and Psilocin**

Psilocybin (4-Phosphoryloxy-*N,N*-dimethyltryptamine) and psilocin (4-Hydroxy-*N,N*-dimethyltryptamine or 4-OH-DMT), are contained in about 190 species of *Psilocybe* mushrooms, but the most well-known varieties are *Psilocybe cubensis*, *Psilocybe semilanceata* and *Psilocybe Mexicana*. Psilocybin is a 4-substituted indoleamine that is dephosphorylated to psilocin, its pharmacologically active metabolite [38]. Albert Hofmann

[35] first isolated and identified psilocin from the *Psilocybe Mexicana* mushroom in 1958. *Psilocybe cubensis* contains the highest concentrations of these two tryptamines, and is available frozen, or as a dry powder or capsule [39]. In addition to its natural origin, synthetic psilocin is available fresh or treated/preserved (dried or cooked). Psilocin is highly unstable in solution, and in the presence of oxygen and alkaline pH, it forms bluish and black degradation products. This tryptamine is an isomer of bufotenine, differing only in the position of the hydroxyl group [38]. Psilocin is orally active with a duration of action of 4-6 h [28]. Psilocin undergoes oxidative deamination and forms the minor metabolite 4-hydroxyindole acetic acid (4-HIAA). This tryptamine is also subject to phase II metabolism to the *O*-glucuronide, the main metabolite detected in human urine. In recent years, fungus' sclerotia, commonly called "magic truffles", frequently supply the psychoactive *Psilocybe* alkaloids, as *Psilocybe sclerotia* are not specifically included in the laws banning the sale, the purchase and the use of such substances [40]. Terms for magic truffles include The Philosopher Stones, Space truffles, Sclerotia Stones or Sclerotia. *Psilocybin* mushroom ingestion produces hallucinations as early as 10 min post ingestion of 1-2 mg dried mushrooms and typically lasts from 4 - 12 h. Common symptoms include dizziness, giddiness, nausea, weakness, muscle aches, shivering, anxiety, restlessness and abdominal pain [41,42]. In 2018, Honyiglo et al. described the death of an 18 year old male in France who jumped from the second floor and died following "hallucinogenic mushroom" intake [43]. The intoxication was confirmed by identification and quantification of psilocin in cardiac and femoral blood (67 and 60 ng/mL respectively), urine (2,230 ng/mL), bile (3,102 ng/mL), and vitreous humor (57 ng/mL). Gas chromatography time-of-flight detection with electron impact ionization (GC-EI-TOF) was the analytical technique employed for identification and quantification.

Currently, there is great interest in *psilocybin* in combination with psychotherapy to treat psychiatric disorders like anxiety, depression, and addiction to nicotine and drugs [44,45]. For example, Grob et al. dispensed 0.2 mg/kg oral *psilocybin*, with a niacin placebo control to advanced-stage cancer patients with anxiety [46]. There was a significant reduction in anxiety at 1 and 3 months after treatment based on patients' Spielberg State-Trait Anxiety Inventory (STAI). Carhart et al. [47] administered *psilocybin* to treat 12 patients with moderate-to-severe, unipolar, treatment-resistant major depression with two oral doses of *psilocybin* (10 mg and 25 mg, 7 days apart) in a supportive setting. In addition, two randomized blinded controlled clinical trials demonstrated significant long-term reductions in anxious depressed mood after *psilocybin* treatment [45,48]. Essential distress also decreased and quality of life improved in terminally ill cancer patients after a single oral dose of *psilocybin*. An open-label pilot study provided *psilocybin* in

combination with cognitive behavioral therapy to 15 treatment-resistant tobacco/nicotine-dependent smokers [49]. Smoking abstinence was observed in 67% of patients at follow-up, documenting that psilocybin was more effective than the most successful FDA-approved medication, varenicline [41]. Finally, a recent open-label pilot study investigated psilocybin for the treatment of 10 alcohol-dependent individuals, with alcohol use decreasing dramatically after the first psilocybin administration [50].

- 5-Methoxy-*N,N*-dimethyltryptamine (5-MeO-DMT)

5-MeO-DMT is a natural tryptamine [28] that requires the presence of a MAOI to produce psychedelic effects [25]. 5-MeO-DMT is ingested, but unpublished reports describe inhalation as a common mean of consumption with effects appearing within 60 sec and lasting 5-20 min [50]. Effects include auditory, visual, and time perception distortions, emotional experiences, memory impairment, asthma (12%), high blood pressure (9%) and chronic fatigue syndrome (8%) [51]. There is also evidence that some people use 5-MeO-DMT for treating psychiatric conditions, including depression, anxiety, post-traumatic stress disorder, and problematic substance use [51,52]. Tryptamine derivatives like DMT, 5-OH-DMT and 5-MeO-DMT are metabolized by MAO-A that catalyzes an oxidative deamination forming IAA [52,53].

Brush et al. reported a poisoning related to 5-MeO-DMT and harmaline ingestion [25,54]. The victim was a 17 year old male found collapsed after insufflation of 15-20 mg 5-MeO-DMT. GC/MS analysis of urine only confirmed the presence of both harmaline and harmine. At ED admission, the patient had hypertension and tachycardia (186 bpm) and was hyperthermic (40.7°C). After administration of 2.5 mg lorazepam, the symptoms began to resolve, and the patient was discharged without complication.

Sklerov et al. described the death of a 25 year old white male found unresponsive in a national park following ingestion of 5-MeO-DMT. Toxicological analyses revealed the presence of 5-MeO-DMT in blood, urine, gastric contents, bile, kidney, brain, and liver. Moreover, the heart blood sample contained DMT (0.02 mg/L), 5-MeO-DMT (1.88 mg/L), tetrahydroharmine (0.38 mg/L), harmaline (0.07 mg/L), and harmine (0.17 mg/L). The medical examiner pronounced the death as due to psychedelic amine intoxication [25,55].

2.2. Tryptamines of Synthetic Origin

2.2.1. Ring Substituted Tryptamines

- Alpha-methyltryptamine (α -MT)

α -MT is a psychedelic tryptamine sold as a white crystalline powder [56]. It was first developed in 1960 as an antidepressant in the Soviet Union, but its marketing was unsuccessful. α -MT's duration of effects is 8-14 h if ingested and 3-6 h when inhaled. α -MT effects are similar to those of 3,4-methylenedioxymethamphetamine (MDMA); both are empathogens and strong stimulants [56]. α -MT strongly inhibits re-uptake and release of monoamines dopamine, serotonin and norepinephrine in mouse brain synaptosomes, also being a strong MAO inhibitor.

In September 2004, the U.S. Controlled Substances Act placed α -MT in Schedule I. α -MT is a hallucinogen [56] and a stimulant with an alpha methyl group similar to amphetamine [57]. α -MT is generally available as a powder, tablet, or capsule with oral doses of 5-10 mg producing stimulation, 20-30 mg hallucinogenic effects for up to 24 h, 60-80 mg considered a "strong" dose, and up to 150 mg α -MT was previously self-administered. Generally, 5-20 mg free base is smoked. Snorting or insufflation is an infrequent route of administration due to burning of the mucosa and a bad odor. Inadequate solubility and lack of increased pharmacological effects limits IV administration [58]. The most frequent adverse effects described in the literature are anxiety, muscle tightness, vomiting, hyperthermia, mild increase in blood pressure or respiratory rate, tachycardia, salivation, nausea, impaired coordination, nervousness and restlessness [58,59].

Recently, Holstege et al. reported the intoxication and ED admission of a 21-year-old man following α -MT ingestion [25]. He was hypertensive (BP 183/93 mmHg, heart rate 52 bpm), had a high fever, felt disoriented, nervous, and trembling. After medical treatment, the patient was discharged without complication. No analytical confirmation was performed. In the same year, another α -MT intoxication involved a 17-year-old male found naked and hallucinating [60]. In the ED, he was hyperthermic and tachycardic (160 beats/min), presented with fever (37.3°C), sweating and reactive 6-7 mm mydriatic pupils. α -MT was identified in his urine by high-performance liquid chromatography coupled with mass spectrometry (HPLC-MS). He was discharged with supportive therapy including benzodiazepines. Boland et al., reported the first known α -MT death of a 22 year old male found unresponsive by his roommate, who said he consumed 1 g α -MT 12 h prior. Iliac vein blood, gastric contents, liver and brain were all α -MT positive at 2.0 mg/L, 9.6 mg/kg; 24.7 mg/kg and 7.8 mg/kg, respectively [61].

There are few α -MT pharmacokinetic data. Hydroxylation or oxidation of the indole ring at the 2-, 6- and/or 7-positions was observed in male Wistar rats [62]. 2-oxo- α -MT, 6-hydroxy- α -MT, 7-hydroxy- α -MT and 10-hydroxy- α -MT metabolites were identified in rat urine. Other rat α -MT metabolic pathways include deamination to indole-3-acetone

followed by oxidation to indole-3-carboxylic acid [62]. Also, an isomer of α -MT, 5-(2-aminopropyl) indole (5-IT, 5API), appeared on the European drug market in 2011 [63].

- Alpha-ethyltryptamine (α -ET)

α -ET was first synthesized in 1947 as a potential synthetic precursor to the β -carbolines but appeared on the clandestine market as an antidepressant (Monase) in the mid-1980s [64]. In 1986, Daldrup et al. described its first illicit use in Germany [65] and in 1993 the U.S. Drug Enforcement Administration (DEA) included it on the Schedule I list [66]. α -ET may produce serotonin neurotoxicity [67], but the exact mechanism is not understood. Serotonin neurotoxicity was produced by the combined administration of a non-neurotoxic serotonin releasing agent and the dopamine releasing agent S-amphetamine [68,69]. Other authors added that α -ET was the first tryptamine derivative, indeed, the first non-phenylisopropylamine, shown to produce stimulus effects similar to those of MDMA on unconditioned motor behaviour in rats [70,71]. Like α -MT, other simple synthetic tryptamines, such as α -ET, possess a methyl group on the alpha carbon, providing protection from MAO metabolism [61]. α -ET has a duration of action of 6–8 h when taken orally [26].

Morano et al., described a fatal intoxication involving α -ET ingestion [65]. The victim's autopsy revealed bilateral "pulmonary edema and generalized visceral congestion with some epicardial petechiae". α -ET intake was confirmed in blood (5.6 mg/L), urine (80.4 mg/L), vitreous (2.4 mg/L), bile (22.0 mg/L), stomach contents (52.9 mg/g), liver (18.3 mg/g), kidney (24.0 mg/g) and brain (16.2 mg/g). Daldrup et al. described another fatal case in which a psychotic man presented with agitation and hyperpyrexia [65]. Blood toxicological analysis identified α -ET at 1.1 mg/L, with the cause of death listed as malignant hyperthermia with α -ET contribution.

- Diethyltryptamine (DET)

DET is the ethyl analogue of DMT. It is orally active because the ethyl group prevents MAO degradation. The active dose is 50–100 mg, with psychoactive effects lasting 2-4 h [72,73]. DET's most common effects include slight generalized tremors to gross athletic movements, visual distortion, hypersensitivity to light, visual hallucinations, auditory perceptual distortions and olfactory hallucinations [74].

- N-methyl-N-ethyltryptamine (MET)

MET is structurally related to DMT, but little scientific information is available on its pharmacology or toxicity in humans. Inhalation of 15 mg freebase MET or 80-100 mg

oral freebase MET produce effects [75]. Anecdotal reports describe the most common physical and psychological effects as physical euphoria, tactile enhancement, increased heart rate and blood pressure, muscle cramps, teeth grinding, pupil dilation, hallucinations and cognitive effects [75].

- *N*-methyltryptamine (NMT)

NMT is the product of methyl group additions to tryptamine by the enzyme indolethylamine-*N*-methyltransferase [76]. In 2014, Gardner et al. demonstrated that NMT was a teratogen in pregnant rats, producing fetal skeletal malformations and cleft palates [77]. MAO metabolism produces its IAA metabolite.

- Dipropyltryptamine (DPT)

DPT is a synthetic tryptamine with a crystalline hydrochloride salt and an oily or crystalline base, first reported in 1973 as a treatment for alcoholism [77]. DPT is a hallucinogen, also known as “The Light”. DPT increases the intensity [77] of music and color, with pleasant flashes of light and sparkles, causing one to lose one’s ego and producing visual experiences [25]. DPT was an adjunct to psychotherapy in the 1960s and 1970s, but few peer-reviewed experimental studies were conducted [77]. Anecdotal internet reports describe it as a hallucinogen in humans following oral administration of 100-250 mg. Adverse physical and psychological “positive” effects include auditory hallucinations, music enhancement, stimulation, euphoria, and relaxation, as well as “negative” effects such as paranoia, psychosis, anxiety, nausea, dizziness, increased heart rate and general tremor [78].

DPT strongly inhibited 5-HT reuptake into rat synaptosomes [13] and had moderate affinity and partial agonism at the human 5-HT_{1A} receptor [79]. In 2008, Fantegrossi et al. reported that DPT elicited head-twitches in mice and rats suggesting that a primary site of action for DPT is the 5-HT_{2A} receptor [80]. Dailey et al. described a DPT intoxication case of a 19-year-old female [81]. The patient arrived at the ED with tachycardia (200 bpm) and psychomotor agitation, and was immediately sedated with 3 mg lorazepam. No analytical confirmation was performed, but a vial of DPT labelled “for research purposed only” was found at the scene.

- Diisopropyltryptamine (DiPT)

DiPT is a synthetic hallucinogen, closely related structurally to DMT, a 5HT_{2A} agonist and a partial 5HT_{1A} agonist that inhibits the serotonin transporter and vesicular monoamine transporter [82]. DiPT produces short-term visual and auditory hallucinations

including hearing voices, and bizarre dream states at high doses, and auditory distortion with deep tones at low doses [83].

2.2.2. 4-Substituted Tryptamines

- 4-Hydroxy-*N*-methyl-*N*-ethyltryptamine (4-OH-MET)

4-OH-MET is one of the most common synthetic tryptamines available online. 4-OH-MET, synthesized by Shulgin et al. [83], has effects lasting 4-6 h. 4-OH-MET can produce a wide range of effects including prickling, decreased ability to move, and later anxiety, nervousness, paranoia, tiredness and insomnia [34].

- 4-Hydroxy-*N,N*-dipropyltryptamine (4-OH-DPT)

4-OH-DPT is the 4-hydroxylated DPT derivative first synthesized by Shulgin et al. [83]. 4-OH-DPT is a light beige or white powder [56] that acts as a 5-HT_{2A} partial agonist. 4-OH-DPT also shares structural similarity with psilocin [84]. Effects are dose dependent, with onset at 15-45 min and duration of 5-8 h. According to user reports, synthetic 4-OH-DPT produces visual effects and hallucinatory states [85].

- 4-Acetoxy-*N,N*-dipropyltryptamine (4-AcO-DPT)

4-AcO-DPT is the 4-acetoxy derivative of DPT, is structurally similar to 4-AcO-DMT and 4-acetoxy-*N,N*-diisopropyltryptamine (4-AcO-DiPT), and is available as a white powder [56]. It is available online and typically administered orally or by insufflation. Its effects are dose dependent and include hallucination, dissociation, confusion and flashbacks, as reported on Erowid by a 4-AcO-DPT user [86].

- 4-Acetyloxy-*N,N*-diallyltryptamine (4-AcO-DALT)

4-AcO-DALT is a tryptamine derivative structurally linked to DALT and 5-MeO-DALT [56]. Users report taking 15-30 mg doses, with effects similar to those of hallucinogenic mushrooms or 4-AcO-DMT [86]. Effects lasted 1 h and were similar to those following mushroom intake, including mental and visual effects, and a slight cough and gagging [86].

- 4-Acetoxy-*N*-methyl-*N*-ethyltryptamine (4-AcO-MET)

4-AcO-MET, also known as matacetin, is a homolog of *O*-acetylpsilocin (4-AcO-DMT), an acetate ester of 4-OH-MET and a homologue of 4-AcO-DMT. It is also a structural and functional psilocin analogue and the 4-hydroxyl MET analogue [72].

Other synthetic 4-substituted tryptamines for which no scientific data are available are: 4-Hydroxy-diethyl-tryptamine (4-OH-DET), 4-OH-DiPT, 4-Hydroxy-*N*-methyl-*N*-isopropyltryptamine (4-OH-MiPT), 4-Hydroxy-*N*-methyl-*N*-propyltryptamine, or meprocin (4-OH-MPT), 4-Methoxy-*N*-methyl-*N*-isopropyltryptamine (4-MeO-MiPT), 4-Methoxy-*N,N*-dimethyltryptamine (4-MeO-DMT), 4-Hydroxy-*N,N*-tetramethylenetryptamine (4-OH-pyr-T) and their acetic acid derivatives (e.g. 4-Acetoxy-*N,N*-dimethyltryptamine (4-AcO-DMT), 4-Acetoxy-*N,N*-diethyltryptamine (4-AcO-DET), and 4-Acetoxy-*N,N*-diisopropyltryptamine (4-AcO-DiPT).

2.2.3. 5-Substituted Tryptamines

- Bufotenine or 5-Hydroxy-*N,N*-dimethyltryptamine (5-OH-DMT)

5-OH-DMT is a serotonin derivative found in the skin secretions of some Brazilian *Rhinella* toads [87], as well as in plants of the Leguminosae family and psychoactive mushrooms (*Amanita muscaria*) [88]. When *Bufo* species are ingested, toxicity ensues, including hemiparesis, muscle jerking and twitching, convulsions, altered mental status, slurred speech, headache, nausea, vomiting, severe dyspnea, and death [89–91]. Furthermore, effective dosage, route of administration and psychedelic effects are widely known and reported in the literature [92,93]. It is metabolized by the enzyme monoamine oxidase A (MAO-A) that catalyzes an oxidative deamination forming IAA [87].

- 5-Methoxy- α -methyltryptamine (5-MeO- α -MT)

At low dosages (15-30 mg orally, 5-20 mg smoked), 5-MeO- α -MT produces powerful hallucinations [60]. Depending upon the individual, negative effects, including death, are more typical at higher dosages (80-100 mg oral 5-MeO- α -MT) [7,94]. Neurologic manifestations that may occur include agitation, restlessness, confusion, and lethargy. Physical manifestations include vomiting, papillary dilation, jaw clenching, tachycardia, mydriasis, salivation, diaphoresis, and mild elevations in blood pressure, temperature, and respiratory rate may also occur [94].

- 5-Methoxy-*N,N*-dipropyltryptamine (5-MeO-DPT)

5-MeO-DPT is a 5-MeO-DMT structural isomer available as a white powder [56]. This molecule is orally active, with dose-dependent effects. The most common reported effects included dizziness, increased heart rate, tremor, anxiety and agitation.

- 5-Methoxy-*N,N*-diisopropyltryptamine (5-MeO-DiPT)

“Foxy Methoxy” or 5-MeO-DiPT is a well-known psychedelic tryptamine in the illicit market [95]. The common routes of administration are oral, smoked and insufflations [96]. Noworyta-Sokołowska et al. showed that 5-MeO-DIPT at doses of 5, 10, and 20 mg/kg induced head-twitch, hallucinations, vomiting and tachycardia in rats [96]. Moreover, long-term exposure to 5-MeO-DIPT resulted in development of post-hallucinogenic perception disorder. As described by Shulgin et al., users feel the effects of 6-10 mg 5-MeO-DIPT 20 to 30 min after administration for 3-6 h [97]. 5-MeO-DIPT is metabolized by five pathways, including hydroxylation, N-dealkylation [98] and reactions of *O*-demethylation, with the *N,N*-diisopropyl groups converted to 5-hydroxy-*N,N*-diisopropyltryptamine (5-OH-DIPT) that is further partly sulfated and glucuronidated [99].

The literature contains several reports of 5-MeO-DIPT intoxications. A 23-year-old male arrived at the ED with paranoia and sensory distortion after ingesting 5-MeO-DIPT. 5-MeO-DIPT intake was confirmed in blood and urine (0.14 and 1.6 µg/mL, respectively), suggesting consumption shortly before intoxication [100]. Smolinske et al. investigated an intoxication case of a psychotic 19-year-old male following ingestion of “Foxy”, transported to the ED and immediately treated with lorazepam [101]. Urine analysis was positive for phencyclidine and cocaine but was negative for 5-MeO-DIPT. In 2003, Meatherall et al. described the intoxication of a 21-year-old man found in a state of confusion [102]. At ED admission, the patient was alert and oriented, with the only clinical observation his inability to move his limbs. After 3.5 h, he was discharged from the hospital. Gas chromatography-mass spectrometry (GC-MS) analysis of his urine revealed 1.7 µg/mL 5-MeO-DIPT, codeine, nicotine, cotinine, acetaminophen and caffeine.

- 5-Methoxy-*N,N*-diallyltryptamine (5-MeO-DALT)

5-MeO-DALT was first synthesized by Shulgin et al. in 1980 [97] and was seized by police in 2006 as a “plant fertilizer” or “plant food” [32]. Active oral doses ranged from 12–20 mg [103], with administration by the oral, nasal insufflation and IV routes. This drug produced dose-dependent effects 15 to 30 min after oral administration that lasted for 2 to 4 h. Adverse effects included vasoconstriction, increased blood pressure, rapid heartbeat, headache, sweating, dilated pupils, bruxism, anxiety and nausea. Meatherall et al. reported a fatal road crash following ingestion of 350 mg 5-MeO-DALT by a 26 year old male [102]. Toxicological findings included the presence of 5-MeO-DALT but there were no data on drug quantification.

Michely et al. [104] identified 5-MeO-DALT phase I and II metabolites by liquid chromatography–high-resolution mass spectrometry (LC–HRMS/MS). Metabolites were

primarily derived from hydroxylations, oxidations to oxo metabolites, *N*-dealkylations and *O*-demethylations.

- 5-Methoxy-*N*-methyl-*N*-isopropyltryptamine (5-MeO-MiPT)

5-MeO-MiPT, or “moxy” was marketed as a “plant fertilizer”. Oral doses ranged from 1-3 mg (light), 3-8 mg (common) and 8-12 mg (strong), with typical 10-20 mg doses if inhaled [105]. The principal effects lasted 3-7 h and included a general heightening of awareness, mild euphoria, psychedelic visual effects, such as enhanced colors, but also anxiety, nausea, confusion and paranoia. Repke et al. studied if the effects of the drug would differ depending upon route of administration [106]. If ingested the effects were stimulating, with visual hallucinations prevailing. 5-MeO-MiPT metabolism studied by LC-HRMS/MS identified six phase I metabolites following *N*-demethylation, *O*-demethylation, demethylation and hydroxylation and *N*-oxide formation and hydroxylation of the parent compound and *N*-*O*-bis-demethylation of the metabolite 5-OH-MiPT [107].

In 2019, Grafinger et al. reported that a 32 year old male went to the ED after the ingestion of an “LSD-like substance” [108]. The cause of the intoxication was attributed to the combined use of psychoactive substances. 5-MeO-MiPT was identified by LC-HR-MS/MS and quantified by liquid chromatography coupled with mass spectrometry in tandem (LC-MS/MS) at 160 ng/mL in blood and 3380 ng/mL in urine. The most abundant metabolites were identified as 5-methoxy-*N*-isopropyltryptamine (5-MeO-NiPT), 5-hydroxy-*N*-methyl-*N*-isopropyltryptamine (5-OH-MiPT), 5-methoxy-*N*-methyl-*N*-isopropyltrypt-amine-*N*-oxide (5-MeO-MiPT-*N*-oxide) and hydroxy-5-methoxy-*N*-methyl-*N*-isopropyl-tryptamine (OH-5-MeO-MiPT).

Shimizu et al. reported an acute intoxication in a 27-year old male from 5-MeO-MiPT and methylone use [109]. At the ED, he had psychomotor agitation, was sweating, had pyrexia (37.8°C) and tachycardia (150 bpm) and was hypertensive. The unknown powder that the man took was analyzed by high-performance liquid chromatography (HPLC) and GC-MS to determine the intoxicating drug(s). The powder contained 60% methylone (120 mg), a synthetic cathinone, and 38% 5-MeO-MiPT (76 mg). No analytical confirmation was performed and rapid drug screening tests did not show immunoreactivity for other common drugs of abuse in urine and gastric fluid samples. He was discharged the day after admission without complications.

- 5-Methoxy-*N*-methyl-*N*-ethyltryptamine (5-MeO-MET)

5-MeO-MET is a tryptamine structurally similar to 4-OH-MET and 4-AcO-MET [56]. This drug is available in powder and crystal forms, with the common routes of

administration ingestion and insufflation. A drug-forum site reported a “threshold” dose of 1-4 mg, a “normal” dose 5-8 mg and a “strong” dose 9-10 mg [110]. The onset of effects occurred at 1 min, with a limited duration of action of only 40 min. The main adverse effects reported by users include euphoria, hallucinations, visual alterations and anxiety.

- 5-Methoxy-*N,N*-diethyltryptamine (5-MeO-DET)

5-MeO-DET is an indolealkylamine structurally similar to DMT [107], with little data on its behavioural effects. In 2011, Gatch et al. observed stimulant effects and increased locomotor activity in rats [82]. After intraperitoneal and intraocular injection of 0.05 to 10 mg/kg 5-MeO-DET, effects occurred within 30 min and lasted 80 to 90 min.

- 5-Methoxy-*N,N*-trimethyltryptamine (5-MeO-TMT)

5-MeO-TMT is a psychedelic tryptamine first synthesized by Shulgin et al. [86] that is smoked or orally administered [106]. Toxicological information is still scarce but users suggest the oral dose is 75-150 mg, but no duration of effects was reported. The effects include euphoria, visual distortions and difficulty in sleeping.

2.3. Analytical Methods to Determine Tryptamines and/or Metabolites in Conventional and Non-Conventional Biological Matrices

From 2010 to 2023, thirty-four analytical methods were presented to determine tryptamines and metabolites. Table 2 summarizes the analytical methods reported for the determination of tryptamines in biological matrices, including information on sample size, sample preparation, instrumentation and validation parameters.

Table 2. Analytical methods to determine tryptamines in conventional and non-conventional biological matrices.

Analytes	Sample (µL)	Sample preparation	Method	Mobile phase	Linear range (ng/mL)	LOD (ng/mL)	LOQ (ng/mL)	Recovery (%)	Concentration (ng/mL)	References
5-MeO-DMT α-MT DiPT DMT DPT MiPT	P: 1000	Dilute; SPE; Evaporate; Resuspend	LC-MS/MS (positive ESI; MRM)	A: 1mM AmFo with 0.1 % FA; B: MeOH with 0.1 % FA	NA	1.0 2.5 1.0 2.5 1.0 2.5	NA	NA	NA	Wohlfarth, 2010 [111]
DMT	B: 1000	Dilute; SPE; Evaporate; Resuspend	LC- QTrap/MS (positive ESI; MRM)	A: 5 mM AmFo with 0.1% FA; B:MeOH with 0.1% FA	NA	0.1	0.2	94.0- 102.9	1.2-19.8	Oliveira, 2012 [112]
Psilocin	P: 500	Dilute; Centrifuge; SPE; Evaporate; Resuspend	LC-MS/MS (positive EI; MRM)	A: MeOH with 0.1% FA; B: 2 mM AmAc with 0.1 % FA	2-100	0.1	0.3	86	NA	Martin, 2012 [113]
Psilocin Bufotenine	S: 1000	Dilute; Centrifuge	LC-MS/MS (positive EI; MRM)	A: ACN with 0.1 % FA; B: 2 mM AmAc buffer with 0.1 % FA (pH3)	1-17.5	0.05 0.05	0.17 0.1	95 91.6	0.2-0.5 0.5	Martin, 2013 [114]

Psilocin Bufotenine	P: 1000	Dilute; Centrifuge	LC-MS/MS (positive EI; MRM)	A: ACN with 0.1 % FA; B: 2 mM AmAc buffer with 0.1 % FA (pH3)	1-17.5	0.05 0.07	0.15 0.27	93.5 91.3	NA	Martin, 2013 [114]
Psilocin Bufotenine	U: 500	Enzymatic hydrolysis; Centrifuge; SPE; Evaporate; Resuspend	LC-MS/MS (positive EI; MRM)	A: ACN with 0.1 % FA; B: 2 mM AmAc buffer with 0.1 % FA (pH3)	1-17.5	0.2 0.1	0.2 0.14	91.8 88.8	11-13 1.6-5.9	Martin, 2013 [114]
5-MeO- DALT 5-MeO-DMT α-MT DiPT DMT DPT	B: 10	Dilute; DBS; Evaporate; Resuspend.	LC-MS/MS (positive ESI; MRM)	A: water with 0.1 % FA; B: ACN with 0.1% FA;	NA	1.0 1.0 2.5 1.0 1.0	NA	NA	NA	Ambach, 2014 [115]
5-MeO- DALT 5-MeO-DMT α-MT DiPT DMT DPT	B: 500	Dilute; Centrifuge; SPE; Wash; Evaporate; Resuspend.	LC-MS/MS (positive ESI; sMRM)	A: 10 mM AmFo with 0.1% FA; B: MeOH with 0.1% FA	2.5- 1000	NA	2.5 2.5 2.5 5 2.5	NA	NA	Ambach, 2015 [116]
5-MeO- DALT 5-MeO-DMT α-MT DiPT	U: 250	LLE: Dilute; Centrifuge; Organic phase: evaporated;	LC-MS/MS (positive ESI; sMRM)	A: 10 mM AmFo with 0.1% FA; B: MeOH with	NA	NA	1 1 2.5 1 2.5	NA	NA	Ambach, 2015 [116]

DMT DPT		Residue: resuspended.		0.1% FA			1			
5-MeO- DALT	B: 500	Protein precipitation; DLLME; Centrifuge; Resuspend	LC-MS/MS (positive ESI; sMRM)	A:5mM AmFo with.1% AF; B: MeOH with 0.1% FA	2-1000	0.2-2	NA	5-110	NA	Odoardi, 2015 [117]
Psilocin Bufotenine	H: 50 mg	Wash; Centrifuge; Resuspend	LC-MS/MS (positive EI; MRM)	A: ACN with 0.1% FA; B: 2 mM AmAc buffer with 0.1% FA	0.04-2	10 pg/mg	16 pg/mg 22 pg/mg	NA	0.14- 1.45	Martin, 2015 [118]
DALT 5-MeO- DALT	U:100	Dilute; Centrifuge; Evaporate; Resuspend	LC-HR- MS/MS (positive ionization; full scan & DDA)	A: 2 mM AmFo with 0.1 % FA; B: 2 mM AmFo : ACN:MeOH (50:50, v/v; 1 % water) with 0.1 % FA	NA	1	NA	NA	NA	Michely, 2015 [104]
DALT 5-MeO- DALT	U: 5000	Acid hydrolysis	GC-MS SUSA (positive EI; full scan)	helium	NA	10 50	NA	NA	NA	Michely, 2015 [104]
4-OH-DET 4-OH-DIPT 4-OH-MET 4-OH-MIPT 4-MeO-DMT	B: 200	Dilute; Protein precipitation; Centrifuge; Evaporate;	LC-MS/MS (positive ESI; dMRM)	A: ACN with 0.1% FA; B: water with 0.1% FA	1-100	0.06 1.05 NA NA 2.98	NA	17.1	DMT:11.1	Adamowicz, 2016 [119]

4-AcO-DiPT		Resuspend									0.99
5-MeO- α -MT											0.11
5-Meo-DALT											1.11
5-MeO-DiPT											0.15
5-MeO-DMT											2.61
5-MeO-MiPT											NA
α -MT											2.61
DiPT											0.88
DMT											0.08
DPT											0.30
MET											NA
NMT											1.50
DET											0.72
DALT											
2-Ph-DALT											
4-AcO-DALT											
4-OH-DALT											
5-Me-DALT											
5-MeO-DALT											
5-MeO-2-Me-DALT	B, P, U: NA	Dilute and shoot	GC-MS; sIR; (positive ESI; full scan & PDA)	helium	NA	NA	NA	NA	NA	NA	Brandt, 2016 [120]
5-EtO-DALT											
5-F-DALT											
5-F-2-Me-DALT											
5-CI-DALT											
5-Br-DALT											
6-F-DALT											
7-Me-DALT											
7-Et-DALT											

DALT 2-Ph-DALT 4-AcO-DALT 4-OH-DALT 5-Me-DALT 5-MeO-DALT 5-MeO-2-Me-DALT 5-EtO-DALT 5-F-DALT 5-F-2-Me-DALT 5-CI-DALT 5-Br-DALT 6-F-DALT 7-Me-DALT 7-Et-DALT	B, P, U: NA	Dilute and shoot	LC-MS; sIR; (positive HESI; full scan & DDA)	A: water with 0.1% FA; B: ACN with 0.1% FA	NA	NA	NA	NA	NA	Brandt, 2016 [120]
5-MeO-DiPT 4-OH-DiPT	B: 200	Protein precipitation; Centrifuge; Evaporate; Resuspend	LC-MS/MS (positive ESI; MRM; full scan & DDA)	A: 5 mM FA B: ACN	1–100	0.1	0.3	84 91	NA	Vaiano, 2016 [121]
DMT 5-MeO-DMT α-MT	OF: 500	Dilution; LLE; Centrifuge; Evaporate; Resuspend	UHPLC-MS/MS (positive ESI; MRM)	A: 10mM AmFo B: meOH	NA	NA	NA	NA	NA	Gjerde, 2016 [122]

5-MeO-MiPT	S: 100	Dilute; Centrifuge; Evaporate; Resuspend	UHPLC- HRMS XEVO G2 QTOFMS (positive ESI)	A: water with 0.01% FA; B:MeOH with 0.01% FA	NA	NA	NA	NA	NA	Fabregat- Safont, 2017 [123]
5-MeO-MiPT	U: 200	Enzymatic hydrolysis; Protein precipitation; Centrifuge	UHPLC- HRMS interfaced to a XEVO G2 QTOF MS (positive ESI)	A: water with 0.01% FA; B:MeOH with 0.01% FA	NA	NA	NA	NA	NA	Fabregat- Safont, 2017 [123]
5-MeO-MiPT	U: 100	Protein precipitation; Centrifuge	UHPLC- HRMS interfaced to a XEVO G2 QTOF MS (positive ESI)	A: water with 0.01% FA; B:MeOH with 0.01% FA	NA	NA	NA	NA	NA	Fabregat- Safont, 2017 [123]
5-F-DALT 7-Me-DALT 6-MD-DALT	U: 100	Dilute; Centrifuge; Evaporate; Resuspend	LC- HRMS/MS (positive HESI; full scan & DDA)	A: 2 mM aqueous AmFo with 0.1% FA (pH 3); B: 2 mM aqueous AmFo with ACN:MeOH (1:1, v/v; 1% water) with 0.1%	NA	NA	NA	NA	NA	Michely, 2017 [124]

5-F-DALT 7-Me-DALT 5,6-MD-DALT DALT 2-Ph-DALT 4-AcO-DALT 4-OH-DALT ED-DALT 5-Me-DALT 5-MeO-DALT 5-MeO-2-Me-DALT 5-EtO-DALT 5-F-DALT 5-F-2-Me-DALT 5-Cl-DALT 5-Br-DALT MD-DALT 6-F-DALT 7-Me-DALT 7-Et-DALT	U: 2500	Acid hydrolysis	GC-MS SUSA (positive ESI; full scan)	FA helium	NA	NA	NA	NA	NA	Michely, 2017 [124]
Psilocin DMT 5-MeO-DMT	B: 1000	Centrifuge; Evaporate; Resuspend	LC-MS/MS (positive ESI; dMRM)	A: 5mM AmFo in water with 0.01% FA; B: ACN with 0.01% FA	NA	2.50	NA	NA	NA	Fagiola, 2018 [125]
	synthesized	Dilute	GC-MS; GC- sIR; (positive ES; full scan)	helium	NA	NA	NA	NA	NA	Brandt, 2017 [120]

Psilocin DMT 5-MeO-DMT	U: 1000	Centrifuge; Evaporate; Resuspend	LC-MS/MS (positive ESI; dMRM)	A: 5mM AmFo in water with 0.01% FA; B: ACN with 0.01% FA	NA	2.50	NA	NA	NA	Fagiola, 2018 [125]
5-MeO-DiPT	H: 30 mg	Wash; Pulverize; Centrifuge	LC-MS/MS (positive ESI; MRM)	A: 20 mM AmAc, 5% ACN and water with 0.1% FA; B: ACN with 0.1% FA	0.1-100 pg/mg	NA	0.1 pg/mg	91.1-112	0.2–7533 pg/mg	Roujia, 2019 [126]
DMT Psilocybin	U: NA	Dilute	LC-QTOF (positive ESI)	A: 5 mM AmFo (pH 3); B: ACN with 0.1% AF	NA	1-2	NA	NA	NA	Pope, 2019 [127]
5-MeO-DiPT 5-OH-DiPT 5-MeO-IPT	U:1000	Centrifuge; Resuspend	GC- Orbitrap- MS (positive EI; full scan)	helium	2-300	1	2	92.4-98.4	2-2.8	Yan, 2020 [128]
5-MeO-DiPT	DUS: 10	Dry; Sonicate; Centrifuge	LC-MS/MS (positive EI; MRM)	A: 10 mM AmAc and water with 0.1% FA; B: ACN	0.2-100	0.1	0.2	78.8- 82.8	0.3- 2.3	Yan, 2020 [129]
5-MeO-DiPT 5-MeO-MiPT 5-MeO- DALT	H: 20 mg	Wash; Pulverize; Centrifuge	UHPLC- MS/MS (ESI; MRM)	A: water with 0.1% FA; B: ACN with	3- 800 pg/mg	0.1 0.1 0.1 1	3 3 3 3	85.5- 101.8 93.8- 94.0 85.3-99.0	5-MeO-DiPT: 110-130000 pg/mg 5-MeO-NiPT:	Shi, 2020 [130]

5-MeO-DMT				0.1% FA	5	50	93.2-	130- 37000		
5-MeO-α-MT					1	3	104.5	pg/mg		
5-OH-DiPT					5	10	93.4-	5-OH-DiPT:		
5-MeO-NiPT					0.1	3	102.6	310- 13000		
DPT					20	50	85.6- 99.0	pg/mg		
NiPT					0.3	3	90.1- 99.7	4-OH-DiPT:		
DMT					5	10	92.3- 95.0	570 pg/mg		
Psilocin					5	10	96.4-			
Psilocybin					1	10	101.6			
4-OH-MiPT					0.1	3	90.2-			
4-OH-DiPT					0.3	10	109.7			
4-AcO-DiPT					5	10	86.0-			
4-OH-MET							101.7			
							88.2-			
							100.8			
							85.6- 93.6			
							85.9-			
							107.7			
							85.2- 88.0			
							86.9- 94.7			
DMT					7.6	25.3	78.3			
5-MeO-DMT					2.6	8.5	86.3			
5-MeO-α-MT					4.3	14.2	36.2			
5-MeO-MiPT					2.7	9.1	72.1			
5-MeO-DALT	H: 25 mg	Wash; Dilute; Hydrolysis; Evaporate; Reconstitute	UHPLC- MS/MS (ESI; MRM)	A: water with 0.1% FA; B: CAN:water (95:5) with 0.1% FA	10- 500 pg/mg	1.3 4.3 1.5 10.3	4.3 14.3 5.1 34.4	65.4 34.6 71.3 53.2	NA	Nzekove, 2021 [131]
4-AcO-DiPT										
5-MeO-DPT										
α-ET										
DMT	P: 50	Protein precipitation;	LC-MS/MS	A: water with 0.1% FA;	0.25- 250	NA	0.25	95.5-99.0	44.5± 12.7	Luethi, 2022 [132]

		Centrifuge		B: MeOH with 0.1% FA							
DMT	P: 200	Protein precipitation; Centrifuge; Evaporate; Reconstitute	QTRAP LC- MS/MS	A: water with 0.1% FA; B: MeOH with 0.1% FA	0.25- 200	NA	0.25	66.2- 68.8	NA	Eckernas, 2022 [133]	

Abbreviations: 5-MeO-DMT, 5-Methoxy-*N,N*-dimethyltryptamine; α -MT, α -methyltryptamine; DiPT, *N,N*-diisopropyltryptamine; DMT, *N,N*-dimethyltryptamine; DPT, *N,N*-dipropyltryptamine; DET, *N,N*-diethyltryptamine; MiPT, *N*-methyl-*N*-isopropyltryptamine; 5-MeO-DALT, 5-Methoxy-*N,N*-diallyltryptamine; DPT, *N,N*-dipropyltryptamine; 4-OH-DET, 4-Hydroxy-*N,N*-diethyltryptamine; 4-OH-DIPT, 4-Hydroxy-*N,N*-diisopropyltryptamine; 4-AcO-DIPT, 4-Acetoxy-*N,N*-diisopropyltryptamine; 4-OH-MET, 4-Hydroxy-*N*-methyl-*N*-ethyltryptamine; 4-OH-MIPT, 4-Hydroxy-*N*-methyl-*N*-isopropyltryptamine; 4-MeO-DMT, 4-Methoxy-*N,N*-dimethyltryptamine; 5-MeO- α -MT, 5-Methoxy- α -methyltryptamine; 5-MeO-DIPT, 5-Methoxy-*N,N*-diisopropyltryptamine; 5-MeO-DMT, 5-Methoxy-*N,N*-dimethyltryptamine; 5-MeO-MiPT, 5-Methoxy-*N*-methyl-*N*-isopropyltryptamine; MET, *N*-methyl-*N*-ethyltryptamine; DET, *N,N*-diethyltryptamine; NMT, *N*-methyltryptamine; DALT, *N,N*-diallyltryptamine; 5-MeO-DALT, 5-Methoxy-*N,N*-diallyltryptamine; 2-Ph-DALT, 2-Phenyl-*N,N*-diallyltryptamine; 4-AcO-DALT, 4-Acetoxy-*N,N*-diallyltryptamine; 4-OH-DALT, 4-Hydroxy-*N,N*-diallyltryptamine; 5-Me-DALT, 5-Methyl-*N,N*-diallyltryptamine; 5-MeO-2-Me-DALT, 5-Methoxy-2-methyl-*N,N*-diallyltryptamine; 5-EtO-DALT, 5-Ethoxy-*N,N*-diallyltryptamine; 5-F-DALT, 5-Fluoro-*N,N*-diallyltryptamine; 5-F-2-Me-DALT, 5-Fluoro-2-methyl-*N,N*-diallyltryptamine; 5-Cl-DALT, 5-Chloro-*N,N*-diallyltryptamine; 5-Br-DALT, 5-Bromo-*N,N*-diallyltryptamine; 6-F-DALT, 6-Fluoro-*N,N*-diallyltryptamine; 7-Me-DALT, 7-Methyl-*N,N*-diallyltryptamine; 7-Et-DALT, 7-Ethyl-*N,N*-diallyltryptamine; 6-MD-DALT, 6-Methylenedioxy-*N,N*-diallyltryptamine; 5,6-MD-DALT, 5,6-Methylenedioxy-*N,N*-diallyltryptamine; 5-MeO-IPT, 5-Methoxy-isopropyltryptamine; 5-MeO-NiPT, 5-Methoxy-*N*-isopropyltryptamine; NiPT, *N*-isopropyltryptamine; H, hair; B, blood; U, urine; S, serum; P, plasma; SPE, solid phase extraction; LLE, liquid liquid extraction; DLLME, dispersive liquid-liquid microextraction; DBS, dried blood spots; DUS, dried urine spots; UPLC, ultra-performance liquid chromatography; LC-MS/MS, liquid chromatography coupled with mass spectrometry in tandem; LC- HRMS/MS, liquid chromatography high resolution coupled with mass spectrometry in tandem; DDA, data dependent acquisition; PDA, photodiode array acquisition; sMRM, scheduled multiple reaction monitoring; dMRM, dynamic multiple reaction monitoring; QTrap, triple quadrupole linear ion trap mass spectrometer; UHPLC-HRMS, ultra-performance liquid chromatography-high resolution mass spectrometry; GC-Orbitrap-MS, gas chromatography coupled with Orbitrap mass spectrometry; HPLC, high performance liquid chromatography; UHPLC, ultra high performance liquid chromatography; LC-QTOF, liquid chromatography coupled to a Quadrupole Time of Flight mass spectrometer; GC-MS, gas chromatography coupled with mass spectrometry; ESI, electrospray ionization; HESI, heated electro spray ionization; EI, electron ionization; MRM, multiple reaction monitoring; GC-sIR, Gas chromatography solid-state infrared analysis; AmAc, ammonium acetate; FA, formic acid; ACN, acetonitrile; AmFo, ammonium formate; MeOH, methanol; LOD, lower limit of detection; LOQ, limit of quantification; NA, not available.

Different biological matrices were employed for forensic purposes including conventional matrices urine, blood, plasma, serum, and unconventional matrices oral fluid and hair. Protein precipitation is a simple sample preparation method, providing sufficient extraction efficiency while simplifying extraction and preparation time. Different protein precipitation methods include different solvents for blood extraction, but methanol is the most common solvent. Different sample preparation techniques include protein precipitation for urine, serum and blood samples, acid hydrolysis for urine, centrifugation for blood, plasma and urine samples, washing for plasma, blood and hair samples, enzymatic hydrolysis for urine samples, solid phase extraction (SPE), liquid-liquid extraction (LLE), dispersive liquid-liquid microextraction (DLLME) and a solvent extraction for dried blood spots (DBS). Tryptamine is a relatively labile analyte, but it remains stable in an acidic environment. Some analytical methods described the use of acidic solvents to extract drugs from blood.

Most analytical methods included chromatographic separations and mass spectrometry detection. LC-MS/MS, LC-HRMS/MS, GC-MS, LC-MS, and ultra-performance liquid chromatography-high resolution mass spectrometry (UHPLC-HRMS/MS) analytical methods are most common for forensic toxicology purposes. Different approaches utilized triple quadrupole full-scan mode, triple quadrupole multiple reaction monitoring (MRM) with data dependent acquisition (DDA) and photodiode array acquisition PDA, single quadrupole time of flight (TOF). Even with powerful analytical instrumentation, these substances' identification can be missed for many reasons including the fact that the reference mass spectrum may not be available in libraries for full-scan mode, and fragments generated in single ion monitoring (SIM) mode show nondescript fragmentation patterns [25].

Low limits of detection (LOD) are key for identifying tryptamines; two analytical methods achieved LODs of 0.10–0.15 ng/mL for 5-MeO-DiPT, with the same sample volume and LC-MS/MS technology, but different sample preparation techniques [120,122]. Michely et al. had LODs of 10-50 ng/mL for DALT and 5-MeO-DALT by GC-MS, with a 2.5 mL urine sample [119], but later achieved LODs of 1-5 ng/mL using LC-HRMS/MS and fifty times lower sample volume [134]. Also, Martin et al. determined psilocin in 500 μ L plasma with a 0.1 ng/mL LOD [113], whereas in their more recent method they present an LOD of 0.05 ng/mL using 1 mL of the same matrix with a different sample preparation [114]. Fagiola et al. detected DMT in blood with a 2.5 ng/mL LOD [134], while Adamowicz et al. identified DMT with a 0.88 ng/mL LOD in a smaller blood volume but a longer sample preparation procedure [119], both with LC-MS/MS. For 5-MeO-DMT, Fagiola et al. [134] had a similar LOD as Adamowicz et al. (2.50 and 2.61 ng/mL, respectively), but the first author employed a higher sample volume. More rigorous sample preparation can reduce background noise and improve detectability. Adamowicz et al.

accomplished a lower 4-MeO-DiPT LOD compared to that of Vaiano et al. [121] with the same sample volume and mass spectrometer.

Yan et al. [128] analyzed urine for 5-MeO-DiPT and metabolites using a GC-Orbitrap-MS method characterized by LODs of 1 ng/mL and a concentration range of 1-2.8 ng/mL in five authentic urine samples. In this study the authors also identified two metabolites, 5-OH-DiPT and 5-MeO-DiPT, but without presenting their LODs. LODs from 0.06-2.98 ng/mL blood were described for 16 tryptamines but sensitivities for some metabolites were not included in the method of Adamowicz et al. [119]. Michely et al. [124] achieved the same LOD for 5-MeO-DALT as Ambach et al. [116], with 100 μ L urine without an extraction technique, while the latter group required 250 μ L urine but had a more comprehensive LLE sample cleanup. Ambach et al. also developed an analytical method for tryptamines in 10 μ L dried blood spots (DBS), reaching LODs of 1-2.5 ng/mL for 5-MeO-DALT, 5-MeO-DMT, AMT, DiPT, DMT and DPT [113]. In the Brandt et al. method for 15 tryptamines, the LODs were not provided, despite their being used to propose a metabolic pathway for tryptamines [121,126]. Generally, the most commonly detected compounds were 5-MeO-DiPT, 5-MeO-DALT and DMT, perhaps because their metabolic pathways are already well known and toxicologists know how to identify the drugs.

Since 2020, other five analytical methods were developed to detect different tryptamines [129–133]. Two of them detected DMT in plasma samples using different sample volume sample preparations. The same LOQ was obtained from both methods. Another author [131] detect 8 tryptamines in 25 mg hair, using a UHPLC-MS/MS as chromatographic separation. Other 16 tryptamines were studied using 20 mg hair and a simple sample preparation. In this case, LODs varied between 0.1 and 20 pg/mg and authors were able to quantify four tryptamines: 5-MeO-DiPT, 5-MeO-NiPT, 5-OH-DiPT and 4-OH-DiPT.

Aims

Tryptamines are not routinely detected in emergency department screening panels and are not included in routine analysis in forensic and clinical settings, which can lead to incorrect interpretation of symptoms or autopsy findings. Indeed, tryptamines induce non-specific effects, and the consumption of specific molecules can only be determined through the analysis of biological samples such as blood and urine. However, analytical methods for identifying many analogues in biological samples and comprehensive screening for tryptamines and metabolites in urine are lacking. Moreover, tryptamines can be active at low doses and quickly metabolized, making drug detection difficult, and focusing on specific metabolite biomarkers to improve detection and prove consumption is frequently preferred. Currently, however, there are few data on the metabolic pathways or specific enzymes involved in tryptamines biotransformation. Data suggest that not all tryptamines have a common metabolic pathway, and those pathways vary based on the nature and position of chemical substitutions. As such, *in vitro* metabolism profiling of NPS is critical for identifying specific consumption markers and elucidating the pharmacokinetic profile.

This dissertation had two main goals:

Part I: Assess the human metabolism of 4-AcO-DiPT, 4-OH-MPT, and α -MT and identify optimal biomarkers of intake in clinical and forensic toxicology. These tryptamines were incubated with 10-donor-pooled human hepatocytes to simulate *in vivo* conditions; samples were analyzed by liquid chromatography-high-resolution tandem mass spectrometry (LC-HRMS/MS) and software-assisted data mining; LC-HRMS/MS analysis and data mining were supported by *in silico* metabolite predictions. Samples from authentic cases of consumption were analyzed in the same conditions when available.

Part II: Develop and validate following international guidelines in forensic toxicology a comprehensive LC-HRMS/MS method to detect or, when possible, to quantify tryptamines and metabolites in urine for forensic and clinical applications. All commercially available reference standards for tryptamines and results from the metabolite identification studies presented in Part I were included in the method.

Part I: Tryptamines' Metabolite Profiling

Tryptamine intoxications and fatalities are increasing, although these NPS are not controlled in most countries. There are few data on the metabolic pathways and enzymes involved in tryptamines biotransformation. This class of NPS have non-specific effects, and the consumption of specific molecules can only be determined in forensic and clinical settings through the analysis of biological samples such as blood and urine. They can, however, be active at low doses and quickly metabolized, making drug detection difficult. As a result, targeting specific metabolite biomarkers is frequently preferred to improve detection and demonstrate consumption.

Therefore, in this first chapter it is presented the metabolic profiling in human hepatocyte incubations for three molecules: 4-AcO-DiPT, 4-OH-MPT and α -MT. A brief introduction is given about the studied molecule, followed by the results obtained, a fully detailed discussion and conclusion.

1. 4-AcO-DiPT Metabolic Profiling in Human Hepatocyte Incubations

4-AcO-DiPT is a synthetic tryptamine related to 4-hydroxy-*N,N*-diisopropyltryptamine (4-OH-DiPT), 4-acetyloxy-*N,N*-dipropyltryptamine (4-AcO-DPT) and 4-acetoxy-*N,N*-dimethyltryptamine (4-AcO-DMT) that currently are not controlled in many countries. 4-AcO-DiPT was identified as early as July 2004, with charges against vendors selling the drug to the public; however, there were no convictions and no determination of the legal status of 4-AcO-DiPT [17]. Although the current use of psychedelics is low, tryptamine intake is increasing [7,68] despite limited data on prevalence and patterns of intake. According to psychonaut's experiences reported on Erowid website, 4-AcO-DiPT is available online and typically administered orally with effects similar to those of hallucinogenic mushrooms and 2-(4-bromo-2,5-dimethoxyphenyl)-ethanamine (2C-B) [135]. 4-AcO-DiPT is a white powder available as the free base and the HCl salt. Both are orally active, with the lower molecular weight freebase about 10% more potent than the same weight of the HCl salt. 4-AcO-DiPT and 4-OH-DiPT have similar effects if taken orally, though dosage might be different. Oral 4-AcO-DiPT doses start at 3-5 mg, 5-15 mg is considered a "light" dose, while higher doses range between 25 and 40 mg. Users self-report 15–30 mg doses, with onset of effects in 20-60 min, depending on dosage form and stomach contents, and duration of 2 to 4 h. Its effects, that can appear from 1 to 4 h, are dose dependent and include hallucination, dissociation, confusion, and flashbacks, as reported on Erowid by a 4-AcO-DPT user [135]. Over the last decade, there were few intoxication cases and even fewer fatalities due to tryptamines reported in the European Union and North America, although this is likely an underestimation due to missed detections. There are few data on metabolic pathways and specific enzymes involved in tryptamine biotransformation, but it appears that there is not a

common metabolic pathway, with the nature and position of substituents changing metabolism. Overall, psychedelic tryptamine use is increasing, raising the importance of laboratory identification of specific metabolites to verify intake and identify potential public health NPS outbreaks. The aim of this study was to determine optimal 4-AcO-DiPT metabolite biomarkers of consumption for clinical and forensic applications, using *in silico* metabolite prediction, human hepatocyte metabolism, LC-HRMS/MS analysis, and software-assisted data-mining.

1.1. Material and Methods

1.1.1. *In Silico* Metabolites Prediction

The metabolites were predicted with the online GLORYx freeware [136,137]. The metabolite list was generated using the tryptamine of interest with the “phase I and phase II metabolism” option. Metabolites with a score higher than 0.40 were selected and reprocessed to simulate a second-step metabolism; the second-generation metabolite score was multiplied by the first-generation metabolite score and scores higher than 0.20 were added to the inclusion list (Table 3).

1.1.2. Chemicals and Reagents

4-AcO-DiPT and 4-OH-MPT were obtained from Cayman Chemical (Ann Arbor, MI, USA), α -MT was purchased from Toronto Research Chemicals (Milan, Italy) and diclofenac was acquired from Sigma Aldrich (Milan, Italy). Stock standards of these chemicals were prepared to 1 mg/mL in LC-MS grade methanol (Carlo Erba; Cornaredo, Italy). Standards were stored at -20°C until analysis. Ten-donor-pooled cryopreserved human hepatocytes, thawing medium (TM), and 0.4% trypan blue were purchased from Lonza (Basel, Switzerland). l-Glutamine, HEPES (2-[4-(2-hydroxyethyl)-1-piperazinyl]ethane-sulfonic acid), and Williams’ Medium E were from Sigma Aldrich. l-Glutamine and HEPES were dissolved in Williams’ Medium E to 2 and 20 mmol/L, respectively, prior to analysis. The supplemented Williams’ Medium E (sWME) was stored at 4°C until incubation. LC-MS grade acetonitrile, water, and formic acid were obtained from Carlo Erba (Cornaredo, Italy).

1.1.3. Hepatocytes Incubation

Incubations were conducted as previously described, with small adjustments [28]. Hepatocytes, thawed at 37°C , were lightly mixed in 50 mL TM in a 50-mL polypropylene conical tube maintained at the same temperature. The tube was centrifuged at 100 g for 5 min and the pellet washed with 50 mL sWME at 37°C . After centrifugation under the same

conditions, cells were resuspended in 2 mL sWME. Hepatocyte viability was evaluated with the trypan blue exclusion test, and sWME volume adjusted to 2×10^6 viable cells/mL. Incubations were prepared in sterile 24-well culture plates with 250 μ L hepatocyte suspension and 250 μ L analyte at 20 μ mol/L in sWME at 37°C. Metabolic reactions were then interrupted with 500 μ L ice-cold acetonitrile. Negative controls, i.e., hepatocytes in sWME without 4-AcO-DiPT and 4-AcO-DiPT in sWME without hepatocytes, were incubated for 3 h under the same conditions. Diclofenac was also incubated under the same conditions to ensure proper metabolic activity.

1.1.4. Sample Preparation

100 μ L hepatocyte supernate was vortexed with 100 μ L acetonitrile, centrifuged at 15,000 g for 10 min at room temperature, and supernates dried under nitrogen at 37°C. Residues were reconstituted with 150 μ L mobile phase A (MPA): mobile phase B (MPB) (8:2 v/v), mixed well, centrifuged for 10 min at 15,000 g at room temperature, and supernates transferred into glass inserts in LC autosampler vials. The sample injection volume was 15 μ L.

1.1.5. Instrumental Conditions

LC-HRMS/MS analyses were performed on a DIONEX UltiMate 3000 liquid chromatograph coupled with a Q-Exactive quadrupole-Orbitrap hybrid high-resolution mass spectrometer with a heated electrospray ionization (HESI) source (Thermo Scientific, Waltham, MA, USA).

1.1.6. Liquid Chromatography

Chromatographic separation occurred on a Kinetex[®] Biphenyl column (150 x 2.1 mm, 2 μ m) (Phenomenex, Castel Maggiore, Italy) maintained at $37 \pm 1^\circ\text{C}$. The 30-min run utilized 0.1% formic acid in water (MPA) and 0.1% formic acid in acetonitrile (MPB) at a 0.4 mL/min flow rate. The gradient was started at 5% MPB for 2 min, increased to 25% MPB by 18 min, increased to 95% MPB within 2 min, and held for 5 min. The return to initial conditions occurred within 0.1 min, followed by a 4.9-min equilibration, for a total run time of 30 min. Autosampler temperature was $10 \pm 1^\circ\text{C}$.

1.1.7. Mass Spectrometry Conditions

Samples were injected twice, once in positive and once in negative ionization mode. HESI source parameters were 50 sheath gas flow rate, 10 auxiliary gas flow rate, ± 3 kV spray voltage, 300°C capillary and auxiliary gas heater temperature, 50 S-lens radio

frequency and sweep gas was not applied. The orbitrap was calibrated prior to analysis, with a lock mass list for better accuracy. Data were acquired from 1 to 25 min in full scan HRMS (FullMS)/data dependent MS/MS (ddMS²) mode. The FullMS acquisition range was m/z 120-700 with a resolution of 70,000 at full width at half maximum (FWHM) at m/z 200. The automatic gain control (AGC) target was 10^6 and maximum injection time (IT) 200 ms. Up to 5 ddMS² scans were triggered, with a dynamic exclusion of 2.0 s and an intensity threshold of 10^4 , for each FullMS scan depending on a priority inclusion list of putative metabolites based on *in silico* predictions and the metabolic fate of 4-AcO-DiPT analogues (Table 3). Other ions not in the inclusion list might also trigger ddMS² scans. Additionally, background m/z values with high intensity were assessed during injection of blank controls and compiled in an exclusion list in positive and negative-ion modes. ddMS² isolation window was $m/z \pm 1.2$ with a resolution of 17,500 and the normalized collision energy (NCE) was 30, 60, and 90 a.u. ddMS² AGC target was 2×10^5 and maximum IT was 64 ms.

1.1.8. Final Metabolite Identification

LC-HRMS data were processed with Thermo Scientific Compound Discoverer (v. 3.1.1.12), using a partially automated approach. Briefly, the ions detected in HRMS were compared to a list of theoretical metabolites (intensity threshold, 5×10^3 ; mass tolerance, 5 ppm). The HRMS/MS spectra and theoretical elemental composition of the ions were compared to online databases (intensity threshold, 10^5 ; HRMS mass tolerance, 5 ppm; HRMS/MS mass tolerance; 10 ppm). The chromatographic peaks detected in controls with a similar or higher intensity than that of the peaks detected in the samples were filtered out.

1.2. Results

1.2.1. *In Silico* Metabolite Predictions

In silico metabolite predictions are reported in Table 3. A total of 47 phase I and II metabolites were predicted, with 10 first-generation metabolites (P 1- P 10) and 37 were second-generation metabolites (P X.1, P X.4, by decreasing score, MX indicating the corresponding first-generation metabolite) (Table 3). First-generation metabolites included hydroxylation, deisopropylation, carboxylation, ester hydrolysis, glucuronidation and deamination. Second-generation metabolites involved phase I (hydroxylation, dealkylation, carboxylation, deisopropylation) and phase II (glucuronidation and sulfation) reactions. All predicted metabolites were incorporated in a ddMS² inclusion list to support LC-HRMS/MS analyses and all predicted metabolic transformations were incorporated in the list of potential reactions to support automatic data mining.

Table 3. Molecular structure, elemental composition, metabolic transformation, and predictive score of in silico predicted 4-AcO-DiPT metabolites.

Predicted Metabolite (M)	Transformation	Elemental composition	Score (%)
P1	<i>N</i> -Hydroxylation	C ₁₈ H ₂₇ N ₂ O ₃	63
P1.1	<i>O</i> -Glucuronidation	C ₂₅ H ₃₀ N ₂ O ₈	30
P1.2	<i>N</i> -Deisopropylation	C ₁₆ H ₂₁ NO ₃	22
P1.3	Hydroxylation	C ₁₉ H ₂₈ NO ₄	22
P1.4	Hydroxylation (C1")	C ₁₈ H ₂₆ N ₀ O ₄	21
P2	Hydroxylation (C2")	C ₁₈ H ₂₆ N ₂ O ₃	63
P2.1	<i>O</i> -Sulfation	C ₁₈ H ₂₄ N ₃ O ₇ S	60
P2.2	<i>O</i> -Glucuronidation	C ₂₄ H ₃₂ N ₂ O ₁₀	39
P 2.3	Dealkylation	C ₁₇ H ₂₄ N ₂ O ₂	21
P 2.4	Hydroxylation (C11)	C ₁₉ H ₂₆ N ₂ O ₄	21
P 2.5	Carboxylation (C9)	C ₁₉ H ₂₄ N ₂ O ₅	21
P3	Deisopropylation	C ₁₅ H ₂₀ N ₂ O ₂	63
P3.1	Hydroxylation (C1")	C ₁₆ H ₂₀ N ₂ O ₃	35
P3.2	Depropylation	C ₁₃ H ₁₄ O ₃	35
P3.3	<i>N</i> -Hydroxylation	C ₁₅ H ₂₀ N ₂ O ₃	35
P3.4	<i>N</i> -Deisopropylation	C ₁₂ H ₁₄ N ₂ O ₂	35
P4	Hydroxylation (acetyl)	C ₁₈ H ₂₆ N ₂ O ₃	34
P4.1	<i>O</i> -Glucuronidation	C ₂₃ H ₃₂ N ₂ O ₉	28
P4.2	<i>O</i> -Sulfation	C ₁₇ H ₂₄ N ₂ O ₆ S	24
P5	Carboxylation (acetyl)	C ₁₉ H ₂₆ N ₂ O ₃	34
P5.1	<i>O</i> -Glucuronidation	C ₂₆ H ₃₆ N ₂ O ₉	31
P5.2	<i>N</i> -Hydroxylation	C ₁₈ H ₂₅ N ₂ O ₅	20
P5.3	Deisopropylation	C ₁₅ H ₁₈ N ₂ O ₄	20
P5.4	Hydroxylation (C1")	C ₁₈ H ₂₄ N ₂ O ₅	20
P6	Ester hydrolysis	C ₁₉ H ₂₆ N ₂ O	34
P6.1	<i>O</i> -Sulfation	C ₁₆ H ₂₄ N ₂ O ₄ S	32
P6.2	<i>O</i> -Glucuronidation	C ₂₂ H ₃₂ N ₂ O ₇	29
P6.3	Hydroxylation (C1")	C ₁₆ H ₂₄ N ₂ O ₂	20
P6.4	<i>N</i> -Hydroxylation	C ₁₆ H ₂₅ N ₂ O ₂	20
P7	Hydroxylation (C2)	C ₁₆ H ₂₄ N ₂ O ₂	25
P8	<i>N</i> -Glucuronidation	C ₁₂ H ₁₃ NO ₃	20
P9	Deamination (to aldehyde)	C ₁₂ H ₁₃ NO ₃	20
P10	Deamination (to alcohol)	C ₁₂ H ₁₁ NO ₃	20

1.2.2. 4-AcO-DiPT Fragmentation Pattern

The 4-AcO-DiPT fragmentation pattern is shown in Figure 2. In positive-ionization mode, ions *m/z* 202.0866 resulted from a loss of the diisopropyl amine group followed by

loss of the acetyl group producing m/z 160.0758, the fragment with the most intense signal. Further fragmentation yielded ions m/z 132.0808 then 115.0539 through carbon monoxide and ammonia losses, respectively. Ion m/z 117.0573 was a radical cation typically yielded by hydroxyindole alkylamines [138]. α - and β -cleavage at the nitrogen of the ethylamine chain yielded fragments m/z 114.1275 and 102.1278, respectively. Fragment m/z 72.0805 was further produced by isopropyl loss from m/z 114.1275. In addition, the fragment m/z 259.1815 on negative ionization mode indicates an acetyl loss on the parent drug.

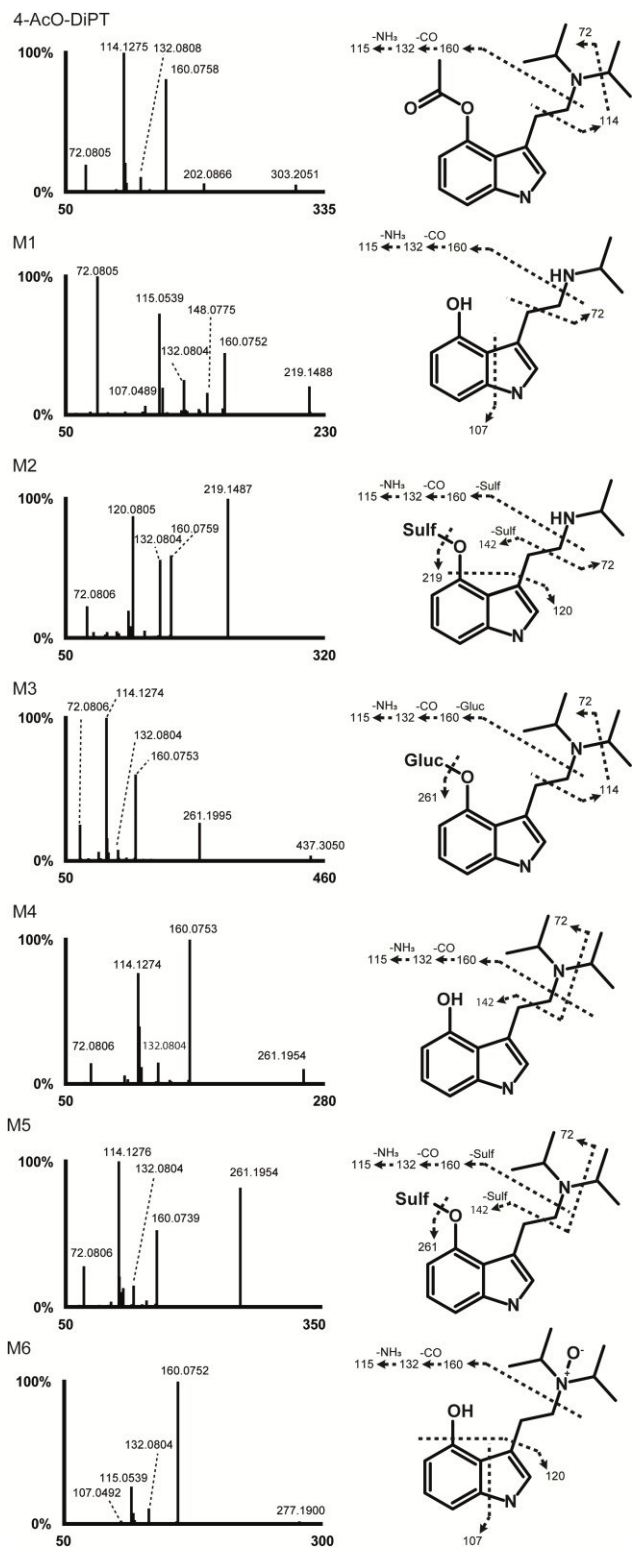


Figure 2. 4-AcO-DiPT high-resolution tandem mass spectrometry spectrum and suggested fragmentation in positive-ionization mode.

1.2.3. Metabolite Identification

LC-HRMS data were automatically processed to produce a list of six potential metabolites that were manually checked by the operators. 4-AcO-DiPT LC-HRMS peak area was 3.00×10^7 in the 3 h incubation with hepatocytes, i.e., 375 times lower than that of the 0 h incubation (1.12×10^{10}). Six metabolites were identified after 3 h incubation following ester hydrolysis, *O*-glucuronidation, *O*-sulfation, *N*-oxidation and *N*-dealkylation. All second-generation metabolites derived from the only first-generation metabolite detected, which was produced by ester hydrolysis (4-OH-DiPT, M4). The metabolites are listed from M1 to M6 by ascending retention time (Table 4). As for the five remaining metabolites, they all derived from M4 with further phase I and II transformations, including *N*-deisopropylation (4-OH-iPT, M1 and 4-OH-iPT-sulfate, M2) and *N*-oxidation at the ethylamine chain (4-OH-DiPT-*N*-oxide, M6), and *O*-sulfation (M2 and 4-OH-DiPT-sulfate, M5) and *O*-glucuronidation (4-OH-DiPT-glucuronidate, M3) in the indole ring. The fragmentation pattern of 4-AcO-DiPT metabolites is shown in Figure 2. The metabolic pathway of the major metabolites is suggested in Figure 3. An extracted-ion chromatogram of 4-AcO-DiPT and metabolites in positive-ionization mode obtained after 3-h incubation with human hepatocytes is presented in Figure 4.

Table 4. Metabolic transformation, retention time (RT), accurate mass of molecular ion (hydrogen adduct in positive-ionization mode [M+H]⁺), elemental composition, deviation from theoretical accurate mass, and liquid chromatography-high-resolution mass spectrometry peak area of 4-AcO-DiPT and metabolites after 3 hours incubation with human hepatocytes (HESI positive mode, HESI negative mode).

ID	Transformation	RT (min)	[M+H] ⁺	Elemental composition	Mass error (ppm)	Peak Areas (HESI +, HESI-)
M1	Ester hydrolysis + <i>N</i> -Deisopropylation	6.31	219.1489	C ₁₃ H ₁₈ N ₂ O	-1.21	1.10 × 10 ⁸
M2	Ester hydrolysis + <i>N</i> -Deisopropylation + <i>O</i> -Sulfation	7.24	299.1057	C ₁₃ H ₁₈ N ₂ O ₄ S	-1.23	3.50 × 10 ⁷ , 5.90 × 10 ⁷
M3	Ester hydrolysis + <i>O</i> -Glucuronidation	8.30	437.2277	C ₂₂ H ₃₂ N ₂ O ₇	-1.45	2.94 × 10 ⁸ , 2.60 × 10 ⁷
M4	Ester hydrolysis	11.82	261.1955	C ₁₆ H ₂₄ N ₂ O	-2.25	4.19 × 10 ⁹
M5	Ester hydrolysis + <i>O</i> -Sulfation	12.11	341.1525	C ₁₆ H ₂₄ N ₂ O ₄ S	-1.42	4.47 × 10 ⁷ , 2.79 × 10 ⁷
M6	Ester hydrolysis + <i>N</i> -Oxidation	12.53	277.1907	C ₁₆ H ₂₄ N ₂ O ₂	-1.35	7.76 × 10 ⁶
Parent	no transformation	15.02	303.2059	C ₁₈ H ₂₆ N ₂ O ₂	-2.67	3.00 × 10 ⁷

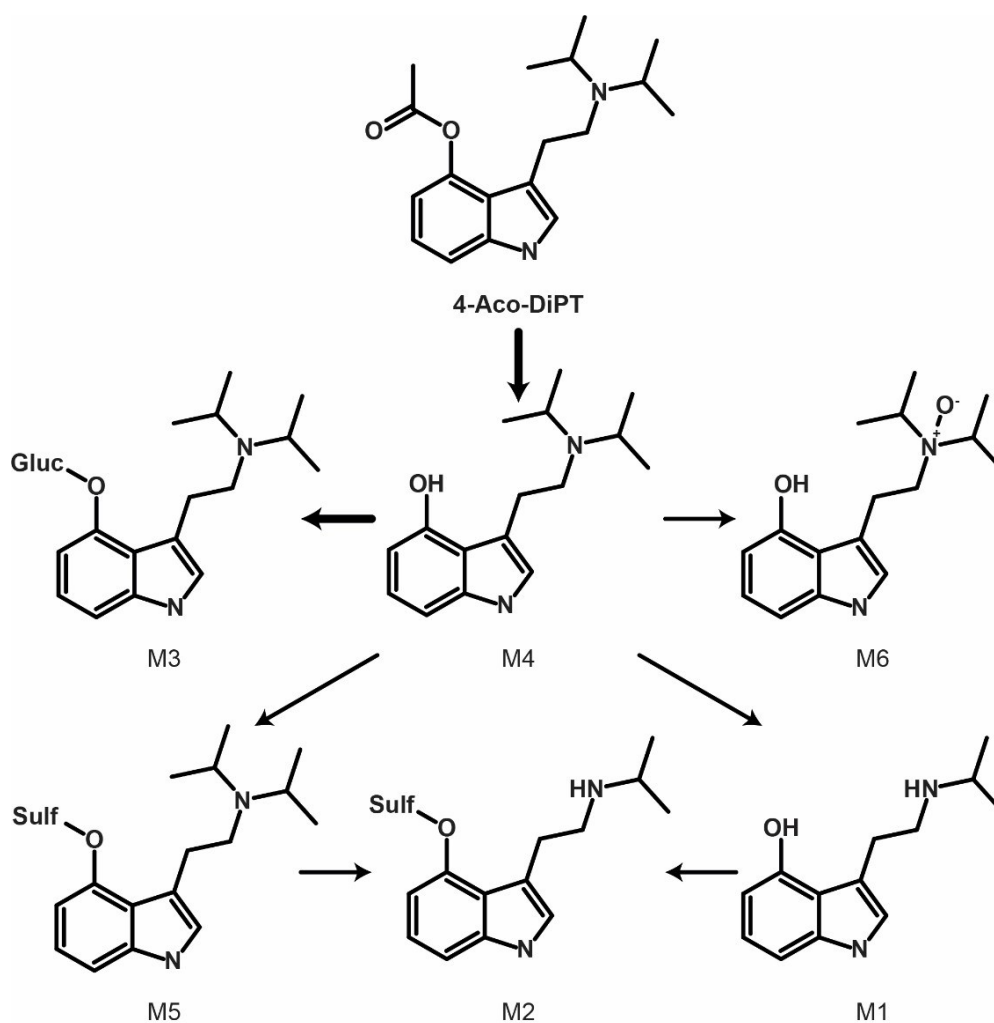


Figure 3. 4-AcO-DiPT suggested metabolic fate. Bold indicates major transformations.

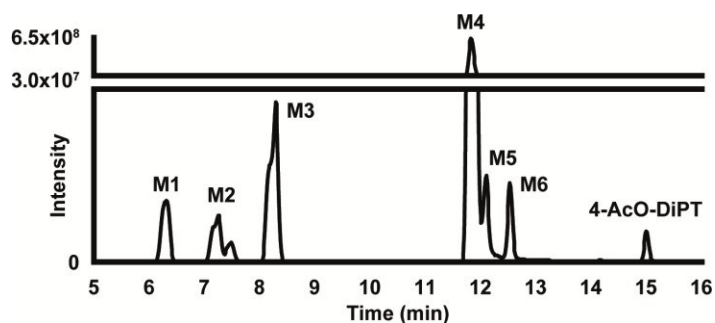


Figure 4. Extracted-ion chromatogram of 4-AcO-DiPT and metabolites in positive-ionization mode obtained after 3-h incubation with human hepatocytes. Mass tolerance, 5 ppm; m/z values, 219.1489, 261.1955, 277.1907, 299.1057, 303.2059, 341.1525, 437.2277.

1.2.3.1. Phase I Metabolites

- Ester Hydrolysis

M4, eluted at 11.82 min, was the metabolite detected with the most intense signal with a base peak at m/z 261.1954. 4-OH-DiPT transformation occurred with the loss of the acetyl group and with hydrolysis occurring in the hydroxyl group of the indole ring, as demonstrated by the production of fragments m/z 160.0753, 114.1274 and 117.0573. The fragments on negative ionization mode m/z 132.0243, 114.1275, 132.0804 and 72.0806 showed that the indole core and the ethylamine chains were intact. The acetyl loss is indicated by the mass shift of +42.0104 Da from parent and a difference of -2C -2H -1O on the elemental composition.

M1, M2, M3, M5 and M6 were produced after ester hydrolysis and other metabolic reactions. M3 was detected as a double peak with the same fragmentation pattern.

- Ester Hydrolysis and *N*-Deisopropylation

M1 eluted at 6.31 min, and was formed after *N*-deisopropylation following ester hydrolysis. Fragment m/z 160.0752 in the MS/MS spectrum clearly identifies that this reaction occurred in the isopropyl group. 4-OH-iPT revealed a mass shift of +84.0570 Da and a difference of elemental composition of -5C -8H - 1O proves this metabolic reaction.

- Ester Hydrolysis and *N*-Oxidation

M6 was detected at 12.53 min and was produced by oxidation on the indole ring after ester hydrolysis. Fragments m/z 160.0752, 107.0492 and 115.0539 showed that this transformation did not occur in the indole ring, but instead in the diisopropyl amine group of the molecule. This metabolite presented a mass shift of + 26.0152 Da and a difference of elemental composition of -2C -2H. 4-OH-DiPT-*N*-oxide retention time was later than that of M4 (4-OH-DiPT), indicating *N*-oxidation [14-16].

1.2.3.2. Phase II Metabolites

- Ester Hydrolysis and *O*-Glucuronidation

M3, detected at 8.20 min, was the second most intense metabolite. This metabolite was formed after ester hydrolysis and glucuronidation. 4-OH-DiPT-glucuronidate presented a mass shift of -134.0218 Da differing in +4C +6H +5O from the elemental composition of the parent drug. The presence of fragments m/z 160.0753, 114.1274 clearly indicates no transformation in the indole core or the ethylamine chain. Actually, the signal that was detected in negative ionization mode suggests that a glucuronidation reaction occurred.

- Ester Hydrolysis and *O*-Sulfation

M5 eluted at 12.11 min, with fragments m/z 160.0752 and 115.0539 indicating no reaction at the indole core or the ethylamine chain. 4-OH-DiPT-sulfate showed a mass shift of -37.9466 Da and a difference of -2C -2H +2O +1S on its elemental composition.

- Ester Hydrolysis, *N*-Deisopropylation and *O*-Sulfation

M2, eluting at 7.24 min, resulted from a ester hydrolysis, *N*-deisopropylation and sulfation (produced by M1 *O*-sulfation). The fragment m/z 120 proves that no changes were made in the indole core. 4-OH-iPT-sulfate had a mass shift of +4.1002 Da and a difference of -5C -8H +2O +1S on its elemental composition. M2 produced fragment m/z 219.1487 by sulfate loss, and similar fragments to those of M1. The fact that a signal was also identified in negative ionization mode, suggests that a sulfation reaction it occurred to generate both metabolites (M2 and M5).

1.3. Discussion

In silico metabolite predictions alone are not sufficient to identify the metabolism of specific drugs; however, compilation of HRMS/MS inclusion and exclusion lists and a list of potential metabolic transformations is key to successful Compound Discoverer processing workflow and helping manual metabolite identification. All 6 metabolites were predicted. The main phase I and II reactions occurred in the hydroxyl group of the indole ring and in the isopropyl group after ester hydrolysis.

4-AcO-DiPT was incubated with human liver hepatocytes proven more suitable for metabolite profiling than human liver microsomes [139]. Hepatocytes are more representative of the physiological liver environment containing both phase I and II drug-metabolizing enzymes, cofactors, and drug transporters [140]. All of these factors allow a better estimation of *in vivo* metabolism.

M4 was the most intense metabolite detected 3 h after incubation with hepatocytes, followed by glucuronidation generating M3. Interestingly, the most intense metabolite (M4), was also detected in the control samples without hepatocytes at 0 and 3 h and at 0 h incubation with hepatocytes but at a much lower intensity than after 3 h incubation, meaning that, although M4 is formed through an enzymatic reaction, it is also spontaneously formed during incubation to a lesser extent. This indicates that M4 formation was overestimated in our experiments. When analyzing authentic samples, digestion (with β -glucuronidase/sulfatase) is preferred to increase the M4 signal. To further understand where the glucuronidation occurred in M3, the 3 h incubations with hepatocytes was re-analyzed after enzymatic hydrolysis with β -glucuronidase, suggesting which part of the molecule was glucuronidated. β -Glucuronidase catalyzes the hydrolysis of *O*-glucuronides and not *N*-glucuronides. Comparing the control sample (same hydrolysis conditions but without β -glucuronidase) to the sample with β -glucuronidase, M3 was not present,

revealing that the reaction occurred at the hydroxyl group of the molecule and not on the amine group.

An additional consideration is that samples were resuspended in a ratio of 80:20 mobile phase (A:B) to guarantee maximum recovery of the analyte. This can explain the double peak detected for M3. Better peak shapes would be obtained if samples were resuspended with a lower percentage of acetonitrile (mobile phase B). To assure that the double peak was not an isomer, another test was made using a ratio of 95:5 mobile phase (A:B) where no double peak was detected.

Since the parent drug is most likely degraded as the acetyl group is eliminated quickly, toxicologists could report 4-OH-DiPT (M4) positive cases as from 4-AcO-DiPT intake. The second most intense metabolite was M3 (4-OH-DiPT-glucuronide) followed by M1 (4-OH-iPT), indicating that glucuronidation and dealkylation are common in this tryptamine's metabolic pathway. Others propose that tryptamines do not have a common metabolic pathway and that metabolism changes depending on the nature and position of their substituents, with demethylation, hydroxylation and dealkylation the most common phase I reactions, followed by glucuronidation or sulfation [99,104,108,123,141–143]. 4-OH-DiPT, 4-OH-iPT and 4-OH-DiPT-N-oxide are proposed as biomarkers of 4-AcO-DiPT consumption, but the rapid enzymatic hydrolysis and lower spontaneous hydrolysis of 4-AcO-DiPT to 4-OH-DiPT might create a problem in discerning 4-AcO-DiPT from 4-OH-DiPT consumption. If the parent drug is present even in low concentrations, the ingested drug would be clear, but there is no available information regarding detection of this drug in authentic samples. These results require *in vivo* confirmation, which is challenging due to the lower prevalence indicated by the small number of 4-AcO-DiPT seizures in recent years.

1.4. Conclusion

For the first time, we characterized the 4-AcO-DiPT metabolic profile in human hepatocytes using *in silico* metabolite predictions, LC-HRMS/MS analysis, and software-assisted data mining. We identified six metabolites through ester hydrolysis followed by *N*-Deisopropylation, *O*-sulfation, *O*-glucuronidation, and/or *N*-Oxidation. We recommend 4-OH-DiPT, 4-OH-iPT, and 4-OH-DiPT-*N*-oxide as metabolite biomarkers of 4-AcO-DiPT consumption in clinical and forensic toxicology. We propose incorporation of HRMS/MS fragmentation patterns in online libraries mzCloud and HighResNPS. These findings underscore the value of experimental data and demonstrate how challenging it is to predict NPS metabolism. Our *in vitro* model offers preliminary findings about 4-AcO-DiPT human metabolism; however, these findings should be verified using samples from authentic positive cases. These data enable analytical toxicologists to identify 4-AcO-DiPT exposure cases.

2. 4-OH-MPT Metabolite Profiling in Human Hepatocyte Incubations

4-hydroxy-N,N-methylpropyltryptamine (4-OH-MPT), also known as meprocin, is a psychedelic tryptamine first identified in seizures in Sweden in October 2018 [144]. 4-OH-MPT is a higher homologue of psilocin, which is internationally controlled under the United Nations 1971 Convention on Psychotropic Substances (Schedule I) [145]. It is therefore regulated in several countries such as the United States under the Controlled Substances Act (Schedule I) and the United Kingdom under the Misuse of Drugs Act 1971 (Class A). Whether *in vitro* or *in vivo*, there are currently no scientific data on 4-OH-MPT pharmacokinetics and pharmacodynamics, potency and efficacy, and active blood concentrations. Users, however, described 4-OH-MPT on drug forums as a hallucinogenic drug inducing visual distortion with exhilarating, calming, and dissociative properties; doses ranged from 8 to 50 mg orally or smoked, similar to DMT or psilocybin, and often taken with cannabis [146]. 4-OH-MPT intake was never reported in the scientific literature or early warning systems.

Due to the lack of specific clinical effects, 4-OH-MPT consumption can be ascertained only through toxicological analyses. However, tryptamines are usually highly potent and active at traces amounts in blood [147] and rapidly metabolized [68], making their detection in biological matrices challenging. In clinical and forensic toxicology, aiming for metabolites is often preferred to preclude sample tampering and increase detection capabilities, as their concentrations is usually higher than that of the parent drug and they can be detected over an extended time course. Detecting specific metabolite biomarkers is therefore critical to document intake. In the present study, 4-OH-MPT human metabolism was assessed to identify optimal metabolite biomarkers of consumption in clinical and forensic cases. The substance was incubated with human hepatocytes, which contain the full range of phase I and II metabolic enzymes and necessary cofactors and transporters to effectively simulate human liver metabolism [137,148–152]. For a comprehensive screening, incubates were analyzed by liquid chromatography-high-resolution tandem mass spectrometry (LC-HRMS/MS) and software-assisted data mining supported by *in silico* metabolite predictions [137].

2.1. Materials and Methods

2.1.1. In Silico Metabolite Prediction

4-OH-MPT putative metabolites were predicted with open-access software GLORYx [143]. A list of metabolites was automatically produced with the “phase I and phase II metabolism” option; metabolites with a prediction score higher than 25% were reprocessed to simulate a second round of metabolic transformations. The score of second-generation metabolites was multiplied by the score of the corresponding first-generation

metabolite to calculate an “adjusted score”, and putative metabolites with an adjusted score higher than 25% were considered.

2.1.2. Chemicals and Reagents

LC-MS grade methanol, acetonitrile, water, and formic acid (FA) were from Carlo Erba (Cornaredo, Italy). 4-OH-MPT and diclofenac reference standards were from Cayman Chemical (Ann Arbor, MI, USA) and Sigma Aldrich (Milan, Italy), respectively. Standards were solubilized in LC-MS grade methanol stock solutions (1 mg/mL) and stored at -20°C until analysis. Ten-donor-pooled cryopreserved human hepatocytes and thawing medium were purchased from Lonza (Basel, Switzerland). Supplemented Williams’ Medium E (sWME) was prepared with 2 mmol/L l-glutamine and 20 mmol/L HEPES (2-[4-(2-hydroxyethyl)-1-piperazinyl]ethanesulfonic acid) in Williams’ Medium E (WME) from Sigma Aldrich, prior to the analysis. β -Glucuronidase (50 units/ μ L) from limpets (*Patella vulgata* L.) was purchased from Sigma Aldrich.

2.1.3. Hepatocyte Incubation

Human hepatocyte incubations were conducted as previously described [137]. Briefly, hepatocytes and thawing medium were warmed at 37°C, the medium was discarded and hepatocytes resuspended in sWME. A volume of 250 μ L 10 μ mol/L 4-OH-MPT in sWME was mixed with 250 μ L 5 x 10⁵ hepatocytes, after evaluating cell viability with the trypan blue exclusion test, in sWME in culture plates, which were then incubated for 0 or 3 h at 37°C. Negative controls including hepatocytes in sWME without 4-OH-MPT, and 4-OH-MPT in sWME without hepatocytes, were also incubated for 0 or 3 h to exclude interferences and non-enzymatic transformations. Diclofenac was also incubated under the same conditions to ensure proper metabolic activity. Reactions were interrupted with 500 μ L ice-cold acetonitrile and samples were centrifuged.

2.1.4. Sample Preparation

The samples were analyzed within 30 min after interrupting metabolic reactions, and stored at -80°C in case of required re-analysis. After centrifugation, 100 μ L supernatant was vortexed with 100 μ L acetonitrile and centrifuged for 10 min at 15,000g, at room temperature. Supernatants were evaporated under a nitrogen stream at 37°C and residues were reconstituted in 150 μ L 0.1% FA in water (mobile phase A):0.1% FA in acetonitrile (mobile phase B) (80:20, v/v). After centrifugation for 10 min at 15,000g, at room temperature, supernatants were transferred into LC autosampler vials, and 15 μ L was injected for LC-HRMS/MS analyses.

2.1.4.1. β -Glucuronidase Hydrolysis

To refine the structure elucidation of specific glucuronides, the 3 h hepatocyte incubate with 4-OH-MPT was re-analyzed after glucuronide hydrolysis. After thawing and centrifugation for 10 min, 15,000g, at room temperature, 100 μ L supernatant was evaporated to approximately 50 μ L under nitrogen at 37°C. The remaining volume was mixed with 50 μ L β -glucuronidase (2,500 units) and incubated for 90 min at 37°C. After hydrolysis, the sample was vortexed with 150 μ L acetonitrile and evaporated to dryness under nitrogen at 37°C. The residue was reconstituted with A:B (80:20, v/v) and centrifuged for 10 min, 15,000g, at room temperature. The supernatant was transferred into an LC autosampler vial with a glass insert, and 15 μ L was injected onto the chromatographic system. A control was prepared with the 3 h hepatocyte incubate with 4-OH-MPT under the same conditions without β -glucuronidase, to ensure that the hydrolysis was enzymatic.

2.1.5. Instrumental Conditions

LC-HRMS/MS analysis was performed with a Dionex UltiMate 3000 chromatographic system coupled with a Thermo Scientific (Waltham, MA, USA) Q Exactive mass spectrometer equipped with a heated electrospray ionization (HESI) source. Each sample was injected once in positive- and once in negative-ionization mode.

2.1.6. Liquid Chromatography

Separation was performed on a Kinetex Biphenyl column (150 x 2.1 mm, 2.6 μ m) from Phenomenex (Castel Maggiore, Italy) with a mobile phase gradient composed of 0.1% FA in water (A) and 0.1% FA in acetonitrile (B) at $37 \pm 1^\circ\text{C}$. LC run time was 20 min with a 0.4 mL/min flow rate. The gradient initiated with 2% B for 2 min; B was linearly increased to 17% at 10 min then 95% at 12 min; B was maintained at 95% for 4 min before returning to 2% at 16.1 min; the column was re-equilibrated for 3.9 min. The temperature of the autosampler was $10 \pm 1^\circ\text{C}$.

2.1.7. Mass Spectrometry Conditions

HESI settings were ramped over multiple injections of 1 μ g/mL 4-OH-MPT in A:B (80:20, v/v) in the LC conditions of the analysis to achieve the most intense 4-OH-MPT LC-HRMS signal. Optimized source parameters were: spray voltage, ± 3.5 kV; sheath gas flow rate, 50 a.u.; auxiliary gas flow rate, 5 a.u.; auxiliary gas temperature, 300°C; capillary temperature, 300°C; S-lens radio frequency level, 50 a.u.

HRMS/MS data were acquired from 1 to 16 min of the gradient using full-scan HRMS (FullMS)/data dependent MS/MS (ddMS2) mode with Xcalibur (v. 4.1.31.9) from Thermo Scientific. FullMS parameters were: mass range, m/z 150–600, resolution, 70,000 (full width at half maximum at m/z 200), automatic gain control (AGC) target, 106; max injection time (IT), 200 ms. ddMS2 parameters were: resolution, 17,500; isolation window, m/z 1.2; normalized collision energy, 30, 75, and 100 a.u.; AGC target, 2×10^5 ; max IT, 64 ms; topN, 5 (pick others if idle); intensity threshold, 104; dynamic exclusion, 2.0 s. An inclusion list compiling potential metabolites based on *in silico* predictions and the metabolic transformations identified in 4-OH-MPT analogues [99,104,124,142,153–157] was employed (Table 6). An exclusion list based on the background noise detected after multiple injections of A:B (80:20, v/v) was also employed. The orbitrap was calibrated prior to analysis and a lock mass list with previously identified background ions (m/z 279.0933, 279.1591, and 391.2843 from 1 to 5 min of the LC gradient) was used throughout the analysis for better accuracy [158].

2.1.8. Final Metabolite Identification

LC-HRMS/MS raw data were mined with Compound Discoverer (v. 3.2.0.421) from Thermo Scientific in a single analysis, as previously described [137]. Briefly, the detected ions were compared to a list of theoretical metabolites generated using combinations of the following transformations: demethylation (C 3H > H, leaving group > arriving group), depropylation (3C 7H > H), desaturation (2H > \emptyset), dihydrodiol formation (\emptyset > 2O 2H), oxidation (\emptyset > O), oxidative deamination to alcohol (2H N > H O), oxidative deamination to ketone (3H N > O), reduction (\emptyset > 2H); acetylation (H > 2C 3H O), glucuronidation (H > 6C 9H 6O), glycine conjugation (H O > 2C 4H N 2O), glutathionylation (\emptyset > 10C 17H 3N 6O S), methylation (H > C 3H), and sulfation (H > H 3O S); the maximum number of dealkylations was 3, the maximum number of phase II reactions was 2, and the maximum number of transformations was 5. LC-HRMS intensity threshold was 5×10^3 and HRMS mass tolerance was 5 ppm. Besides, the HRMS/MS spectra and theoretical elemental composition of the ions were compared to mzCloud (Drugs of Abuse/Illegal Drugs, Endogenous Metabolites, and Natural Products/Medicines libraries), ChemSpider (Cayman Chemical and DrugBank libraries), and HighResNPS online databases. LC-HRMS intensity threshold was 105, HRMS mass tolerance was 5 ppm, and HRMS/MS mass tolerance was 10 ppm. The chromatographic peaks detected in controls with a similar or higher LC-HRMS intensity than that of the peaks detected in the samples were filtered out.

2.2. Results

2.2.1. *In Silico* Metabolite Prediction

Twelve first-generation metabolites (P1–P12 by decreasing score) and 29 second-generation metabolites (PX-1–PX-11 by decreasing adjusted score, PX being the corresponding first-generation metabolite) were predicted with a score higher than 25%; 13 metabolites were redundant. Phase II *O*-sulfation and *O*-glucuronidation at the hydroxyindole core were major transformations; other common reactions included hydroxylation and carboxylation at the propyl chain and further *O*-sulfation or *O*-glucuronidation, *N*-oxidation at the ethylamine side chain, *N*-demethylation, *N*-depropylation, and **O**-methylation at the hydroxyindole core. Predicted metabolites were reported in the LC-HRMS/MS inclusion list, prior to the analysis (Table 6).

Table 6. Inclusion lists for liquid chromatography-high-resolution tandem mass spectrometry analysis of human hepatocyte incubates.

Transformation	Elemental composition	[M+H] ⁺ , <i>m/z</i>	[M-H] ⁻ , <i>m/z</i>	Reference transformation
-	C ₁₄ H ₂₀ N ₂ O	233.1648	231.1503	None (parent)
+3O +S	C ₁₄ H ₂₀ N ₂ O ₄ S	313.1216	311.1071	Sulfation
+6C +8H +6O	C ₂₀ H ₂₈ N ₂ O ₇	409.1969	407.1824	Glucuronidation
+C +2H	C ₁₅ H ₂₂ N ₂ O	247.1805	245.1659	Methylation
+O	C ₁₄ H ₂₀ N ₂ O ₂	249.1598	247.1452	Hydroxylation
-3C -6H	C ₁₁ H ₁₄ N ₂ O	191.1179	189.1033	<i>N</i> -Depropylation
-C -2H	C ₁₃ H ₁₈ N ₂ O	219.1492	217.1346	<i>N</i> -Demethylation
-2H +2O	C ₁₄ H ₁₈ N ₂ O ₃	263.1390	261.1245	Carboxylic acid formation (<i>ω</i> -alkyl)
-4C -9H -N +O	C ₁₀ H ₁₁ NO ₂	178.0863	176.0717	<i>N</i> -Dealkylation to alcohol
-4C -11H -N +O	C ₁₀ H ₉ NO ₂	176.0706	174.0561	<i>N</i> -Dealkylation to aldehyde
-2H	C ₁₄ H ₁₈ N ₂ O	231.1492	229.1346	Dehydrogenation
-2H +O	C ₁₄ H ₁₈ N ₂ O ₂	247.1441	245.1296	Oxidation
+4O +S	C ₁₄ H ₂₀ N ₂ O ₅ S	329.1166	327.1021	Sulfation + Hydroxylation
-3C -6H +3O +S	C ₁₁ H ₁₄ N ₂ O ₄ S	271.0747	269.0602	Sulfation + <i>N</i> -Depropylation
-C -2H +3O +S	C ₁₃ H ₁₈ N ₂ O ₄ S	299.1060	297.0914	Sulfation + <i>N</i> -Demethylation
-2H +5O +S	C ₁₄ H ₁₈ N ₂ O ₆ S	343.0958	341.0813	Sulfation + Carboxylic acid formation (<i>ω</i> -alkyl)
+6C +8H +7O	C ₂₀ H ₂₈ N ₂ O ₈	425.1918	423.1773	Glucuronidation + Hydroxylation
+3C +2H +6O	C ₁₇ H ₂₂ N ₂ O ₇	367.1500	365.1354	Glucuronidation + <i>N</i> -Depropylation
+5C +6H +6O	C ₁₉ H ₂₆ N ₂ O ₇	395.1813	393.1667	Glucuronidation + <i>N</i> -Demethylation
+6C +6H +8O	C ₂₀ H ₂₆ N ₂ O ₉	439.1711	437.1566	Glucuronidation + Carboxylic acid formation (<i>ω</i> -alkyl)
+C +2H +O	C ₁₅ H ₂₂ N ₂ O ₂	263.1754	261.1609	Methylation + Hydroxylation
-2C +4H	C ₁₂ H ₁₆ N ₂ O	205.1336	203.1190	Methylation + <i>N</i> -Depropylation
+C +2O	C ₁₅ H ₂₀ N ₂ O ₃	277.1547	275.1401	Methylation + Carboxylic acid formation (<i>ω</i> -alkyl)

+2O	$C_{14}H_{20}N_2O_3$	265.1547	263.1401	Dihydroxylation
-2C -6H +2O	$C_{12}H_{14}N_2O_3$	235.1077	233.0932	<i>N</i> -Depropylation + <i>N</i> -Carboxylation
-C -2H +O	$C_{13}H_{18}N_2O_2$	235.1441	233.1296	<i>N</i> -Demethylation+ Hydroxylation
+C +2H +4O +S	$C_{15}H_{22}N_2O_5S$	343.1322	341.1177	Sulfation + Methylation + Hydroxylation
+7C +10H +7O	$C_{21}H_{30}N_2O_8$	439.2075	437.1929	Glucuronidation + Methylation + Hydroxylation

2.2.2. 4-OH-MPT Fragmentation Pattern

LC-HRMS/MS analysis employed a ramped collision energy based on 4-OH-MPT fragmentation to generate suitable fragments for metabolite structure elucidation, although optimal collision energy might differ from one metabolite to another. 4-OH-MPT HRMS/MS fragmentation pattern in positive-ionization mode is displayed in Figure 5. The nitrogen atom of the ethylamine side chain was the main site of initial ionization, 4-OH-MPT yielding major fragments m/z 160.0756 ($C_{10}H_{10}NO^+$) and 86.0963 ($C_5H_{12}N^+$) through α - and β -cleavage, respectively, at the ethyl linker. Further m/z 86.0963 β -cleavage at the propyl chain produced fragment m/z 58.0653 ($C_3H_8N^+$). Carbon monoxide loss and subsequent ammonia loss from m/z 160.0756 produced fragments m/z 132.0806 ($C_9H_{10}N^+$) and 115.0541 ($C_9H_7^+$), respectively, as confirmed by pseudo-MS/MS/MS experiments, which is a typical fragmentation pathway of hydroxyindole alkylamines [138]. Fragment m/z 160.0756 also yielded radical cation m/z 117.0572 ($C_8H_7N^{+\bullet}$), another common fragment of hydroxyindole alkylamines [138,159]. 4-OH-MPT did not produce a signal in negative-ionization mode under the present analytical conditions.

2.2.3. Metabolite Identification

After automatic data mining, a list of 237 potential metabolites was manually checked by the operators. 4-OH-MPT LC-HRMS peak area was 1.1×10^9 and 5.1×10^8 in 0-h and 3 h incubates, respectively. Three phase I and 4 phase II metabolites were identified and listed from M1 to M7 by ascending retention time (Figure 5). Phase I transformations were *N*-oxidation (M4 and M7) and *N*-demethylation (M3 and M5) at the ethylamine side chain. Phase II transformations were *O*-glucuronidation (M2 and M4) and sulfation (M5 and M6) at the hydroxyindole core; the LC-HRMS signal of phase II metabolites was approximately three quarters of the total signal of 4-OH-MPT metabolites. The fragmentation pattern of 4-OH-MPT metabolites is reported in Figures 6 (positive ionization) and 7 (negative ionization). 4-OH-MPT metabolic fate is suggested in Figure 8. The elemental composition, retention time, accurate mass of molecular ion, diagnostic HRMS/MS fragments, and LC-HRMS peak area of 4-OH-MPT and metabolites in positive- and negative-ionization mode after 3 h incubation with hepatocytes are reported in Table 7. Deviation from HRMS theoretical masses was low, i.e., -0.73–0.10 ppm in positive-ionization mode and -0.65–0.26 in negative-ionization mode, thanks to customized internal and external orbitrap calibration.

Table 7. Metabolic transformation, elemental composition, retention time, accurate mass of molecular ion, deviation from theoretical accurate mass, diagnostic product ions, and liquid chromatography-high-resolution mass spectrometry peak area of 4-OH-MPT and metabolites in positive- and negative-ionization modes after 3-h Incubation with human hepatocytes. Mass tolerance, 5 ppm.

ID	Transformation	Elemental composition	RT, min	Positive-ionization mode				Negative-ionization mode			
				[M+H] ⁺ , m/z	Mass error, ppm	Diagnostic product ions, m/z	Peak area at T _{3h}	[M-H] ⁻ , m/z	Mass error, ppm	Diagnostic product ions, m/z	Peak area at T _{3h}
M1	+O +2H (indole)	C ₁₄ H ₂₂ N ₂ O ₂	6.60	251.1754	0.10	58, 86, 117, 132, 160	2.2x10 ⁷	249.1608	-0.05	131, 144, 145, 231	1.4x10 ⁶
M2	<i>O</i> -Glucuronidation	C ₂₀ H ₂₈ N ₂ O ₇	7.48	409.1967	-0.58	58, 86, 115, 160, 233	3.1x10 ⁸	407.1822	-0.38	85, 113, 131, 144, 231	8.2x10 ⁷
M3	<i>N</i> -Demethylation	C ₁₃ H ₁₈ N ₂ O	7.96	219.1492	0.05	72, 115, 117, 132, 148, 160	3.0x10 ⁷	ND	ND	ND	ND
M4	<i>O</i> -Glucuronidation + <i>N</i> -Oxidation (alkyl)	C ₂₀ H ₂₈ N ₂ O ₈	8.41	425.1915	-0.73	115, 117, 132, 160, 249	1.6x10 ⁷	423.1774	0.26	85, 113, 131, 158, 187	4.2x10 ⁶
M5	Sulfation (indole) + <i>N</i> -Demethylation	C ₁₃ H ₁₈ N ₂ O ₄ S	8.62	299.1059	-0.35	115, 120, 148, 160, 219	1.6x10 ⁶	297.0915	0.03	80, 131, 144, 158, 217	3.8x10 ⁶
4-OH-MPT	Parent	C₁₄H₂₀N₂O	9.18	233.1648	-0.39	58, 86, 115, 117, 132, 160	5.1x10⁸	ND	ND	ND	ND
M6	Sulfation (indole)	C ₁₄ H ₂₀ N ₂ O ₄ S	9.55	313.1214	-0.72	58, 86, 115, 160,	1.4x10 ⁷	311.1069	-0.65	80, 131, 144, 158,	2.4x10 ⁷

						233			231		
M7	<i>N</i> -Oxidation (alkyl)	C ₁₄ H ₂₀ N ₂ O ₂	10.20	249.1597	-0.22	115, 117, 132, 160	5.2x10 ⁷	ND	ND	ND	ND

Abbreviation: RT, Retention time.

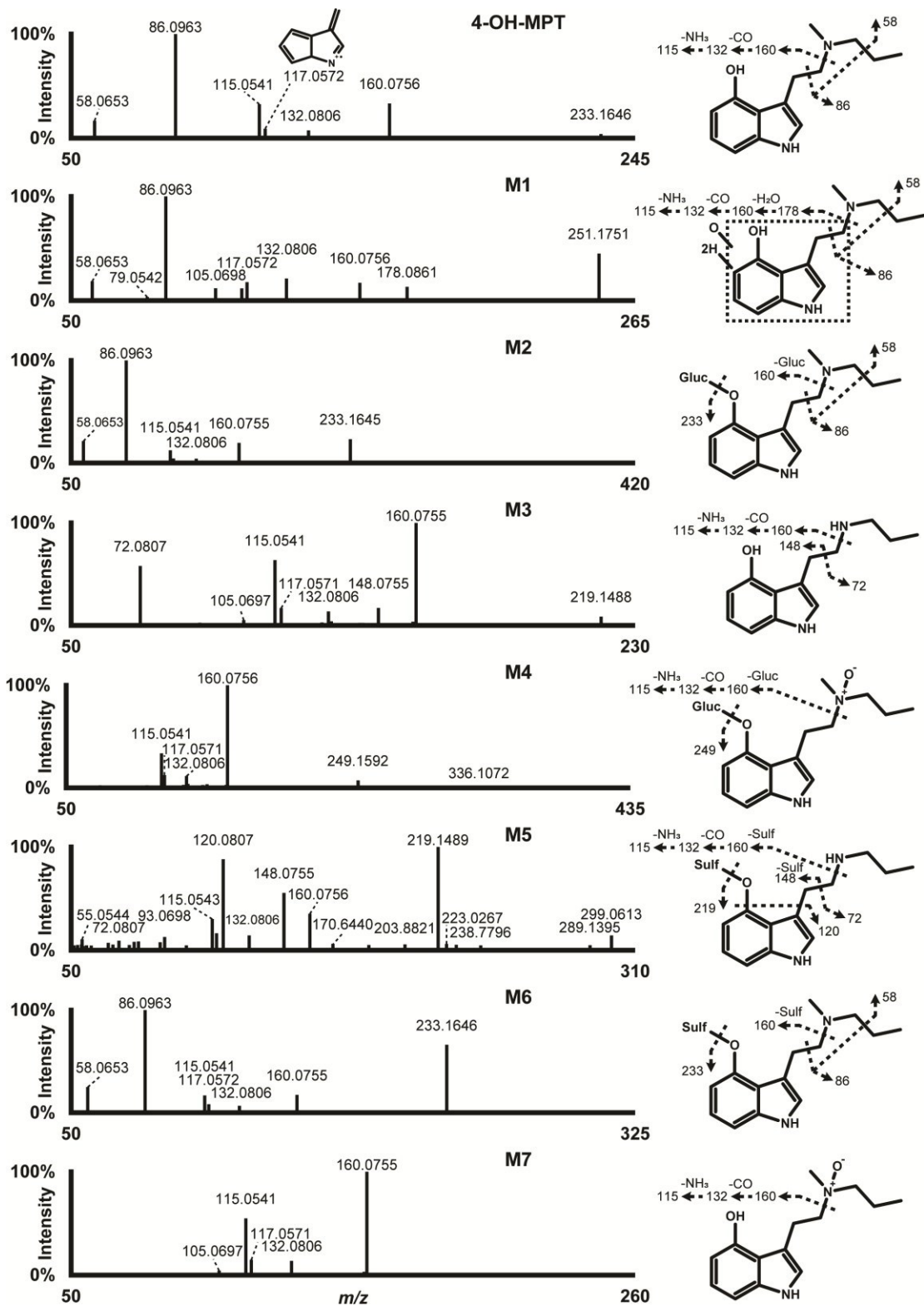


Figure 5. High-resolution tandem mass spectrometry spectrum and suggested fragmentation of 4-OH-MPT and metabolites in positive-ionization mode.

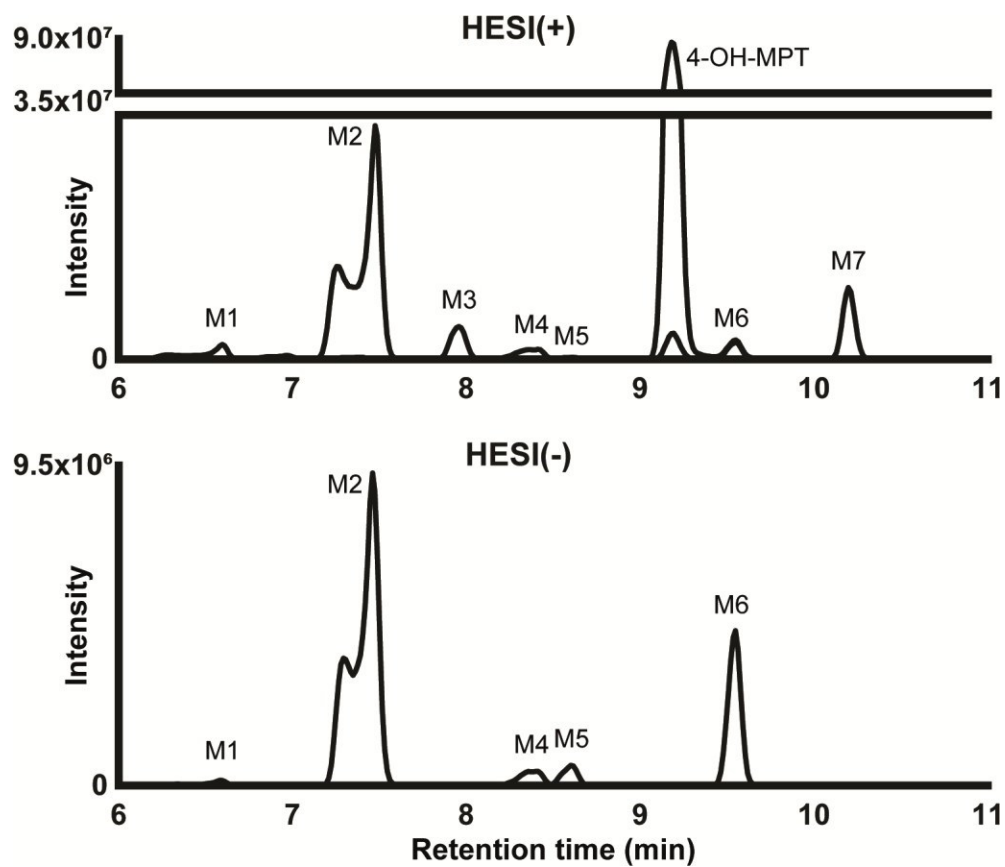


Figure 6. Extracted-ion chromatogram of 4-OH-MPT and metabolites in positive- and negative-ionization modes [HESI(+) and HESI(-), respectively] obtained after 3-h incubation with human hepatocytes. Mass tolerance, 5 ppm.

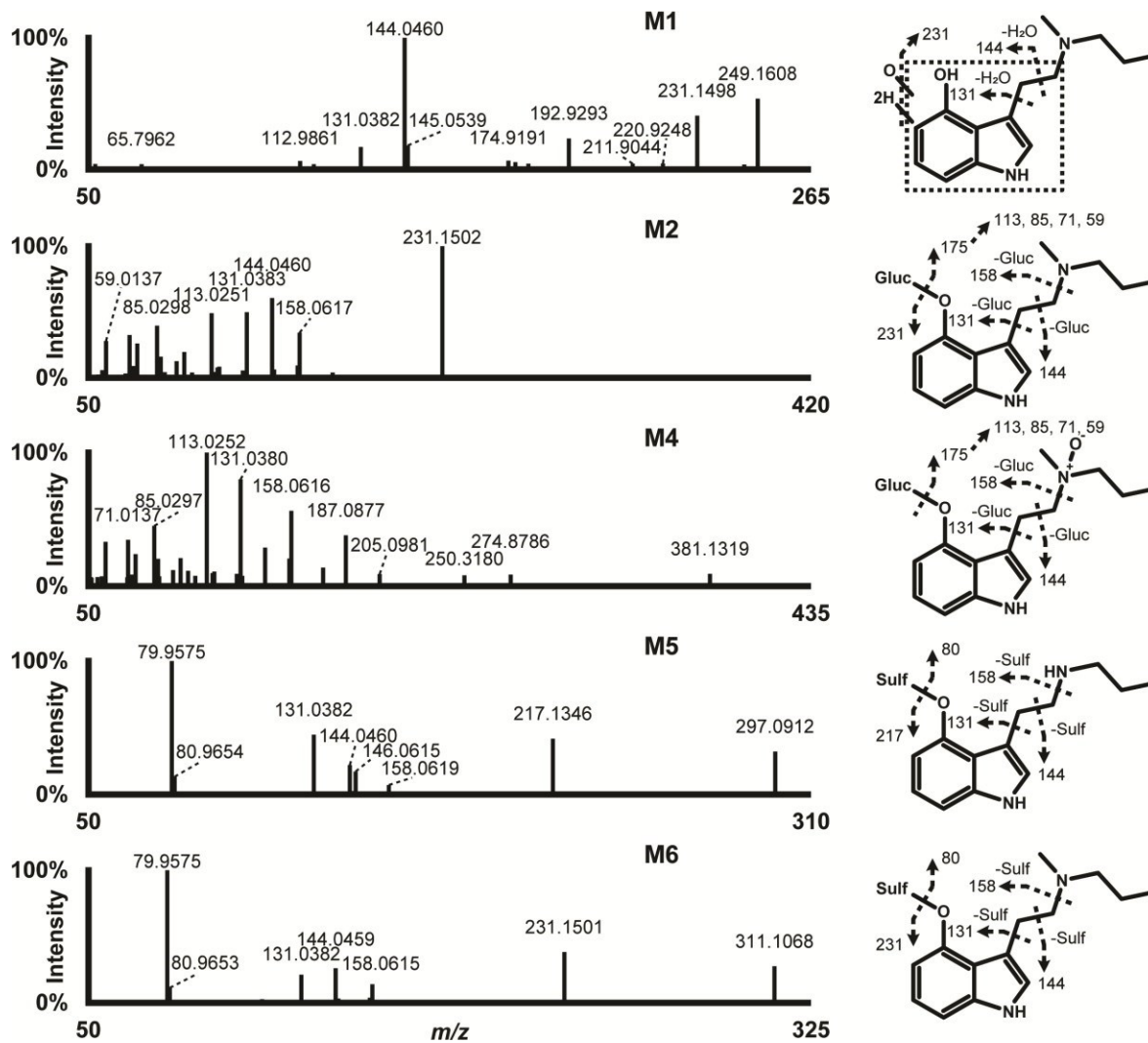


Figure 7. 4-OH-MPT metabolites high-resolution tandem mass spectrometry spectrum and suggested fragmentation in negative-ionization mode.

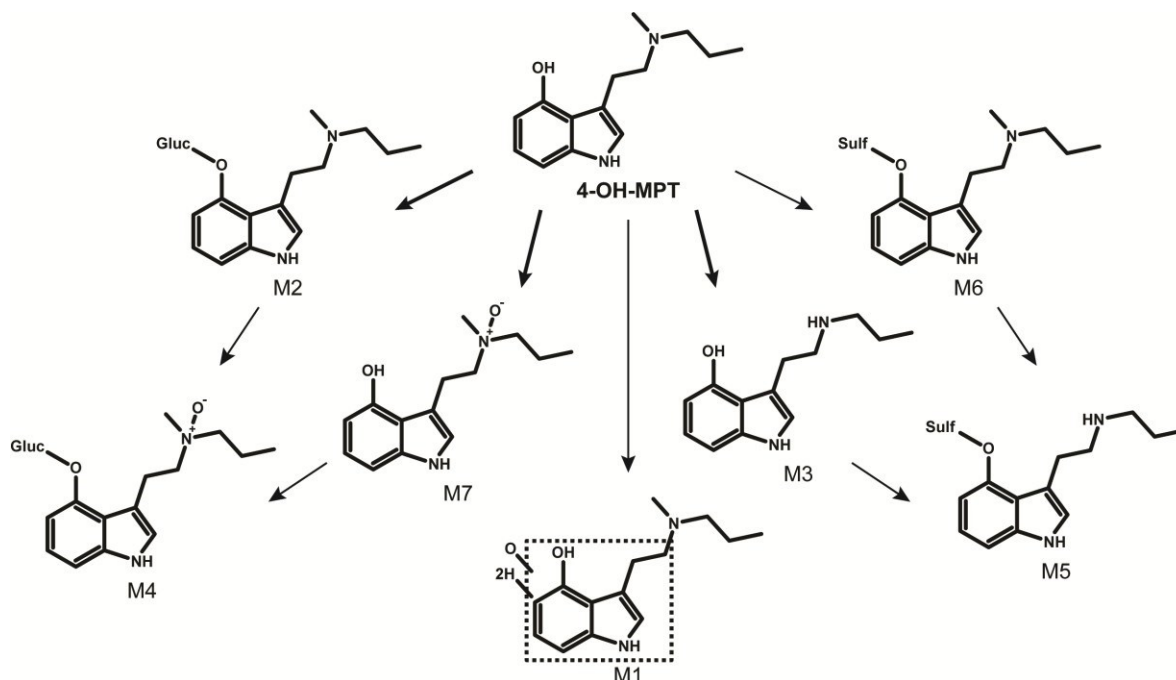


Figure 8. 4-OH-MPT suggested metabolic fate. Gluc, glucuronide; Sulf, sulfate; bold arrow indicates major transformation.

2.2.3.1. *O*-Glucuronidation

M2 was the metabolite with the highest LC-HRMS area, representing approximately 70% of total metabolite signal. M2 eluted at 7.48 min with a molecular ion of m/z 409.1967 in positive-ionization mode (+176.0319 Da mass shift from parent) and yielded characteristic fragment m/z 233.1646 by neutral loss of glucuronide, indicating 4-OH-MPT glucuronidation (+C₆H₈O₆). Fragments m/z 58.0653, 86.0963, 115.0541, 132.0806, and 160.0755, detected with a similar relative intensity after 4-OH-MPT fragmentation, confirmed the transformation. Minor fragment m/z 336.1066 was produced by amine α -cleavage at the ethyl linker, ruling out *N*-glucuronidation at the alkylamine side chain. Moreover, additional hydrolysis experiments showed that M2 was susceptible to β -glucuronidase (complete hydrolysis after 90 min incubation at 37°C), indicating *O*-glucuronidation. Therefore, M2 was formed by 4-OH-MPT *O*-glucuronidation at the hydroxyindole core. Due to the carboxylic acid of the glucuronide, M2 also produced a signal in negative-ionization mode (m/z 407.1822), yielding fragment m/z 231.1502 by glucuronide loss, and fragments m/z 158.0617, 144.0460, and 131.0383 by further fragmentation at the ethyl linker. M2 LC-HRMS trace presented a broad shoulder peak at 7.25 min in positive- and negative-ionization modes, with consistent fragmentation throughout the signal. After re-preparing the samples with a reconstitution mix composed of A:B (98:2, v/v), i.e., identical to the initial gradient conditions, the peak was perfectly resolved without splitting or tailing.

2.2.3.2. Sulfation

M6 molecular mass was m/z 313.1214 after positive ionization (+79.9566 Da mass shift from parent) and produced 4-OH-MPT fragments m/z 58.0653, 86.0963, 115.0541, 117.00572, 132.0806, and 160.0755 with a similar relative intensity, suggesting sulfation (+SO₃). Fragment m/z 233.1646 was produced by sulfate loss and was also detected in HRMS with a higher intensity than that of M6 (2.0×10^7), indicating substantial in-source fragmentation. Consistent with sulfation, M6 produced a high LC-HRMS signal in negative-ionization mode (m/z 311.1069), yielding fragments m/z 79.9575 and 231.1501 by sulfate cleavage, and fragments m/z 158.0615, 144.0459, and 131.0382 by further fragmentation at the ethyl linker. N-sulfation at the alkylamine side chain was excluded due to M6 signal in negative-ionization mode. O-sulfation is a well-known metabolic pathway of hydroxyindole analogues [99,104,124,154,155,160], while the formation of sulfamate indoles was not reported in humans, strongly pointing towards 4-OH-MPT O-sulfation. However, the sulfate position at the hydroxyindole core cannot be ascertained under the present analytical conditions. M6 retention time, i.e., 9.55 min, was delayed compared to that of 4-OH-MPT.

2.2.3.3. N-Oxidation

M7 molecular mass was m/z 249.1597 in positive-ionization mode, representing a +15.9949 Da mass shift from 4-OH-MPT, suggesting oxidation or hydroxylation (+O). 4-OH-MPT fragments m/z 160.0755, 132.0806, 117.0571, and 115.0541 were prominent in the M7 HRMS/MS spectrum, showing that the metabolic reaction did not occur at the hydroxyindole core or the ethyl linker, which was corroborated by the lack of fragments m/z 58.0653 and 86.0963. M7 eluted later than the parent (10.20 min), ruling out aliphatic hydroxylation and indicating N-oxidation, which typically delays retention times in reversed-phase liquid chromatography [150,155,161,162]. M7 was formed through 4-OH-MPT N-oxidation at the alkylamine side chain.

M4 was produced by N-oxidation at the alkylamine side chain and O-glucuronidation at the hydroxyindole core (+O, +C₆H₈O₆) as per the mass shift from 4-OH-MPT (+192.0267 Da); M4 fragmentation after positive and negative ionization, similar to that of M7 (4-OH-MPT N-oxide); and M4 retention time (8.41 min), higher than that of M2 (4-OH-MPT O-glucuronide). Interestingly, M4 LC-HRMS peak presented a shoulder, in positive- and negative-ionization modes, with identical HRMS/MS spectra throughout the signal. This double peak was also observed when using A:B (98:2, v/v) as reconstitution mix during sample preparation, which may indicate the resolution of two diastereoisomers depending on the N-oxide position. In this hypothesis, M7

diastereoisomers were not chromatographically resolved due to the late retention time, during a steeper part of the elution gradient.

2.2.3.4. *N*-Demethylation

M3 was formed by 4-OH-MPT demethylation (-CH₂), as suggested by the -14.0156 Da mass shift from parent. Fragments *m/z* 160.0755, 132.0806, 117.0571, and 115.0541 indicated that the hydroxylindole core and the ethyl linker were not transformed, and fragment *m/z* 72.0807 (*m/z* 86.0963-CH₂) indicated that the demethylation indeed occurred at the alkylamine side chain through N-dealkylation.

M5 was produced by N-demethylation at the alkylamine side chain and sulfation at the hydroxylindole core (-CH₂, +SO₃), as suggested by the mass shift from parent (+65.9411 Da); M5 fragmentation after positive ionization, similar to that of M3 (*N*-demethyl 4-OH-MPT); M5 fragmentation in negative-ionization mode; and M5 retention time (8.62 min), higher than that of M3. M5 underwent substantial in-source fragmentation to *m/z* 219.1492 in positive-ionization mode due to sulfate loss (2.1 x 10⁶).

2.2.3.5. Other

M1 molecular ion was *m/z* 251.1754 in positive-ionization mode, representing a +18.0106 Da mass shift from parent (+O, +2H). M1 might result from the opening of the phenyl ring of the hydroxylindole core at the α carbon of the hydroxyl group, forming a carboxylic acid, as suggested by M1 early retention time (6.60 min) and signal in negative-ionization mode. However, M1 HRMS/MS spectra were not conclusive, and the structure cannot be fully elucidated based on the present analytical conditions. During positive-ionization, fragment *m/z* 178.0861 was produced by β -cleavage at the nitrogen atom of the ethylamine side chain, similar to 4-OH-MPT fragmentation. Further water and carboxylic acid loss might produce fragments *m/z* 160.0756 and 132.0806, respectively, and further ammonia loss from *m/z* 132.0806 produced fragment *m/z* 115.0541. Fragment *m/z* 86.0963, detected in both 4-OH-MPT and M1 HRMS/MS spectra indicated that no reaction occurred at the alkylamine side chain. M1 spectrum in negative-ionization mode was not informative as there was interference by *m/z* 192.9293 and other fragments from trifluoroacetic acid ([2M+Na-2H]⁻, *m/z* 248.9604), a common contaminant that was detected throughout the LC runtime and fragmented along with M1 [158]. Similar to M2, M1 LC-HRMS trace presented a double peak at 6.28 min. Re-preparing the samples with a reconstitution mix composed of mobile phases A:B (98:2, v/v) after evaporation resulted in a single perfectly resolved peak.

2.3. Discussion

Alone, *in silico* metabolite predictions are insufficient to accurately anticipate drug metabolism, and *in vitro* or *in vivo* models are necessary as a first approach. For this purpose, predictions are an interesting tool to optimize LC-HRMS/MS analysis (inclusion and exclusion lists) and help metabolite identification [163]. However, it is important to consider the predictions with a critical eye to avoid skewed interpretation of the sample results. In the present experiments, 6 of 7 metabolites detected after 4-OH-MPT incubation with human hepatocytes were also predicted (Table 7). M2 was predicted with a 84.0% score (P2), M3 with a 43.0% score (P9), and M7 with a 43.0% score (P7). M4 was predicted twice with an adjusted score of 40.0% (P2-8) and 36.1% (P7-2). M6 likely matched P1 (93.0%), and M5 likely matched P1-6 (44.6%) and P9-1 (40.0%). M1 was not predicted. Conversely, 35 predicted metabolites were not detected in 4-OH-MPT hepatocyte incubations.

Phase II transformations at the indole core, especially *O*-glucuronidation and *O*-sulfation, are major pathways of tryptamine metabolism *in vivo*, either by direct glucuronidation or following hydroxylation or *O*-dealkylation, consistent with the present results (M2, M4–6) [99,164,165]. *O*-glucuronide is the main metabolite of psilocin in human urine, through uridine 5'-diphospho-glucuronosyltransferase (UGT) 1A6, 1A7, 1A8, 1A9, and 1A10, and is the main biomarker of Psilocybe mushroom species consumption in clinical and forensic toxicology [165]. *O*-glucuronide and *O*-sulfate are major 5-methoxy-*N,N*-diisopropyltryptamine (5-MeO-DiPT) metabolites after *O*-demethylation and/or indole hydroxylation in human urine [99].

N-demethylation also is a major metabolic pathway of *N*-methyl tryptamines, as observed with 4-OH-MPT (M3 and M5) [156,164]. Remarkably, due to the protective propyl group, no metabolites were produced by alkylamine side chain oxidative deamination in 4-OH-MPT, which is a typical detoxification pathway of *N,N*-dimethyl tryptamines such as DMT, bufotenine (5-OH-DMT), and 5-methoxy-*N,N*-dimethyltryptamine (5-MeO-DMT). These tryptamines are commonly taken along with monoamine oxidase inhibitors to prevent oxidative deamination and effectively induce psychedelic effects (e.g., DMT is taken with harmala alkaloids from Banisteriopsis plant species) [164].

Indole hydroxylation was reported as a minor metabolites of tryptamines *in vivo* [99,156,164,165], but was not detected in 4-OH-MPT metabolism with an intensity higher than the established threshold. *N*-oxidation at the alkylamine side chain also is a common metabolic reaction of tryptamines, as observed with 4-OH-MPT (M4 and M6), their occurrence depending on the amine substituents [104,124,142,156,164,166]. To the best of the authors' knowledge, M1 transformation (+O, +2H) was not reported in the metabolic fate of structural analogues.

We suggest 4-OH-MPT-*N*-oxide (M7) and 4-hydroxy-*N,N*-propyltryptamine (4-OH-PT, M3) as metabolite biomarkers of 4-OH-MPT intake after glucuronide/sulfate hydrolysis in biological samples to improve 4-OH-MPT, M7, and M3 detection. When hydrolysis is not performed, we propose 4-OH-MPT-glucuronide (M2) as an additional biomarker of 4-OH-MPT use. The HRMS/MS spectra of M2, M3, and M7 were provided to online databases mzCloud and HighResNPS, which are openly available to analytical toxicologists to update their drug screenings.

M2 and M7 were not reported as metabolites of structural analogues. However, M3 was a major metabolite of *N,N*-ethylpropyltryptamine (EPT), through *N*-deethylation and hydroxylation, in incubations with human liver S9 fraction, and a minor metabolite in Wistar rat urine following EPT oral administration; M5 might be a major metabolite in S9 fraction only [142]. Additionally, there are currently no data on 4-hydroxy-*N,N*-dipropyltryptamine (4-OH-DPT), 4-acetoxy-*N,N*-dipropyltryptamine (4-AcO-DPT), *N,N*-methylpropyltryptamine (MPT), and 4-acetoxy-*N,N*-methylpropyltryptamine (4-AcO-MPT) metabolism [68], although they can theoretically produce similar metabolites. M3 might be produced by 4-OH-DPT *N*-depropylation and 4-AcO-DPT ester hydrolysis and *N*-depropylation, making M7 crucial to document 4-OH-MPT consumption. 4-OH-MPT and metabolites might be produced by MPT hydroxylation and subsequent reactions, as indole hydroxylation is a common metabolic transformation of tryptamines [104,142,156,165–167]; MPT, however, likely produces other specific metabolites. More importantly, similar to 4-hydroxy-*N,N*-diisopropyltryptamine (4-OH-DiPT) and 4-acetoxy-*N,N*-diisopropyltryptamine (4-AcO-DiPT) [167], 4-AcO-MPT and 4-OH-MPT might produce the same major metabolites, considering the reactivity of the ester bond in 4-AcO-MPT. Therefore, the distinction between 4-OH-MPT and 4-AcO-MPT consumption may be possible only through parent detection in cases of 4-AcO-MPT intake.

Although NPS incubation with human hepatocytes has proved to provide similar results as *in vivo* in humans [137,148–152], the results need to be confirmed with biological samples after 4-OH-MPT intake. Except for a few molecules, clinical studies involving NPS controlled administration are not allowed, and 4-OH-MPT-positive samples can only be obtained through authentic cases of consumption. Unfortunately, we were unable to obtain such samples. This study will help toxicologists identify human cases of 4-OH-MPT intake and generate biological samples to refine the present results.

Another study limitation is the lack of comparison of the metabolites to synthetic reference standards. These standards were not available at the time of writing, as the study provides the first data on 4-OH-MPT metabolism. The present results will help standard manufacturers orientate their synthesis effort to provide suitable standards. Although the structure of all metabolites beside M1 (minor) is unequivocal, considering their fragmentation pattern and the additional hydrolysis experiments, reference standards are critical to quantify the metabolites in biological samples to further understand 4-OH-MPT metabolism.

2.4. Conclusion

The detection of tryptamine metabolites in biological samples is paramount to document consumption. Remarkably, however, tryptamines are structurally similar and often produce the same metabolites, especially when the substitution is located at the alkylamine side chain that is prone to *N*-dealkylation, or at position 4 of the indole core. 4-OH-MPT metabolic fate was consistent with the metabolism of structural analogues in humans: 4-OH-MPT-glucuronide (M2), 4-OH-MPT-*N*-oxide (M7), and 4-OH-PT (M3) were identified as metabolite biomarkers of 4-OH-MPT consumption. However, research on the metabolism of structural analogues, especially 4-OH-DPT, 4-AcO-DPT, MPT, and 4-AcO-MPT, is necessary to evaluate M2, M3, and M7 specificity to identify 4-OH-MPT only. Additionally, the relative abundance of 4-OH-MPT metabolites likely varies with the dose, route of administration, collection time after consumption, and interindividual genetic variations, and further studies in humans are necessary to complete these results. Although 4-OH-MPT was detected in illegal products, there are currently no reports of intoxications involving this tryptamine, possibly due to lack of intake biomarkers. The results were presented during the annual congress of The International Association of Forensic Toxicologists (TIAFT) in Versailles, France, in September 2022.

3. α -MT Metabolite Profiling in Human Hepatocyte Incubations and Urine

α -MT is a synthetic tryptamine available as a white and crystalline powder packaged in vials or capsules or pressed into tablets. It was initially developed in the Soviet Union in the 1960s as an antidepressant due to its monoamine oxidase inhibitor activity, but selling was unsuccessful [56]. Recreational use, however, has gained popularity in the 2000s due to prolonged psychedelic effects such as visual hallucinations and euphoria [60]. However, anxiety and depression are often reported the day after use [168], and high blood pressure, tachycardia, hyper-vigilance, mydriasis, tremor, delayed response time, restlessness, and exaggerated startle reaction can be observed in acute intoxication cases [59,101]. α -MT was involved in several fatalities in the United States, Great Britain, Sweden, Norway, and Japan [169]. Boland et al. reported two α -MT-overdose deaths, with a postmortem peripheral blood concentration of 2.0 $\mu\text{g/mL}$ in one case, and an antemortem serum concentration of 1.5 $\mu\text{g/mL}$ in the other case [61]. Although not scheduled under the United Nations 1971 Convention on Psychotropic Substances, it is controlled in several countries such as the United States since 2003, Germany, Spain, and Austria [56].

Tryptamines induce non-specific effects, and the consumption of specific molecules can only be determined through the analysis of biological samples, such as blood and urine,

in forensic and clinical settings. However, they can also be active at low doses and quickly metabolized, making challenging the drug detection. For these reasons, targeting specific metabolite biomarkers is often preferred to improve detection and prove consumption [164]. α -MT metabolism was studied *in vitro* with rat liver microsomes [170], and *in vivo* with rat urine [170,171]. Incubation with rat liver microsomes produced 3-indolyacetone through oxidative deamination, 6-hydroxy- α -MT, and 6-hydroxy-3-indolyacetone, as identified by paper chromatography and color reactions; further glucuronide conjugates were also detected in rat urine [170]. More recently, Kanamori et al. identified four hydroxy- α -MT metabolites (1'-, 6-, and 7-hydroxy and 2-oxo) in rat urine by gas chromatography-mass spectrometry (GC-MS) after glucuronide/arylsulfate hydrolysis and derivatization; 4-, 5-, 3'-, and *N*-hydroxy- α -MT were not detected [171]. In the two studies, only specific metabolites were targeted, and the detection might not have been suitable due to lack of sensitivity [170] or potential thermosensitivity [171]. More importantly, whether *in vitro* or *in vivo*, there is currently no data on α -MT metabolism in humans.

To identify the most relevant biomarkers of α -MT consumption in clinical and forensic caseworks, we assessed α -MT human metabolism with 1) *in silico* metabolite predictions to assist sample analysis and data mining, 2) *in vitro* incubations with primary human hepatocytes to simulate phase I and phase II metabolism in conditions similar to *in vivo* [139,151,152,172–174], and 3) the analysis of *postmortem* samples from an authentic overdose death to verify the *in vitro* results. Incubates and samples were analyzed by liquid chromatography-high-resolution tandem mass spectrometry (LC-HRMS/MS) in positive- and negative-ionization modes and software-assisted data mining for an all-inclusive screening of α -MT metabolites.

3.1. Materials and Methods

3.1.1. *In Silico* Metabolite Prediction

BioTransformer freeware (v.3.0) was employed to predict α -MT first- and second-generation metabolites in humans [163,175]. The metabolite list was generated using α -MT simplified molecular-input line-entry system (SMILES) string with the “Human and human gut microbial transformation (All human)” option and “combined” CYP450 mode. The accurate mass of predicted metabolites were compiled in an inclusion list for LC-HRMS/MS analysis to prioritize the fragmentation of specific targets. All predicted metabolic reactions and combinations were included in the list of possible transformations for data mining.

3.1.2. Chemicals and Reagents

LC-MS grade methanol, acetonitrile, water, and formic acid (FA) were bought from Carlo Erba (Cornaredo, Italy). LC-MS grade acetic acid and ammonium acetate were acquired by Levanquimica (Bari, Italy). α -MT and diclofenac analytical standards were purchased from Toronto Research Chemicals (North York, Canada) and Sigma Aldrich (Milan, Italy), respectively. Standards were solubilized in LC-MS grade methanol to 1 mg/mL stock solutions and stored at -20°C until analysis. Ten-donor-pooled cryo-preserved human hepatocytes and thawing medium (TM) were obtained from Lonza (Basel, Switzerland). Supplemented Williams' Medium E (sWME) was prepared with 2 mmol/L l-glutamine and 20 mmol/L HEPES (2-[4-(2-hydroxyethyl)-1-piperazinyl]ethanesulfonic acid) in Williams' Medium E from Sigma Aldrich, prior to the analysis. β -Glucuronidase (50 units/ μ L) from limpets (*Patella vulgata* L.) was purchased from Sigma Aldrich.

3.1.3. Hepatocyte Incubations

Incubations were carried out as previously described with a few minor modifications [137]. Hepatocytes were thawed at 37°C and gently mixed with 50 mL TM in a 50 mL polypropylene conical tube at 37°C. After centrifugation at 50g for 5 min, the cells were washed with 50 mL sWME at 37°C then resuspended in 2 mL sWME after centrifugation in the same conditions. Hepatocyte viability was 87%, as evaluated with the trypan blue exclusion test, and sWME volume adjusted to 1.65×10^6 viable cells/mL. In a sterile 24-well culture plate, 200 μ L hepatocyte suspension was gently mixed with 200 μ L α -MT at 20 μ mol/L in sWME, and the plate was immediately incubated at 37°C. Metabolic re-actions were then interrupted with 400 μ L ice-cold acetonitrile after 0 or 3 h incubation. The incubates were centrifuged at 15,000g for 5 min then stored at -80°C. Negative controls, i.e., hepatocytes in sWME without α -MT and α -MT in sWME without hepatocytes, were incubated for 0 or 3 h under the same conditions. Diclofenac was also incubated under the same conditions to ensure proper metabolic activity.

3.1.4. Authentic Samples

Femoral/peripheral blood, cardiac blood, urine, and bile were collected from a fatal case of acute cardiac circulatory collapse secondary to a polydrug intoxication involving α -MT. The subject was a 35-year-old Caucasian male weighing 50 kg and 178 cm tall. Samples were stored at -20°C until analysis and between tests. α -MT concentrations were 4.7 μ g/mL in peripheral and cardiac blood and higher than 5.0 μ g/mL, the upper limit of quantification, in urine and bile. Additionally, in-house toxicology screenings and subsequent confirmation methods by gas or liquid chromatography-tandem mass spectrometry (GC- or LC-MS/MS, respectively) revealed co-exposure to ephedrine,

diazepam, and benzofuran derivative 5-MAPB. 5-MAPB concentrations were 101, 27.4, 4,170, and 1,450 ng/mL in peripheral blood, cardiac blood, urine, and bile, respectively; concentrations of major metabolite 5-APB were 9.33, 5.74, 262, and 43.6 ng/mL, respectively. α -MT metabolite profiling was conducted in peripheral blood and urine, as described below.

3.1.5. Sample Preparation

3.1.5.1. Incubates

After thawing at room temperature and mixing, incubates were centrifuged at 15,000g for 5 min. A volume of 100 μ L supernatant was vortexed with 100 μ L acetonitrile and centrifuged at 15,000g for 10 min. The supernatants were dried under nitrogen at 37°C in conical glass tubes, and the residues were reconstituted with 100 μ L 0.1% FA in water. After centrifugation at 15,000g for 10 min, the supernatants were transferred into glass inserts in LC autosampler vials with a glass insert. Controls were prepared with the samples under the same conditions without β -glucuronidase to rule out non-enzymatic hydrolysis.

3.1.5.2. Urine and Blood

Samples were thawed at room temperature, and 100 μ L blood or 50 μ L urine was mixed with 200, or 100 μ L acetonitrile, respectively, and centrifuged at 15,000g for 10 min. The supernatants were evaporated to dryness under nitrogen at 37°C and the residues were reconstituted with 100 μ L 0.1% FA in water. After centrifugation at 15,000g for 10 min, the supernatants were transferred in autosampler vials with a glass insert.

Additionally, to study phase II metabolites, urine was prepared after glucuronide hydrolysis. A volume of 50 μ L sample was mixed with 50 μ L water, 10 μ L 10 mol/L ammonium acetate, pH 5.0, and 100 μ L β -glucuronidase in conical glass tubes and incubated at 37°C for 90 min. After hydrolysis, the samples were vortexed with 400 μ L ice-cold acetonitrile and dried under nitrogen at 37°C in a conical glass tube. The residues were reconstituted with 100 μ L 0.1% FA in water and centrifuged at 15,000g for 10 min. The supernatants were transferred into LC autosampler vials with a glass insert. Controls were prepared with the samples under the same conditions without β -glucuronidase to rule out non-enzymatic hydrolysis.

3.1.6. Instrumental conditions

LC-HRMS/MS analysis was performed with a Dionex UltiMate 3000 chromatographic system coupled with a Thermo Scientific (Waltham, MA, USA) Q

Exactive mass spectrometer equipped with a heated electrospray ionization (HESI) source. Each sample was injected once in positive- and once in negative-ionization mode (15 μ L).

3.1.7. Liquid Chromatography

Separation was performed with a Kinetex Biphenyl column (150 x 2.1 mm, 2.6 μ m) from Phenomenex (Castel Maggiore, Italy) with a mobile phase gradient composed of 0.1% FA in water (MPA) and 0.1% FA in acetonitrile (MPB) at 37 ± 1 °C. Run time was 21 min with a 0.4 mL/min flow rate. The gradient started with 2% MPB for 2 min; MPB was increased to 15% within 10 min then 95% within 2 min and held for 4 min before returning to initial conditions within 0.1 min; re-equilibration time was 2.9 min. Autosampler temperature was 10 ± 1 °C.

3.1.8. Mass Spectrometry

HESI source parameters were: sheath gas flow rate, 50 u.a.; auxiliary gas flow rate, 10 u.a.; spray voltage, ± 3.5 kV; capillary temperature, 300°C; auxiliary gas heater temperature, 100°C; S-lens radio frequency, 50 u.a.; sweep gas was not applied. The orbitrap was calibrated prior to analysis, and a lock mass list composed of previously identified contaminants was used during injections for better accuracy (phthalates with m/z 279.1591, 301.1410, and 391.2843 in positive-ionization mode, and trifluoro-acetic acid with m/z 248.9604 in negative-ionization mode [158]).

Data were acquired from 1 to 18 min in full scan HRMS (FullMS)/data-dependent MS/MS (ddMS²) mode. The FullMS acquisition range was m/z 150-520 with a resolution of 70,000 at full width at half maximum (FWHM) at m/z 200; the automatic gain control (AGC) target was 10^6 and the maximum injection time (IT) 200 ms. Up to five ddMS² scans were triggered, with a dynamic exclusion of 2.0 s and an intensity threshold of 10^4 , for each FullMS scan depending on a priority inclusion list of putative metabolites based on *in silico* predictions and the metabolic fate of α -MT analogues [62,99,104,124,142,153,154,156,157,170] (Table 8). ddMS² isolation window was m/z 1.2 with a resolution of 17,500 and the normalized collision energy (NCE) was 20, 90, and 110 a.u.; AGC target was 2×10^5 and maximum IT was 64 ms. Additionally, background m/z values with high intensity were assessed during the injection of blank controls and compiled in an exclusion list in positive and negative-ionization modes.

3.1.9. Final metabolite identification

LC-HRMS data were processed with Thermo Scientific Compound Discoverer (v.3.1.1.12), using a partially automated targeted/untargeted approach, as previously described with minor modifications [137]. Briefly, the ions detected in HRMS were

compared to a list of theoretical metabolites based on in silico predictions, the metabolic fate of α -MT analogues, and postulation, and generated using combinations of the following transformations: desaturation ($2H > \emptyset$), dihydrodiol formation ($\emptyset > 2O\ 2H$), ketone formation ($2H > O$), oxidation ($\emptyset > O$), oxidative deamination to alcohol ($2H\ N > H\ O$), oxidative deamination to ketone ($3H\ N > O$), reduction ($\emptyset > 2H$); acetylation ($H > 2C\ 3H\ O$), glucuronidation ($H > 6C\ 9H\ 6O$), glycine conjugation ($H\ O > 2C\ 4H\ N\ 2O$), glutathionylation ($\emptyset > 10C\ 17H\ 3N\ 6O\ S$), methylation ($H > C\ 3H$), and sulfation ($H > H\ 3O\ S$); in-source amine loss, abundant for α -MT, was added to the phase I transformation list ($3H\ N > \emptyset$); the maximum number of dealkylations was 2, the maximum number of phase II reactions was 2, and the maximum number of transformations was 4. LC-HRMS intensity threshold was 5×10^3 and HRMS mass tolerance 5 ppm. The HRMS/MS spectra and theoretical elemental composition of the ions were compared to mzCloud (Drugs of Abuse/Illegal Drugs, Endogenous Metabolites, and Natural Products/Medicines libraries), ChemSpider (Cayman Chemical and DrugBank libraries), and HighResNPS online databases; intensity threshold, 10^5 ; HRMS mass tolerance, 5 ppm; HRMS/MS mass tolerance; 10 ppm. The chromatographic peaks detected in controls with a similar or higher intensity than that of the peaks detected in the samples were disregarded. Molecules with a signal intensity lower than 0.5% of that of the metabolite with the most intense signal were also disregarded.

3.2. Results

3.2.1. In Silico Metabolite Predictions

A total of ten first-generation and 67 second-generation metabolites were predicted. First-generation metabolites were produced by hydroxylation, *N*-oxidation, terminal desaturation, and oxidative deamination, and second-generation metabolites also included desaturation to ketone, ketoreduction, *O*-glucuronidation, and *O*-sulfation; glucuronidation and sulfation were the only phase II reactions. To assist in LC-HRMS/MS analysis, all the predicted metabolites were included in an inclusion list. To support automatic data mining, all predicted metabolic transformations were included in the list of potential reactions.

3.2.2. α -MT Fragmentation Pattern

α -MT main site of ionization was the primary amine of the alkyl side chain in positive-ionization mode, major fragment m/z 158.0964 ($C_{11}H_{12}N^+$) being yielded through α -cleavage (amine loss). Further β -cleavage produced fragments m/z 143.0730 ($C_{10}H_9N^+$) and 130.0651 ($C_9H_8N^+$). Fragments m/z 117.0573 ($C_8H_7N^+$) and 115.0542 ($C_9H_7^+$) were typical of the indole group (Figure 9). Despite the optimization of the ion source settings, α -

MT signal intensity was low compared to that of other tryptamines in similar LC-HRMS conditions [157].

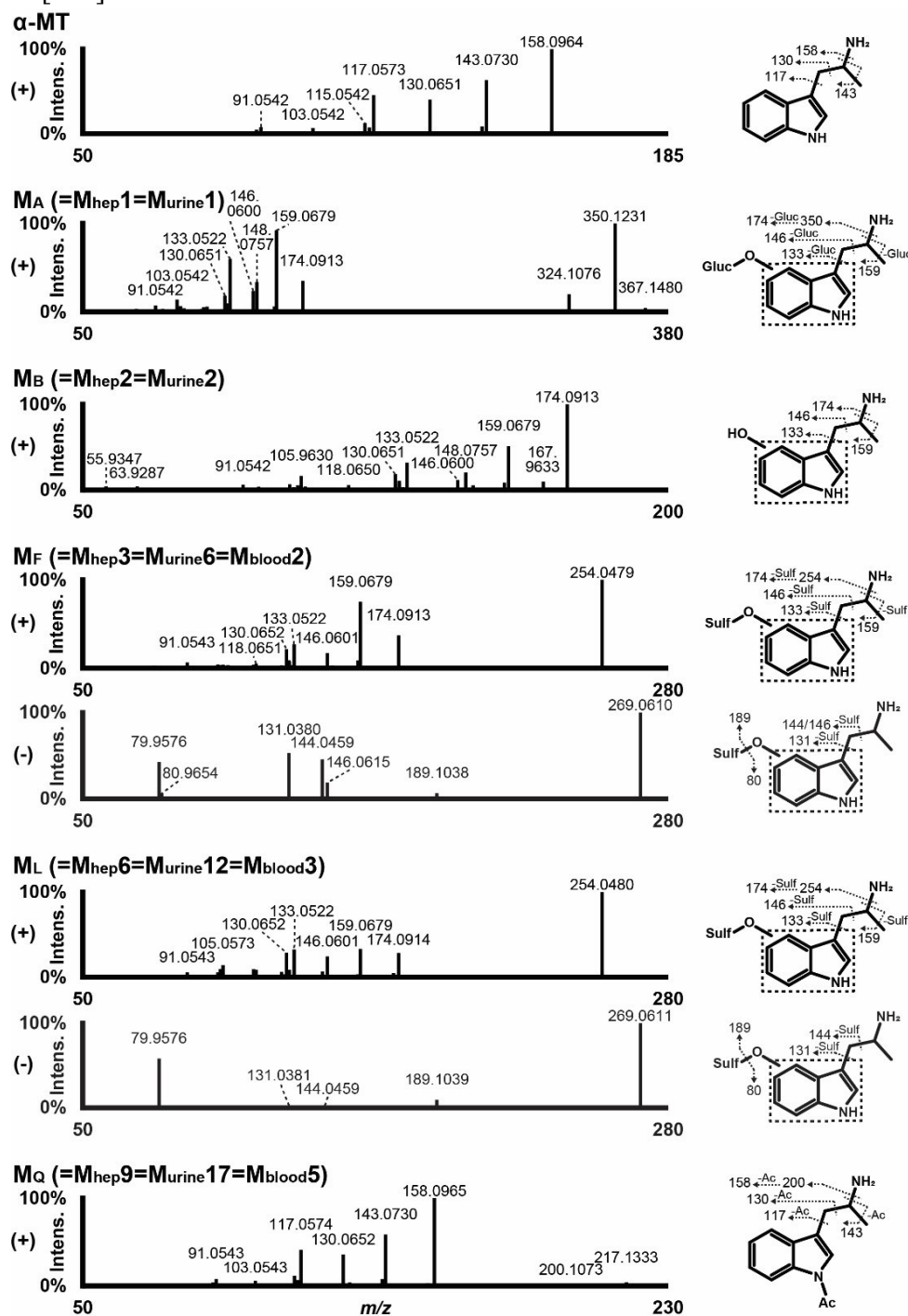


Figure 9. Fragmentation pattern of α -MT and major metabolites in liquid chromatography-high-resolution tandem mass spectrometry. We suggest MA, MF, and ML as biomarkers of α -MT use in non-hydrolyzed urine; α -MT and MB in hydrolyzed urine; and

α -MT, MF, ML, and MQ in blood. (+), positive-ionization mode; (-), negative-ionization mode; Ac, acetyl; Gluc, glucuronide; Sulf, sulfate; dotted box, Markush structure.

This can be partly explained by a considerable in-source amine loss, as m/z 158.0964 intensity was approximately 3.3 times higher than that of parent. α -MT did not produce a signal in negative-ionization mode in the experimental conditions.

3.2.3. α -MT metabolites identification

Diclofenac metabolization to 4'-hydroxydiclofenac and acyl- β -D-glucuronide diclofenac after 3 h incubation as a control alongside α -MT in the same conditions indicated that α -MT *in vitro* metabolism occurred properly. α -MT signal intensity was 6.0×10^7 and 4.5×10^7 in human hepatocyte incubations for 0 and 3 h, respectively. Nine metabolites were identified after 3 h incubation and listed from $M_{\text{hep}1}$ to $M_{\text{hep}9}$ by ascending retention time. Metabolic reactions were hydroxylation ($M_{\text{hep}2}$ and $M_{\text{hep}4}$) and further *O*-sulfation ($M_{\text{hep}3}$ and $M_{\text{hep}6}$) or *O*-glucuronidation ($M_{\text{hep}1}$ and $M_{\text{hep}5}$), *N*-acetylation ($M_{\text{hep}9}$), and combinations ($M_{\text{hep}7}$ and $M_{\text{hep}8}$).

The fragmentation pattern of α -MT major metabolites in positive- and negative-ionization mode (when applicable) is reported in Figure 9. The elemental composition, retention time, accurate mass of molecular ion, and LC-HRMS peak area of α -MT and metabolites in positive- and negative-ionization mode after 3 h incubation with hepatocytes are reported in Table 8.

Table 8. Metabolic transformation, elemental composition, retention time (RT), accurate mass of molecular ion in positive- and negative-ionization modes ($[M+H]^+$ and $[M-H]^-$, respectively) with mass error, and liquid chromatography–high-resolution mass spectrometry peak area of α -MT and metabolites after 3 h incubation with human hepatocytes.

ID	Metabolic transformation	Elemental composition	RT, min	m/z (Δ ppm):	
				$[M+H]^+$	$[M-H]^-$
Peak area					
$[M+H]^+$					
$[M-H]^-$					
$M_{\text{hep}1}$	Hydroxylation (indole) + <i>O</i> -Glucuronidation	$C_{17}H_{22}N_2O_7$	3.06	367.1501 (0.39)	5.2×10^5
				365.1353 (-0.34)	3.6×10^5
$M_{\text{hep}2}$	Hydroxylation (indole)	$C_{11}H_{14}N_2O$	4.65	191.1180 (0.42)	4.5×10^6
				ND	ND
$M_{\text{hep}3}$	Hydroxylation (indole) + <i>O</i> -Sulfation	$C_{11}H_{14}N_2O_4S$	5.40	271.0747 (-0.2)	4.1×10^5
				269.0599 (-0.93)	1.6×10^6
$M_{\text{hep}4}$	Hydroxylation (indole)	$C_{11}H_{14}N_2O$	6.15	191.1180 (0.63)	1.2×10^5
				ND	ND

M_{hep5}	Hydroxylation (indole) + <i>O</i> -Glucuronidation	C ₁₇ H ₂₂ N ₂ O ₇	6.35	367.1502 (0.69) 365.1353 (-0.34)	1.6 × 10 ⁵ 1.3 × 10 ⁵
M_{hep6}	Hydroxylation (indole) + <i>O</i> -Sulfation	C ₁₁ H ₁₄ N ₂ O ₄ S	7.48	271.0748 (0.28) 269.0600 (-0.56)	9.1 × 10 ⁵ 3.1 × 10 ⁶
α-MT (Parent)	No transformation	C ₁₁ H ₁₄ N ₂	9.12	175.1231 (0.54) ND	4.5 × 10 ⁷ ND
M_{hep7}	Hydroxylation (indole) + <i>O</i> -Sulfation + <i>N</i> -Acetylation (indole)	C ₁₃ H ₁₆ N ₂ O ₅ S	9.48	313.0854 (0.58) 311.0707 (-0.05)	1.2 × 10 ⁵ 6.7 × 10 ⁵
M_{hep8}	Hydroxylation (indole) + <i>O</i> -Glucuronidation + <i>N</i> -Acetylation (indole)	C ₁₉ H ₂₄ N ₂ O ₈	9.62	409.1609 (0.85) 407.1460 (0.02)	2.9 × 10 ⁵ 5.2 × 10 ⁵
M_{hep9}	<i>N</i> -Acetylation (indole)	C ₁₃ H ₁₆ N ₂ O	14.07	217.1336 (0.46) ND	2.7 × 10 ⁶ ND

3.2.4. α-MT Hydroxylation and Further *O*-Sulfation or *O*-Glucuronidation

M_{hep2} and M_{hep4} eluted at 4.65 and 6.15 min of the LC run time, respectively, with a +15.9949 Da mass shift from parent, indicating oxidation (+O). Both molecules presented a fragmentation pattern similar to that of α-MT in positive-ionization mode, fragments *m/z* 174.0913, 159.0679, 146.0600, and 133.0522 carrying the metabolic transformation (*m/z* 158.0964, 148.0730, 130.0651, and 117.0573, respectively, from parent +O) and indicating an hydroxylation at the indole core. The exact position of the hydroxyl group at M_{hep2} and M_{hep4} indole core cannot be ascertained in the present analytical conditions. M_{hep2} and M_{hep4} were fragmented along with *m/z* 190.9795 and other minor ions detected during the whole LC separation, producing interferences such as *m/z* 105.9630, 149.9527, and 167.9633.

M_{hep3} and M_{hep6} eluted at 5.40 and 7.48 min of the chromatographic gradient, respectively, with a +95.9516 Da mass shift from parent, indicating oxidation (+O) and sulfation (+SO₃). Interestingly, sulfation delayed retention times when compared to M_{hep2} and M_{hep4}, as observed previously with other tryptamines in similar LC conditions [176]. In positive-ionization mode, amine loss (*m/z* 254.0480) and fragments *m/z* 174.0914, 159.0679, 146.0601, and 133.0522, also observed in hydroxy-α-MT metabolites, pointed towards *O*-sulfation at the indole core. M_{hep3} and M_{hep6} also produced a more intense signal in negative-ionization mode due to the sulfate proneness to form an anion. After negative ionization, sulfate cleavage produced fragments *m/z* 79.9576 and 189.1039, and fragments *m/z* 144.0459 and 131.0381 confirmed that the metabolic reactions occurred at the indole core.

M_{hep1} and M_{hep5} eluted at 3.06 and 6.35 min, respectively, with a +192.0270 Da mass shift from α-MT, indicating oxidation (+O) and glucuronidation (+C₆H₈O₆). In

positive-ionization mode, amine loss (m/z 350.1231) and fragments m/z 174.0913, 159.0679, 146.0600, and 133.0522 pointed towards O-glucuronidation at the indole core in both molecules.

3.2.5. α -MT *N*-Acetylation and Combinations

$M_{\text{hep}9}$ was highly retained and eluted at 14.07 min of the LC gradient with a +42.0105 Da mass shift from α -MT, indicating *N*-acetylation (+C₂H₂O). $M_{\text{hep}9}$ fragmentation pattern after positive ionization contained ion m/z 200.1073 through amine loss, indicating that the reaction did not occur at the primary amine of the molecule but rather at the secondary amine of the indole core; fragments m/z 158.0965, 143.0730, 130.0652, and 117.0574 were also detected in α -MT HRMS/MS spectrum.

$M_{\text{hep}7}$ and $M_{\text{hep}8}$ eluted at 9.48 and 9.62 min, respectively. Based on $M_{\text{hep}7}$ retention time and HRMS/MS in positive- and negative-ionization modes, it was produced by hydroxylation (+O) and subsequent *O*-sulfation (+SO₃) and *N*-acetylation (+C₂H₂O) at the indole core. Similarly, $M_{\text{hep}8}$ was the result of hydroxylation (+O) and subsequent *O*-glucuronidation (+C₆H₈O₆) and *N*-acetylation (+C₂H₂O) at the indole core.

3.2.6. α -MT Metabolites in *Postmortem* Urine

Seventeen metabolites were identified in urine and listed from $M_{\text{urine}1}$ to $M_{\text{urine}17}$ by ascending retention time. α -MT signal was 10 times higher than that of the metabolite with the most intense signal ($M_{\text{urine}6}$). All the metabolites identified after 3 h incubation with human hepatocytes were detected in urine: $M_{\text{hep}1}=M_{\text{urine}1}$, $M_{\text{hep}2}=M_{\text{urine}2}$, $M_{\text{hep}3}=M_{\text{urine}6}$, $M_{\text{hep}4}=M_{\text{urine}8}$, $M_{\text{hep}5}=M_{\text{urine}9}$, $M_{\text{hep}6}=M_{\text{urine}12}$, $M_{\text{hep}7}=M_{\text{urine}13}$, $M_{\text{hep}8}=M_{\text{urine}14}$, and $M_{\text{hep}9}=M_{\text{urine}17}$. Eight additional metabolites were identified with hydroxylation and further *O*-sulfation ($M_{\text{urine}5}$) or *O*-glucuronidation ($M_{\text{urine}3}$, $M_{\text{urine}4}$, and $M_{\text{urine}7}$), *N*-glucuronidation ($M_{\text{urine}10}$, $M_{\text{urine}11}$, and $M_{\text{urine}15}$), and combination ($M_{\text{urine}16}$). Beside $M_{\text{urine}7}$, whose signal was approximately reduced of a factor 10, none of the *O*-glucuronides ($M_{\text{urine}1}$, $M_{\text{urine}3}$, $M_{\text{urine}4}$, $M_{\text{urine}9}$, and $M_{\text{urine}14}$) were detected after hydrolysis. In contrast, the signal of hydroxy- α -MT metabolites $M_{\text{urine}2}$ and $M_{\text{urine}8}$ increased 34 and 25 times, respectively. Considering their structure, the metabolites identified in *postmortem* samples could not be produced by the other substances detected during toxicology analyses, including the benzofuran derivative 5-MAPB.

The fragmentation pattern of α -MT major metabolites in positive- and negative-ionization mode (when applicable) is reported in Figure 9. The elemental composition, retention time, accurate mass of molecular ion, and LC-HRMS peak area of α -MT and metabolites in positive- and negative-ionization mode in urine with and without hydrolysis in Table 9.

Table 9. Metabolic transformation, elemental composition, retention time (RT), accurate mass of molecular ion in positive- and negative-ionization modes ($[M+H]^+$ and $[M-H]^-$, respectively) with mass error, and liquid chromatography–high-resolution mass spectrometry peak area of α -MT and metabolites in postmortem urine with and without enzymatic hydrolysis with β -glucuronidase.

ID	Metabolic transformation	Elemental composition	RT, min	m/z (Δ ppm): [M+H] ⁺ [M-H] ⁻	Peak area	
					[M+H] ⁺	[M-H] ⁻
					Non-hydrolyzed	Hydrolyzed
M_{urine1}	Hydroxylation (indole) + <i>O</i> -Glucuronidation	C ₁₇ H ₂₂ N ₂ O ₇	2.86	367.1500 (0.06) 365.1357 (0.75)	2.4 × 10 ⁸ 4.5 × 10 ⁷	ND
M_{urine2}	Hydroxylation (indole)	C ₁₁ H ₁₄ N ₂ O	4.62	191.1179 (0.05) ND	2.5 × 10 ⁶ ND	8.4 × 10 ⁷ ND
M_{urine3}	Hydroxylation (indole) + <i>O</i> -Glucuronidation	C ₁₇ H ₂₂ N ₂ O ₇	4.81	367.1499 (-0.21) ND	2.7 × 10 ⁶ ND	ND
M_{urine4}	Hydroxylation (indole) + <i>O</i> -Glucuronidation	C ₁₇ H ₂₂ N ₂ O ₇	4.88	367.1498 (-0.48) ND	2.1 × 10 ⁶ ND	ND
M_{urine5}	Hydroxylation (indole) + <i>O</i> -Sulfation	C ₁₁ H ₁₄ N ₂ O ₄ S	5.08	271.0746 (-0.38) 269.0604 (1.00)	4.4 × 10 ⁷ 9.7 × 10 ⁷	3.9 × 10 ⁷ 1.1 × 10 ⁸
M_{urine6}	Hydroxylation (indole) + <i>O</i> -Sulfation	C ₁₁ H ₁₄ N ₂ O ₄ S	5.36	271.0746 (-0.38) 269.0604 (0.92)	3.4 × 10 ⁸ 5.3 × 10 ⁸	3.8 × 10 ⁸ 5.6 × 10 ⁸
M_{urine7}	Hydroxylation (indole) + <i>O</i> -Glucuronidation	C ₁₇ H ₂₂ N ₂ O ₇	5.98	367.1502 (0.60) 365.1361 (1.80)	1.2 × 10 ⁷ 5.2 × 10 ⁶	2.6 × 10 ⁶ 1.0 × 10 ⁶
M_{urine8}	Hydroxylation (indole)	C ₁₁ H ₁₄ N ₂ O	6.11	191.1181 (1.10) ND	8.5 × 10 ⁵ ND	2.1 × 10 ⁷ ND
M_{urine9}	Hydroxylation (indole) + <i>O</i> -Glucuronidation	C ₁₇ H ₂₂ N ₂ O ₇	6.28	367.1501 (0.33) 365.1357	3.4 × 10 ⁷ 1.0 × 10 ⁷	ND

(-0.75)						
M_{urine10}	<i>N</i> -Glucuronidation (indole)	C ₁₇ H ₂₂ N ₂ O ₆	7.06	351.1548 (-0.75) 349.1409 (1.03)	5.2 × 10 ⁶ 1.6 × 10 ⁶	5.2 × 10 ⁶ 1.6 × 10 ⁶
M_{urine11}	<i>N</i> -Glucuronidation (indole)	C ₁₇ H ₂₂ N ₂ O ₆	7.15	351.1550 (-0.18) 349.1412 (1.20)	6.6 × 10 ⁶ 2.0 × 10 ⁶	7.1 × 10 ⁶ 1.9 × 10 ⁶
M_{urine12}	Hydroxylation (indole) + <i>O</i> -Sulfation	C ₁₁ H ₁₄ N ₂ O ₄ S	7.44	271.0747 (-0.02) 269.0605 (1.29)	8.5 × 10 ⁷ 2.3 × 10 ⁸	8.0 × 10 ⁷ 2.3 × 10 ⁸
α-MT (Parent)	No transformation	C ₁₁ H ₁₄ N ₂	8.56	175.1231 (-0.02) ND	3.5 × 10 ⁹ ND	3.6 × 10 ⁹ ND
M_{urine13}	Hydroxylation (indole) + <i>O</i> -Sulfation + <i>N</i> -Acetylation (indole)	C ₁₃ H ₁₆ N ₂ O ₅ S	9.60	313.0853 (0.71) 311.0711 (1.24)	1.8 × 10 ⁷ 1.0 × 10 ⁸	1.6 × 10 ⁷ 9.3 × 10 ⁷
M_{urine14}	Hydroxylation (indole) + <i>O</i> -Glucuronidation + <i>N</i> -Acetylation (indole)	C ₁₉ H ₂₄ N ₂ O ₈	9.61	409.1609 (0.88) 407.1464 (1.00)	4.2 × 10 ⁶ 4.0 × 10 ⁶	ND
M_{urine15}	<i>N</i> -Glucuronidation (alkyl)	C ₁₇ H ₂₂ N ₂ O ₆	10.55	351.1551 (0.16) 349.1412 (1.46)	1.5 × 10 ⁷ 7.3 × 10 ⁶	1.5 × 10 ⁷ 9.0 × 10 ⁶
M_{urine16}	<i>N</i> -Acetylation (indole) + <i>N</i> -Glucuronidation	C ₁₉ H ₂₄ N ₂ O ₇	12.98	393.1661 (1.15) 391.1517 (1.68)	3.0 × 10 ⁷ 4.4 × 10 ⁷	3.2 × 10 ⁷ 4.4 × 10 ⁷
M_{urine17}	<i>N</i> -Acetylation (indole)	C ₁₃ H ₁₆ N ₂ O	14.08	217.1336 (0.28) ND	5.8 × 10 ⁶ ND	5.8 × 10 ⁶ ND

3.2.7. α-MT Hydroxylation and *O*-Sulfation or *O*-Glucuronidation

M_{urine1} (M_{hep1}) and M_{urine9} (M_{hep5}) susceptibility to β-glucuronidase hydrolysis confirmed the formation of *O*-glucuronides.

M_{urine3}, M_{urine4}, and M_{urine7} eluted at 4.81, 4.88, and 5.98 min of the LC gradient, respectively, with a +192.0268 Da mass shift from α-MT, indicating oxidation (+O) and glucuronidation (+C₆H₈O₆); M_{urine3} and M_{urine4} partially coeluted. M_{urine3}, M_{urine4}, and

M_{urine7} fragmentation pattern was similar to that of previously identified *O*-glucuronides, with fragments *m/z* 350.1239, 174.0914, 159.0678, 146.0599, and 133.0522 in positive-ionization modes, indicating *O*-glucuronidation at the indole core. In M_{urine3} and M_{urine4}, fragment relative intensity differed from that of previously identified *O*-glucuronides, the amine loss (*m/z* 350.1239) being substantially less intense.

M_{urine5} eluted at 5.08 min, with a +95.9515 Da mass shift from α -MT and a fragmentation pattern similar to that of previously identified *O*-sulfates in positive- and negative-ionization modes, indicating *O*-sulfation at the indole core (+O +SO₃).

3.2.8. α -MT *N*-Glucuronidation and Combination

M_{urine10} and M_{urine11} partially co-eluted at 7.06 and 7.15 min of the LC gradient, respectively, with a +176.0317 Da mass shift from α -MT, indicating *N*-glucuronidation (+C₆H₈O₆). In positive-ionization mode, M_{urine10} and M_{urine11} produced fragment *m/z* 334.1281 through amine loss and fragments *m/z* 158.0964, 143.0730, 130.0651, and 117.0573, also observed in parent, indicating *N*-glucuronidation at the indole core. M_{urine10} and M_{urine11} were not affected by the enzymatic hydrolysis, which indeed catalyzes the breakdown of *O*-glucuronides.

M_{urine15} eluted much later, at 10.55 min of the gradient, also with a +176.0320 Da mass shift from parent, indicating *N*-glucuronidation (+C₆H₈O₆). However, in addition to fragments *m/z* 158.0965, 143.0730, 130.0651, and 117.0573, also observed in α -MT, fragment *m/z* 220.0814, produced by β -cleavage at the amine of the alkyl side chain, carried the transformation and indicated *N*-glucuronidation at the alkyl side chain. Fragment *m/z* 334.1281 was not detected confirming the position of the transformation. M_{urine15} was not affected by the enzymatic hydrolysis.

Considering M_{urine16} retention time (12.98 min), and HRMS/MS in positive-ionization mode, it was produced by *N*-glucuronidation (+C₆H₈O₆) and *N*-acetylation (+C₂H₂O) at the indole core.

3.3. α -MT Metabolites in *Postmortem* Blood

Five metabolites were identified in blood and listed from M_{blood1} to M_{blood5} by ascending retention time. α -MT signal was 10 times higher than that of the metabolite with the most intense signal (M_{blood2}). All the metabolites identified in urine were detected in blood: M_{blood1}=M_{urine5}, M_{blood2}=M_{urine6}, M_{blood3}=M_{urine12}, M_{blood4}=M_{urine13}, and M_{blood5}=M_{urine17}.

The fragmentation pattern of α -MT major metabolites in positive- and negative-ionization mode (when applicable) is reported in Figure 9. The elemental composition, retention time, accurate mass of molecular ion, and LC-HRMS peak area of α -MT and metabolites in positive- and negative-ionization mode in blood in Table 10.

Table 10. Metabolic transformation, elemental composition, retention time (RT), accurate mass of molecular ion in positive- and negative-ionization modes ($[M+H]^+$ and $[M-H]^-$, respectively) with mass error, and liquid chromatography–high-resolution mass spectrometry peak area of α -MT and metabolites in postmortem blood.

ID	Metabolic transformation	Elemental composition	RT, min	m/z (Δ ppm): [M+H] ⁺ [M-H] ⁻	Peak area [M+H] ⁺ [M-H] ⁻
M_{blood1}	Hydroxylation (indole) + <i>O</i> -Sulfation	C ₁₁ H ₁₄ N ₂ O ₄ S	5.11	271.0750 (1.09) 269.0602 (0.18)	8.5 × 10 ⁵ 2.3 × 10 ⁶
M_{blood2}	Hydroxylation (indole) + <i>O</i> -Sulfation	C ₁₁ H ₁₄ N ₂ O ₄ S	5.38	271.0750 (1.09) 269.0603 (0.55)	9.2 × 10 ⁶ 3.1 × 10 ⁷
M_{blood3}	Hydroxylation (indole) + <i>O</i> -Sulfation	C ₁₁ H ₁₄ N ₂ O ₄ S	7.47	271.0750 (1.09) 269.0603 (0.55)	3.5 × 10 ⁶ 1.3 × 10 ⁷
α-MT (Parent)	No transformation	C ₁₁ H ₁₄ N ₂	9.04	175.1233 (2.08) ND	1.0 × 10 ⁸ ND
M_{blood4}	Hydroxylation (indole) + <i>O</i> -Sulfation + <i>N</i> -Acetylation (indole)	C ₁₃ H ₁₆ N ₂ O ₅ S	9.52	313.0857 (1.38) 311.0711 (1.24)	5.9 × 10 ⁵ 3.6 × 10 ⁶
M_{blood5}	<i>N</i> -Acetylation (indole)	C ₁₃ H ₁₆ N ₂ O	14.07	217.1338 (1.20) ND	2.1 × 10 ⁶ ND

3.4. Discussion

3.4.1. General Analytical Considerations

The structure elucidation of α -MT metabolites is challenging for several reasons: 1) α -MT has a low molecular mass (174.2 g/mol) and α -MT and metabolites therefore produce poor HRMS/MS spectra and are often interfered by ions with the same elemental composition in HRMS and HRMS/MS; 2) α -MT and metabolites produce a low signal intensity in HRMS, which can be partly explained by a substantial in-source fragmentation due to amine loss; and 3) the detection of α -MT metabolites after in-source fragmentation may prompt misinterpretation of the metabolic transformations. To limit isomer coelution and the occurrence of interferences, the LC gradient was developed using a 15-cm-long

analytical column with a biphenyl stationary phase (π - π interaction with the indole group of the molecules) and a particularly slow increase of the organic phase percentage. To limit in-source fragmentation, the auxiliary gas heater temperature was maintained to the minimal recommended value, and amine loss was added to the list of potential reactions for data mining to avoid missing any potential metabolite due to a lack of sensitivity.

In silico metabolite predictions helped in compiling LC-HRMS/MS inclusion and exclusion lists and implementing the transformation list for data mining with Compound Discoverer. Except for *N*-acetylation, all reactions were predicted; predicted reactions such as hydroxylation/oxidation at the alkyl chain, oxidative deamination, and terminal desaturation were not detected. *In silico* metabolite predictions alone are not sufficient to accurately anticipate *in vivo* metabolism, warranting the use of *in vitro* models and the analysis of authentic samples. Additionally, they should be considered carefully when analyzing sample results to avoid biased interpretation [163].

3.4.2. *In Vitro Versus Postmortem* Metabolites

Table 11 summarizes *in vitro* and *postmortem* findings, renaming the metabolites from MA to MQ for better clarity; the elemental composition, retention time in urine, and theoretical accurate mass of molecular ion of α -MT and metabolites in positive- and negative-ionization modes. α -MT metabolic fate in humans is suggested in Figure 9.

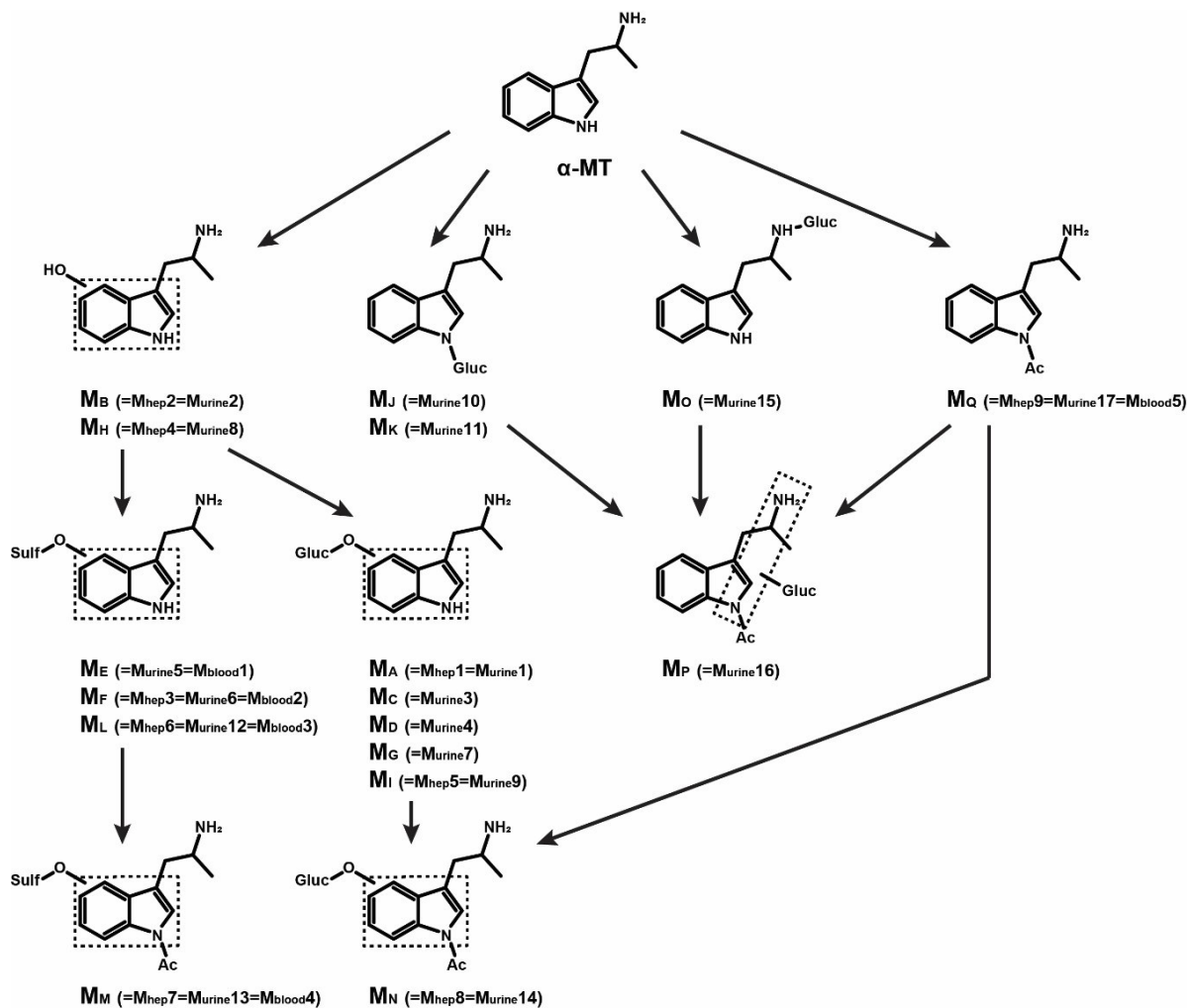


Figure 9. α -MT suggested metabolic fate in humans. Ac, acetyl; Gluc, glucuronide; Sulf, sulfate; dotted box, Markush structure.

Table 11. Metabolic transformation, elemental composition, retention time (RT) in urine, and theoretical accurate mass of molecular ion in positive- and negative-ionization modes ($[M+H]^+$ and $[M-H]^-$, respectively) of α -MT and metabolites in hepatocyte incubations and postmortem samples. We suggest MA, MF, and ML as biomarkers of α -MT use in non-hydrolyzed urine; α -MT and MB in hydrolyzed urine; and α -MT, MF, ML, and MQ in blood.

ID	ID in samples	Metabolic transformation	Elemental composition	Theoretical m/z : $[M+H]^+$ $[M-H]^-$	RT, min
M_A	= M_{hep1} = M_{urine1}	Hydroxylation (indole) + <i>O</i>-Glucuronidation	C₁₇H₂₂N₂O₇	367.1500 365.1354	2.86
M_B	= M_{hep2} = M_{urine2}	Hydroxylation (indole)	C₁₁H₁₄N₂O	191.1179 189.1033	4.62
M_C	= M_{urine3}	Hydroxylation (indole) + <i>O</i> -Glucuronidation	C ₁₇ H ₂₂ N ₂ O ₇	367.1500 365.1354	4.81
M_D	= M_{urine4}	Hydroxylation (indole) + <i>O</i> -Glucuronidation	C ₁₇ H ₂₂ N ₂ O ₇	367.1500 365.1354	4.88
M_E	= M_{urine5} = M_{blood1}	Hydroxylation (indole) + <i>O</i> -Sulfation	C ₁₁ H ₁₄ N ₂ O ₄ S	271.0747 269.0602	5.08
M_F	= M_{hep3} = M_{urine6} = M_{blood2}	Hydroxylation (indole) + <i>O</i>-Sulfation	C₁₁H₁₄N₂O₄S	271.0747 269.0602	5.36
M_G	= M_{urine7}	Hydroxylation (indole) + <i>O</i> -Glucuronidation	C ₁₇ H ₂₂ N ₂ O ₇	367.1500 365.1354	5.98
M_H	= M_{hep4} = M_{urine8}	Hydroxylation (indole)	C ₁₁ H ₁₄ N ₂ O	191.1179 189.1033	6.11
M_I	= M_{hep5} = M_{urine9}	Hydroxylation (indole) + <i>O</i> -Glucuronidation	C ₁₇ H ₂₂ N ₂ O ₇	367.1500 365.1354	6.28
M_J	= M_{urine10}	<i>N</i> -Glucuronidation (indole)	C ₁₇ H ₂₂ N ₂ O ₆	351.1551 349.1405	7.06
M_K	= M_{urine11}	<i>N</i> -Glucuronidation (indole)	C ₁₇ H ₂₂ N ₂ O ₆	351.1551 349.1405	7.15
M_L	= M_{hep6} = M_{urine12} = M_{blood3}	Hydroxylation (indole) + <i>O</i>-Sulfation	C₁₁H₁₄N₂O₄S	271.0747 269.0602	7.44
α -MT (Parent)	NA	No transformation	C₁₁H₁₄N₂	175.1230 173.1084	8.56

MM	=M _{hep} 7 =M _{urine} 13 =M _{blood} 4	Hydroxylation (indole) + <i>O</i> -Sulfation + <i>N</i> -Acetylation (indole)	C ₁₃ H ₁₆ N ₂ O ₅ S	313.0853 311.0707	9.60
MN	=M _{hep} 8 =M _{urine} 14	Hydroxylation (indole) + <i>O</i> -Glucuronidation + <i>N</i> -Acetylation (indole)	C ₁₉ H ₂₄ N ₂ O ₈	409.1605 407.1460	9.61
MO	=M _{urine} 15	<i>N</i> -Glucuronidation (alkyl)	C ₁₇ H ₂₂ N ₂ O ₆	351.1551 349.1405	10.55
MP	=M _{urine} 16	<i>N</i> -Acetylation (indole) + <i>N</i> -Glucuronidation	C ₁₉ H ₂₄ N ₂ O ₇	393.1656 391.1511	12.98
MQ	=M _{hep} 9 =M _{urine} 17 =M _{blood} 5	<i>N</i>-Acetylation (indole)	C₁₃H₁₆N₂O	217.1335 215.1190	14.08

All nine metabolites identified after 3 h incubation with human hepatocytes were detected in postmortem urine. Eight additional metabolites were identified in urine: MC-E, MG, MJ, MK, MO, and MP. The additional metabolites were all minor, suggesting that the incubation with 10-donor-pooled human hepatocytes is a good model to predict α -MT human metabolism. However, the relative intensity of *O*-glucuronides and *O*-sulfates was much higher in urine than *in vitro*, which may be due to extrahepatic metabolism, and the relative intensity of *N*-acetyl metabolites were lower. Therefore, while MB (hydroxy- α -MT), ML (hydroxy- α -MT sulfate), and MQ (*N*-acetyl- α -MT) were the most intense metabolites in hepatocyte incubations, MA (hydroxy- α -MT glucuronide), MF (hydroxy- α -MT sulfate), and ML (hydroxy- α -MT sulfate) were preponderant in non-hydrolyzed urine, and MB (hydroxy- α -MT), MF (hydroxy- α -MT sulfate), and ML (hydroxy- α -MT sulfate) were preponderant in urine after β -glucuronide hydrolysis.

Expectedly, fewer metabolites were identified in postmortem blood due to elimination. Glucuronides were quickly excreted and were not detected in blood. More interestingly, however, hydroxy- α -MT metabolites also were not detected, likely due to low intensity, considering the overall intensity of α -MT and metabolites. Consistent with *in vitro* and urinary results, MF (hydroxy- α -MT sulfate), ML (hydroxy- α -MT sulfate), and MQ (*N*-acetyl- α -MT) were the most intense metabolites detected in blood.

Remarkably, α -MT signal was much more intense than that of the metabolites in postmortem samples, possibly because the individual died of overdose. However, it cannot be excluded that a significant proportion of α -MT is eliminated without alteration. α -MT metabolization was slow in hepatocyte incubations, considering α -MT signal intensity after 0 and 3 h (-25% difference), corroborating the latter statement. A slow metabolism could also explain α -MT prolonged psychedelic effects [60]. Postmortem samples were obtained from a single case of α -MT overdose, and α -MT metabolism may differ with the dose, the route of administration, the time of collection after intake, *postmortem* redistribution (when

applicable), and interindividual genetic variations. Additionally, the stability of α -MT metabolites in postmortem samples after multiple freeze/thaw cycles is unknown. For these reasons, the analysis of other samples from authentic clinical and forensic caseworks are necessary to better understand α -MT pharmacokinetics.

3.4.3. Comparison to Analogues

Consistent with the present results, phase II transformations at the indole core are major pathways of tryptamine metabolism, either by direct glucuronidation or following hydroxylation or *O*-dealkylation [99,164,165,176]. *O*-Glucuronide is the main metabolite target of psilocin consumption in human urine [165] and *O*-glucuronide and *O*-sulfate are major 5-methoxy-*N,N*-diisopropyltryptamine (5-MeO-DiPT) metabolites in urine [99]. Indole hydroxylation was minor (before hydrolysis) in the present experiments, consistent with the metabolism of tryptamine analogues [99,156,165,177].

5-HT can undergo *N*-acetylation at the alkyl chain through the aralkylamine *N*-acetyltransferase, mainly expressed in the central nervous system, and the arylamine *N*-acetyltransferases, ubiquitously expressed, as a step of melatonin biosynthesis in vertebrates [178]; other 2-arylethylamines, such as tryptamine, 5-methoxytryptamine, and phenylethylamine, also are aralkylamine *N*-acetyltransferase substrates [179]. Interestingly, however, indole *N*-acetylation was not reported in the metabolic fate of structural analogues and was not predicted in silico, highlighting the necessity of an untargeted screening of LC-HRMS/MS data for metabolite identification studies. Comparison to reference standards, which are yet to be synthesized, is necessary to definitely confirm the position of the acetylation.

3.4.4. Comparison to α -MT Metabolism in Rats

Szara et al. identified 3-indolyacetone through oxidative deamination, 6-hydroxy- α -MT, 6-hydroxy-3-indolyacetone, and further *O*-glucuronide conjugates as α -MT metabolites in rats [170]. More recently, Kanamori et al. identified 1'-, 6-, and 7-hydroxy- and 2-oxo- α -MT also in rats [62]. Although these two studies only targeted specific metabolites, the overall results were different in humans. Most metabolites identified in humans were phase II metabolites, but glucuronides were minor in Szara et al.'s study [170], and phase II metabolism was not assessed by Kanamori et al., who performed β -glucuronidase/arylsulfatase hydrolysis prior to sample analysis [62]. Importantly, oxidative deamination, a major detoxication pathway of *N,N*-dimethyl tryptamines, was not detected in the present experiments, likely due to the methyl group protective effect [164]. Consistent with users' reports, the lack of 3-indolyacetone suggests that α -MT does not require co-administration of a monoamine oxidase inhibitor to effectively induce psychedelic effects [60]. The differences between rat and human metabolism is not

surprising, due to inter-species discrepancies. Although metabolic studies in rats are a convenient model to predict human drug metabolism, studies in humans are necessary to confirm these preliminary results.

3.4.5. Recommended Biomarkers of Consumption

We suggest α -MT and major metabolites MA (hydroxy- α -MT glucuronide), MF (hydroxy- α -MT sulfate), and ML (hydroxy- α -MT sulfate) as biomarkers of α -MT consumption in urine in clinical and forensic toxicology; MF and ML detectability is notably higher in negative-ionization mode. At present, due to the lack of analytical standards for the newly identified metabolites, hydrolysis is not recommended as there is no guarantee to completely cleave *O*-glucuronides and *O*-sulfates without proper optimization of the hydrolysis conditions. Additionally, the total signal of *O*-glucuronides without hydrolysis was more intense than that of hydroxy- α -MT metabolites with hydrolysis, and targeting *O*-glucuronides seems therefore more rational. Nonetheless, in case of urinary hydrolysis, we suggest α -MT and MB (hydroxy- α -MT) as biomarkers of consumption.

We suggest α -MT and major metabolites MF (hydroxy- α -MT sulfate), ML (hydroxy- α -MT sulfate), and MQ (N-acetyl- α -MT) as biomarkers of α -MT consumption in blood.

To the best of our knowledge, these metabolites were not identified in the metabolism of structural analogues and are specific to α -MT. It should be kept in mind, however, considering the novel psychoactive substance market dynamics, that new analogues potentially sharing metabolites with α -MT such as hydroxy- α -MT may emerge onto the illicit drug market in the future.

3.5. Conclusion

We studied α -MT metabolism in humans for the first time. We identified α -MT metabolites in human hepatocytes and *postmortem* urine and whole blood in an overdose casework using *in silico* metabolite predictions, LC-HRMS/MS analysis, and software-assisted data mining. Seventeen metabolites were identified in authentic samples with hydroxylation, *O*-sulfation, *O*-glucuronidation, *N*-glucuronidation, and *N*-acetylation; the transformations mainly occurred at the indole core of the molecule. We suggest α -MT, hydroxy- α -MT glucuronide M_A, and hydroxy- α -MT sulfates M_F and M_L as biomarkers of α -MT use in non-hydrolyzed urine. We suggest α -MT, hydroxy- α -MT sulfates M_F and M_L and *N*-acetyl- α -MT M_Q as biomarkers of α -MT use in blood. The findings in *postmortem* samples were consistent with those observed *in vitro*, confirming the suitability of 10-donor-pooled human hepatocyte incubations as a model to predict tryptamine metabolism in humans. Tryptamines are prone to phase II conjugations, which are usually quickly

excreted after formation. All nine metabolites identified in hepatocytes were indeed found in urine, eight additional minor metabolites being found in urine.

However, further studies on α -MT clinical and forensic caseworks with different doses and routes of administration are necessary to explore α -MT metabolism, particularly to understand parent detectability compared to that of its metabolites in authentic samples. Our results provide important data to orientate analytical standard manufacturers' synthesis effort and will help toxicologists identify new cases to generate biological samples to refine the present results.

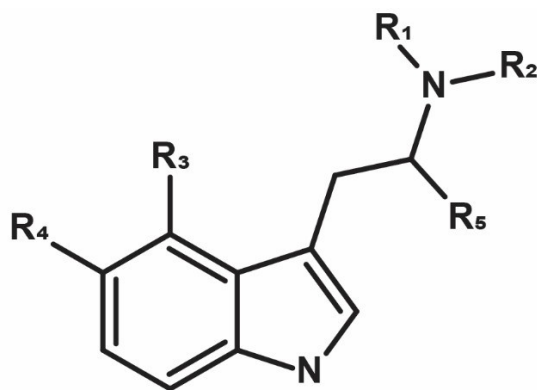
Part II: Tryptamines' Detection In Urine Using LC-HRMS/MS

Tryptamines are indolealkylamines sharing their core structure with the neurotransmitter serotonin (5-hydroxy-*N,N*-tryptamine, 5-HT) [164]. Tryptamines can induce psychotropic effects, such as synesthesia, altered perception, and hallucinations, mainly through 5-HT receptors. However, overdose can induce a 5-HT syndrome with high blood pressure, high body temperature, tachycardia, mydriasis, and tremor, potentially leading to seizures and death [25,164,180]. Several analogues are internationally regulated by the United Nations Convention on Psychotropic Substances of 1971, such as alpha-ethyltryptamine (α -ET), diethyltryptamine (DET), *N,N*-dimethyltryptamine (DMT), and psilocin [181]. Other tryptamines are locally controlled either specifically or by structural analogy, such as in the United States under the Controlled Substances Act and the United Kingdom under the Misuse of Drugs Act of 1971. However, many analogues are not regulated. To circumvent regulation and analytical detection while imitating the recreational psychedelic effects of controlled tryptamines, new structural analogues are synthesized for the first time every year, following the recent trend of new psychoactive substances (NPSs). Recently, psychedelics and tryptamines have raised attention from scientists and media, as they showed tremendous therapeutic potential to treat depression and tobacco, alcohol, and drug addiction. In 2018, the US Federal Drug Administration (FDA) gave psilocybin “breakthrough therapy” status, speeding the process of approval as a pharmaceutical [177,182,183]. According to the 2019 Global Drug Survey (GDS), 40% of drug users reported using psychedelics, with tryptamine use showing the highest increase compared to other substances [184]. The consumption of natural and synthetic tryptamines for self-medication, the manufacturing of new analogues, and the occurrence of clinical and forensic cases involving these tryptamines are expected to rise. Analytical toxicology laboratories should be prepared to cope with the emergence of new cases.

The analytical methods developed for detecting or quantifying tryptamines in biological matrices in forensic and clinical settings were recently reviewed [177]. One major concern was the lack of analytical method for many analogues and the lack of comprehensive screening in urine. Another major concern was the lack of analytical method for detecting metabolite biomarkers of consumption in biological samples, due to the poor understanding of tryptamines' metabolism [177]. The detection of tryptamines and metabolites in biological fluids can be challenging for several reasons: 1) the concentration of several tryptamines and/or their metabolites in biological fluids after a recreational dose can be low and requires sensitive detection such as mass spectrometry [185]; 2) similar to any other NPS subclass, structural isomers with the same elemental composition and major fragments in tandem mass spectrometry (MS/MS) are frequent and should be clearly resolved with a suitable separation method such as gas or liquid chromatography (GC or LC, respectively) [144]; 3) similar to any other NPS subclass, the substantial number of analogues requires a highly specific analytical method and precludes immunodetection due

to cross-reactivity [144]; and 4) tryptamines have a low molecular mass and therefore produce few transitions in MS/MS and are prone to interferences in MS and MS/MS. Moreover, considering the NPS market dynamics, a quantitative method intended to exhaustively identify tryptamines should be easily updatable.

In the present study, we aimed to develop a liquid chromatography-high-resolution tandem mass spectrometry (LC-HRMS/MS) method to specifically and accurately quantify trace amounts of 15 tryptamines and detect 11 additional analogues and metabolites in human urine, which can be collected non-invasively and allows for extended detection windows for the parent drug and metabolites. Alpha-ethyltryptamine (α -ET), alpha-methyltryptamine (α -MT), 4-acetoxy-*N,N*-diisopropyltryptamine (4-AcO-DiPT), 4-hydroxy-*N,N*-diethyltryptamine (4-OH-DET), 4-hydroxy-*N,N*-dimethyltryptamine (psilocin, 4-OH-DMT), 4-hydroxy-*N*-methyl-*N*-propyltryptamine (4-OH-MPT), 5-methoxy-*N,N*-diisopropyltryptamine (5-MeO-DiPT), 5-methoxy-*N,N*-dimethyltryptamine (5-MeO-DMT), 5-methoxy-*N*-methyl-*N*-isopropyltryptamine (5-MeO-MiPT), 5-hydroxy-*N,N*-dimethyltryptamine (bufotenine, 5-OH-DMT), *N,N*-diethyltryptamine (DET), *N,N*-diisopropyltryptamine (DiPT), *N,N*-dimethyltryptamine (DMT), *N,N*-dipropyltryptamine (DPT), and *N*-methyltryptamine (NMT) were included for quantification. 4-Hydroxy-*N,N*-dimethyltryptamine (4-AcO-DMT), 5-methoxy-*N,N*-diallyltryptamine (5-MeO-DALT), 5-methoxy-*N,N*-dipropyltryptamine (5-MeO-DPT), and 4-phosphoryloxy-*N,N*-dimethyltryptamine (psilocybin) were added for detection only, due to the low quantities of analytical standards available. Metabolite biomarkers of α -MT, 4-AcO-DiPT, and 4-OH-MPT consumption identified with human hepatocyte incubations were added to the method for detection only.



	R ₁	R ₂	R ₃	R ₄	R ₅
α-ET	H	H	H	H	CH ₂ CH ₃
α-MT	H	H	H	H	CH ₃
4-AcO-DiPT	CH(CH ₃) ₂	CH(CH ₃) ₂	OCOCH ₃	H	H
4-AcO-DMT	CH ₃	CH ₃	OCOCH ₃	H	H
4-OH-DET	CH ₂ CH ₃	CH ₂ CH ₃	OH	H	H
4-OH-DMT	CH ₃	CH ₃	OH	H	H
4-OH-MPT	(CH ₂) ₂ CH ₃	CH ₃	OH	H	H
5-MeO-DALT	CH ₂ CHCH ₂	CH ₂ CHCH ₂	H	OCH ₃	H
5-MeO-DiPT	CH(CH ₃) ₂	CH(CH ₃) ₂	H	OCH ₃	H
5-MeO-DMT	CH ₃	CH ₃	H	OCH ₃	H
5-MeO-DPT	(CH ₂) ₂ CH ₃	(CH ₂) ₂ CH ₃	H	OCH ₃	H
5-MeO-MiPT	CH(CH ₃) ₂	CH ₃	H	OCH ₃	H
5-OH-DMT	CH ₃	CH ₃	H	OH	H
DET	CH ₂ CH ₃	CH ₂ CH ₃	H	H	H
DiPT	CH(CH ₃) ₂	CH(CH ₃) ₂	H	H	H
DMT	CH ₃	CH ₃	H	H	H
DPT	(CH ₂) ₂ CH ₃	(CH ₂) ₂ CH ₃	H	H	H
NMT	CH ₃	H	H	H	H
Psilocybin	CH ₃	CH ₃	OPO(OH) ₂	H	H

Figure 10. Structure of the tryptamines included in the analytical method.

1. Materials and Methods

1.1. Standards and Reagents

5-OH-DMT analytical standard was purchased from Cerilliant (Round Rock, TX, USA); α-ET, 4-AcO-DiPT, 4-OH-DET, 4-OH-DMT, 4-OH-MPT, 5-MeO-DMT, 5-MeO-

MiPT, DiPT, DPT, and NMT standards were from Cayman Chemicals (Ann Arbor, MI, USA); 5-MeO-DiPT and α -MT standards were from Toronto Research Chemicals (North York, Canada); DET and DMT standards were from the National Measurement Institute of Australia (Australia). 4-AcO-DMT, 5-MeO-DPT, 5-MeO-DALT, and psilocybin standards were kindly provided by Comedical (Trento, Italy) as methanolic solution at 50 μ g/mL. Deuterated internal standard (IS) psilocin-D₁₀ was acquired from Cayman Chemical (Ann Arbor, MI, USA). As per the providers' recommendations, psilocin-D₁₀ was stored at -80°C and all other standards were stored at -20°C until analysis.

LC-MS grade water, methanol, acetonitrile, and formic acid, and LC/MS grade ammonium acetate ACS reagent ($\geq 98\%$ purity) was acquired from Honeywell Fluka (Morristown, NJ, USA), diethyl ether, and ethyl acetate were obtained from Carlo Erba (Cornaredo, Italia). Ammonium hydroxide (25% purity), sodium hydroxide, and hydrochloric acid (37% purity) were purchased from Honeywell Fluka (Morristown, NJ, USA). β -Glucuronidase (110,200 units/mL) from type HP-2 (*Helix Pomatia*) was purchased from Sigma Aldrich (Milan, Italy).

1.2. Calibrators and Quality Controls

α -ET, α -MT, 4-AcO-DiPT, 4-OH-DET, 4-OH-DMT, 4-OH-MPT, 5-MeO-DiPT, 5-MeO-DMT, 5-MeO-MiPT, 5-OH-DMT, DET, DiPT, DMT, DPT, and NMT were solubilized in acetonitrile to 1 mg/mL in glass amber vials, and each standard was equally split into two aliquots (I and II). The IS stock solution consisted of psilocin-D₁₀ at 500 ng/mL in acetonitrile. Stock solutions were stored at -20°C until use.

Preliminary experiments were conducted to anticipate the working range and determine the best calibration model for each analyte. The calibrator stock solution was prepared with all analytes from aliquots I at 50 μ g/mL in acetonitrile. Successive dilutions were prepared in acetonitrile to reach the following final concentrations in urine: 0.1, 0.5, 2, 10, 50, and 100 ng/mL for DMT, DET, 5-MeO-MiPT, DPT, and 5-MeO-DiPT; 0.2, 0.5, 2, 10, 50, and 100 ng/mL for 5-OH-DMT, 4-OH-DMT, NMT, 5-MeO-DMT, and 4-OH-MPT; 0.5, 1, 2, 10, 50, 100, and 1000 ng/mL for α -ET; 2, 5, 20, 50, 100, and 500 ng/mL for α -MT; and 0.1, 0.5, 2, 10, 100, and 1000 ng/mL for 4-OH-DET, 4-AcO-DiPT, and DiPT. Quality controls (QCs) were prepared in acetonitrile from aliquots II at a low (QC1), medium (QC2), and high concentration (QC3) to reach the following final concentrations in urine: QC1–3 were 0.3, 8 and 80 ng/mL, respectively, for 5-OH-DMT, 4-OH-DMT, DMR, 4-OH-DET, 5-MeO-DMT, 4-OH-MPT, DET, 5-MeO-MiPT, and 5-MeO-DiPT; QC1–3 were 1.5, 8 and 80 ng/mL, respectively, for NMT; QC1–3 were 6, 40 and 400 ng/mL, respectively, for α -MT and DPT; QC1–3 were 1.5, 80, and 800 ng/mL, respectively, for α -ET, 4-AcO-DiPT, and DiPT.

1.3. Sample Preparation

In glass tubes, 500 μL urine was mixed with 10 μL QC, calibrator, or acetonitrile; 10 μL IS; 20 μL ammonium acetate at 10 mol/L, pH 5; and 100 μL β -glucuronidase. Hydrolysis was performed at 37°C for 90 min. Liquid-liquid extraction was then performed with 500 μL sodium hydroxide at 1 mol/L and 3 mL ethyl acetate:diethyl ether (75:25, v/v) under agitation for 10 min. Samples were centrifuged at 1300g for 5 min and supernatants were evaporated to dryness with 20 μL acidic methanol (0.25% HCl) under nitrogen at room temperature. Residues were reconstituted in 100 μL water: acetonitrile (98:2, v/v) with 0.1% formic acid and transferred into microtubes. After centrifugation for 10 min, 15,000g, at room temperature, the supernatants were transferred into LC autosampler vials with a glass insert prior to injection onto the chromatographic system.

1.4. Liquid Chromatography-High-Resolution Tandem Mass Spectrometry

LC-HRMS/MS analysis was performed with a Dionex UltiMate 3000 chromatographic system coupled with a Thermo Scientific (Waltham, MA, USA) Q Exactive mass spectrometer equipped with a heated electrospray ionization (HESI) source operating in positive-ionization mode.

1.4.1. Liquid Chromatography Settings

Separation was performed with a Kinetex Phenyl-Hexyl column (100 x 2.1 mm, 2.6 μm) from Phenomenex (Castel Maggiore, Italy) with a mobile phase gradient composed of 0.1% formic acid in water (MPA) and 0.1% formic acid in acetonitrile (MPB) at $40 \pm 1^\circ\text{C}$. Run time was 13 min with a 0.4 mL/min flow rate. The gradient started with 2% MPB for 1 min; MPB was increased to 30% within 6 min then 95% within 1 min and held for 2 min before returning to initial conditions within 0.1 min; re-equilibration time was 2.9 min. Autosampler temperature was $10 \pm 1^\circ\text{C}$.

1.4.2. High-Resolution Tandem Mass Spectrometry Settings

HESI source parameters were: sheath gas flow rate, 50 u.a.; auxiliary gas flow rate, 5 u.a.; spray voltage, 3.5 kV; capillary temperature, 300°C; auxiliary gas heater temperature, 300°C; S-lens radio frequency, 50 u.a.; sweep gas was not applied. The orbitrap was calibrated prior to analysis, and a lock mass list composed of previously identified contaminants was used during injections for better accuracy (triphenylphosphine with m/z 279.09333 and phthalate with m/z 279.15909 [8]).

Data were acquired from 1 to 10 min in full scan HRMS (FullMS)/data-dependent MS/MS (ddMS2) mode. FullMS parameters were: acquisition range, m/z 140–370;

resolution at full width at half maximum (FWHM) at m/z 200, 70,000; automatic gain control (AGC) target, 10^6 ; and maximum injection time (IT), 200 ms. ddMS2 parameters were: resolution, 17,500; isolation window, m/z 1; normalized collision energy (NCE), 20, 90, and 110 a.u.; AGC target, 2×10^5 ; maximum IT; 64 ms; topN, 5 (pick others if idle); intensity threshold, 104; dynamic exclusion, 2.0 s. A scheduled inclusion list with optimized NCE was used to prioritize the fragmentation of the tryptamines included in the present method.

1.4.3. Data Processing and Identification Criteria

LC-HRMS/MS data were processed with TraceFinder 4.1. – Forensic from Thermo Scientific. Peak integration was performed in full-scan MS using the theoretical accurate mass of the analytes' molecular ion with a 5 ppm mass tolerance; analytes were expected to elute within 0.1 min of the theoretical retention time; two specific fragments were expected to be detected for each analyte in MS/MS with a 5 ppm mass tolerance and within 20% of the target ion ratio (average calibrator transition ion ratio); the detection of the other ions of the analytes' isotopic pattern was not a prerequisite for identification. Theoretical accurate mass of the molecular ion and targeted fragments, retention time, and NCE for each analyte are displayed in Table 12.

Table 12. LC-HRMS/MS parameters and identification criteria for analytes and internal standard.

Tryptamine	Elemental composition	Molecular ion [M+H]⁺, m/z	MS/MS fragments, m/z	NCE, a.u.	RT, min
Psilocybin	C ₁₂ H ₁₇ N ₂ O ₄ P	285.0998	205.1336; 58.0654	30	1.59
Bufotenine	C ₁₂ H ₁₆ N ₂ O	205.1335	58.0654; 160.0757	30	1.77
4-OH-DMT-D ₁₀	C ₁₂ H ₁₆ D ₁₀ N ₂ O	215.1963	66.1155; 164.1009	55	2.54
4-OH-DMT	C ₁₂ H ₁₆ N ₂ O	205.1335	58.0654; 160.0757	55	2.66
NMT	C ₁₁ H ₁₄ N ₂	175.1229	144.0808; 132.0808	40	3.28
α-MT	C ₁₁ H ₁₄ N ₂	175.1229	143.0729; 158.0964	60	3.64
DMT	C ₁₂ H ₁₆ N ₂	189.1386	58.0654; 144.0808	40	3.73
4-OH-DET	C ₁₄ H ₂₀ N ₂ O	233.1648	86.0964; 160.0758	55	4.03
5-MeO-DMT	C ₁₃ H ₁₈ N ₂ O	219.1492	58.0653; 131.0729	80	4.07

4-AcO-DMT	C ₁₄ H ₁₈ N ₂ O ₂	247.1441	58.0654; 223.9196	30	4.21
4-OH-MPT	C ₁₄ H ₂₀ N ₂ O	233.1648	86.0963; 160.0756	60	4.21
α-ET	C ₁₂ H ₁₆ N ₂	189.1386	173.1154; 130.0650	35	4.59
DET	C ₁₄ H ₂₀ N ₂	217.1699	86.0964; 155.0704	55	5.01
5-MeO-MiPT	C ₁₅ H ₂₂ N ₂ O	247.1805	86.0963; 174.0911	30	5.15
4-AcO-DiPT*	C ₁₆ H ₂₄ N ₂ O*	261.1961*	114.1276; 160.0756	40	5.22
5-MeO-DALT	C ₁₇ H ₂₂ N ₂ O	271.1805	110.0963; 174.0912	40	5.84
DPT	C ₁₆ H ₂₄ N ₂	245.2012	144.0806; 114.1276	40	6.13
5-MeO-DiPT	C ₁₇ H ₂₆ N ₂ O	275.2118	131.0729; 159.0679	80	6.16
5-MeO-DPT	C ₁₇ H ₂₆ N ₂ O	275.2118	86.0964; 159.0677	80	6.29
DiPT	C ₁₆ H ₂₄ N ₂	245.2012	144.0806; 114.1276	40	6.63

*, 4-AcO-DiPT was detected as 4-OH-DiPT due to acetoxy group cleavage (4-AcO-DiPT initial composition is C₁₈H₂₆N₂O₂)

1.5. Method Validation

Linearity, analytical bias, imprecision, limit of detection (LOD), lower limit of quantification (LLOQ), carryover, interferences, matrix effect (ME), recovery (RE), dilution integrity, and stability were evaluated during method validation in accordance with recommendations from the Organization of Scientific Area Committees (OSAC) for Forensic Science, USA [186].

1.5.1. Linearity

For each analyte, six calibration curves were determined on six separate days with six calibrators from the lower (LLOQ) to the upper (ULOQ) limit of quantification using linear least squares regression. A Mandel test was used to assess curve linearity [187]. Calibrators had to quantify within 15% of the target concentration (or 20% at the LLOQ) and meet the identification criteria described in Section 1.4.3.

1.5.2. Bias and Imprecision

Intra- and inter-day bias and imprecision were calculated with blank urine fortified with the analytes at QC1, QC2, and QC3 in quadruplicates on five different days. For each analyte, QCs had to quantify within 20% of the target concentration and meet the identification criteria described in Section 1.4.3. Imprecision was expressed as a coefficient

of variation (CV) of calculated concentrations, and intra- and inter-day differences were tested via one-way analysis of variance (ANOVA).

1.5.3. Limit of Detection and Quantification

LLOQ was tested with five different sources of blank urine fortified with the analytes at the lowest calibrator concentration. For each analyte, the calibrator had to quantify within 20% of the target concentration and meet the identification criteria described in Section 1.4.3.

LOD was tested with five different sources of blank urine fortified with the analytes at a concentration 2- and 5-fold lower than LLOQ. For each analyte, samples had to meet the identification criteria described in Section 1.4.3. and present a signal/noise ratio higher than 3, regardless of the measured concentration.

1.5.4. Carryover

Lack of carryover was verified in triplicate with blank urine fortified with the analytes at a concentration 5-fold higher than ULOQ, followed by a negative sample (blank urine fortified with the IS only). Carryover was negligible if no peak eluted within 0.1 min of the theoretical retention time, with a signal/noise ratio higher than 3 in negative samples.

1.5.5. Interferences

Matrix interferences were evaluated with five different sources of blank urine. Interferences were negligible if no peak eluted within 0.1 min of the theoretical retention time, with a signal/noise ratio higher than 3.

Interferences from common drugs of abuse and metabolites were evaluated with blank urine fortified with amphetamine (0.5 µg/mL), methamphetamine (0.5 µg/mL), 3,4-methylenedioxyamphetamine (MDA) (2 µg/mL), 3,4-methylenedioxymethamphetamine (MDMA) (1 µg/mL), 3,4-methylenedioxy-*N*-ethylamphetamine (MDEA) (2 µg/mL), Δ^9 -tetrahydrocannabinol (THC) (1 µg/mL), cocaine (1.5 µg/mL), ecgonine methyl ester (1 µg/mL), cocaethylene (1 µg/mL), benzoylecgonine (1 µg/mL), morphine (0.5 µg/mL), 6-acetylmorphine (0.5 µg/mL), codeine (1.5 µg/mL), methadone (1 µg/mL), EDDP (1 µg/mL), diazepam (5 µg/mL), flurazepam (1 µg/mL), and clonazepam (1 µg/mL) in urine. Interferences were negligible if no peak eluted within 0.1 min of the theoretical retention time, with a signal/noise ratio higher than 3.

Between-analyte interferences were evaluated with blank urine fortified with the analytes at 50 µg/mL, separately. Interferences were negligible if no peak eluted within 0.1 min of the theoretical retention time, with a signal/noise ratio higher than 3, for all analytes except for the fortified one.

1.5.6. Matrix Effect and Recovery

Matrix effect and recovery were evaluated with blank urine from five different sources fortified with the analytes at QC1, QC2, and QC3. Three sample sets were prepared, with set A) blank urine fortified with the analytes before extraction, set B) blank urine extracted and fortified with the analytes immediately before evaporation, and set C) neat standards in 3 mL ethyl acetate: diethyl ether (75:25, v/v) and 20 μ L acidic methanol (0.25% HCl) evaporated under nitrogen at room temperature and reconstituted with MPA: MPB (98:2, v/v). For each analyte and each concentration, analytical recovery was calculated by dividing the mean peak area of set A) by the mean peak area of set B). Ion suppression or enhancement was calculated by dividing the mean peak area of set B) by the mean peak area of set C) minus 1. Additionally, the samples were required to quantify within 20% of the target concentration and meet the identification criteria described in Section 1.4.3.

1.5.7. Dilution Integrity

Dilution integrity was assessed in quintuplicates with blank urine fortified with the analytes at a concentration 5-fold higher than ULOQ. Samples were diluted ten- and fifty-fold in blank urine before analysis. Samples were required to quantify within 20% of the target concentration and meet the identification criteria described in Section 1.4.3.

1.5.8. Stability

Analyte stability was assessed in urine at room temperature and at +4°C for 24 h and 1 week, in urine following 3 freeze/thaw cycles (-20°C), and in the LC reconstitution solvent 24 h after extraction and storage in the autosampler (+10°C). Internal standard was added immediately before extraction. Stability was assessed in 4 replicates at QC1, QC2, and QC3 concentrations. Analytes were considered stable if the measured concentrations were within 20% of the target concentration and meet the identification criteria described in Section 1.4.3.

1.5.9. Proof of Method

A urine sample from a fatal case of acute intoxication involving α -MT was analyzed as proof of concept. α -MT concentration was estimated to be higher than 5.0 μ g/mL (ULOQ) in LC-MS/MS [188].

1.6. Updating the Method with New Analogues and Metabolites

4-AcO-DMT, 5-MeO-DPT, 5-MeO-DALT, and psilocybin were individually fortified in urine to reach a final concentration of 10 ng/mL and the samples were analyzed as described above to include their molecular ion in HRMS, two major fragments in HRMS/MS, and their retention time to the method (Table 1). Due to low quantities of stock solutions, the method validation did not include these analogues.

α -MT, 4-AcO-DiPT, and 4-OH-MPT were incubated with 10-donor-pooled human hepatocytes to identify major metabolite biomarkers of consumption, and 100 μ L incubates were evaporated to approximately 50 μ L and mixed with 450 μ L blank urine before being analyzed in the same conditions as described above. The molecular ion in HRMS, two major fragments in HRMS/MS, and the retention time of major metabolite biomarkers were included in the method (Table 13); the details of the metabolite identification studies were previously reported [157,188,189]. 4-AcO-DiPT metabolites were 4-hydroxy-*N*-isopropyltryptamine (4-OH-iPT, 4-AcO-DiPT M1) and 4-OH-MPT-*N*-oxide (4-AcO-DiPT M2); 4-OH-MPT metabolites were 4-hydroxy-*N*-propyltryptamine (4-OH-PT, 4-OH-MPT M1) and 4-OH-MPT-*N*-oxide (4-OH-MPT M2); and α -MT metabolites were two hydroxyls at the indole core (the exact position cannot be ascertained in present analytical conditions) α -MT M1 and α -MT M2.

2. Results

4-AcO-DiPT analytical recovery and matrix effect could not be properly measured due to the cleavage of the acetoxy group during the extraction. Table 13 displays the values for dilution integrity and stability for all analytes. No carryover or interference were detected. Extracted-ion chromatograms in blank urine and in blank urine fortified at the LLOQ are displayed in Figure 11 for each analyte.

Extracted-ion chromatograms in blank urine and in blank urine fortified at the LLOQ are displayed in Figure 2 for each analyte.

α -MT concentration in urine from an authentic case of intoxication was higher than 50 μ g/mL; the sample was diluted 50 times before analysis. Extracted-ion chromatograms in the authentic specimen for α -MT and major hydroxylated metabolites α -MT M1 and M2 are displayed in Figure 12.

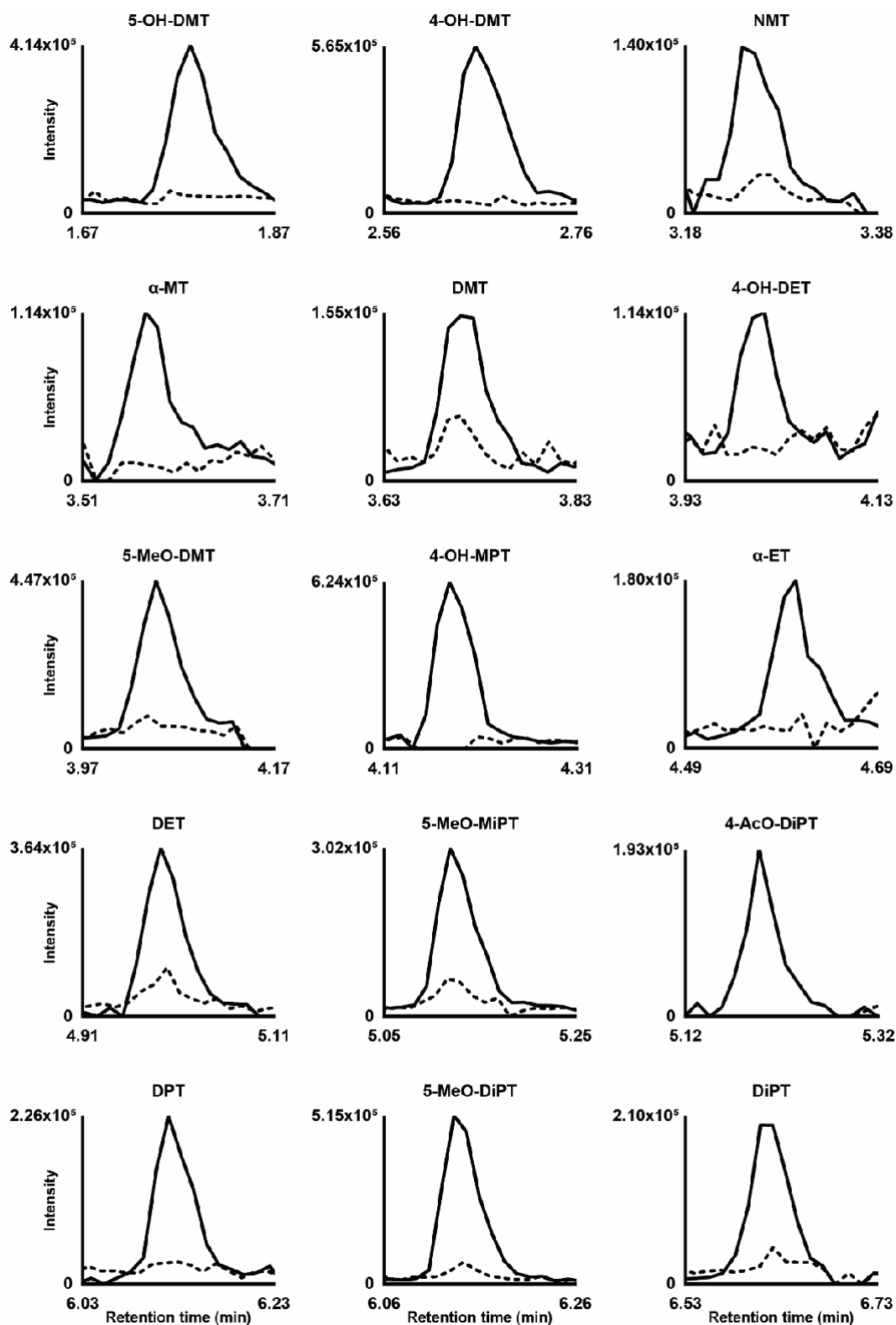


Figure 11. Extracted-ion chromatogram of blank urine (dotted line) and blank urine fortified with the analytes at the lowest limit of quantification (plain line) for all analogues included in the method validation. Mass tolerance, 5 ppm.

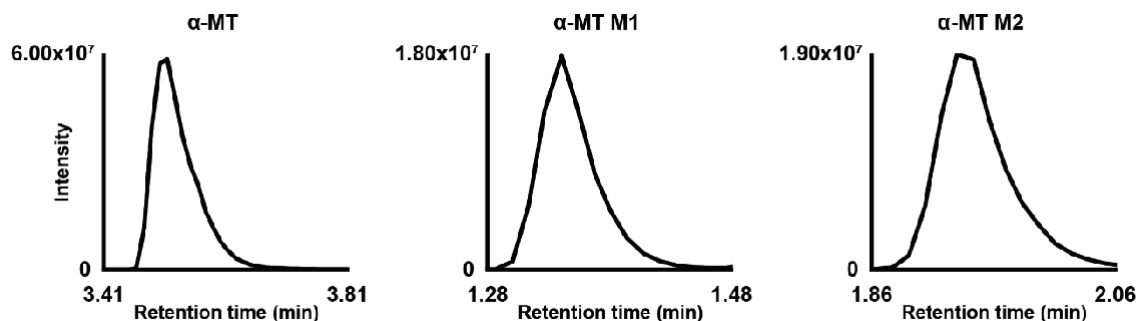


Figure 12. Extracted-ion chromatogram of α -MT and metabolites from an authentic case of intoxication involving α -MT (concentration was higher than 50 $\mu\text{g}/\text{mL}$); the sample was diluted 50 folds. Mass tolerance, 5 ppm.

3. Discussion

3.1. Method Optimization

3.1.1. Liquid Chromatography Optimization

A phenyl-hexyl analytical column was employed for LC separation as it is commonly used in toxicology laboratories for routine analyses and is also suitable for effectively retaining tryptamines to allow for better separation (π - π interactions with the indole core and hydrophobic interactions with the alkyl chain). A good retention is particularly needed for tryptamines, due to their low mass and high polarity. No buffer was used in mobile phases to limit adduct formation and ion suppression. However, 0.1% formic acid was added to favor ionization in positive-ionization mode (Section 3.1.2.). The column temperature was maintained at 40°C to mimic *in vivo* conditions, since the stability of future tryptamines and metabolites to be added to the method is unknown. The analytes were well separated across the 13-min gradient, and position isomers were perfectly resolved.

3.1.2. Mass Spectrometry Optimization

Electrospray ionization was employed as interface between chromatography and MS as it is suitable for polar to mildly polar low-mass molecules. The analytical standards of tryptamines and IS were individually infused directly through the source at 1 $\mu\text{g}/\text{mL}$ in water:acetonitrile (50:50, v/v) at a 10 $\mu\text{L}/\text{min}$ flow rate to select the ionization mode, identify specific fragments in HRMS/MS, and optimize the collision energy. Ionization was performed in positive mode as none of the analytes produced a signal in negative-ionization mode. For each analyte, a specific intermediary NCE was selected to generate two major fragments with approximately the same signal intensity, two fragments being required for

identification; non-specific fragments due to water loss or amine loss were excluded. A generic ramped NCE was employed for all other compounds to ensure the production of multiple fragments. To optimize the source parameters, a mix of the analytes at 1 µg/mL in MPA: MPB (98:2, v/v) was injected multiple times in the LC conditions of the analysis with different HESI settings ramping spray voltage, sheath gas flow rate, and auxiliary gas flow rate and heater temperature; capillary temperature was maintained at the lowest recommended value to avoid thermal degradation of future analytes. While the values of the spray voltage and sheath gas flow rate did not affect the signal intensity, increasing the auxiliary gas flow rate substantially decreased the signal of all analytes and was therefore maintained at 5 a.u. Decreasing the auxiliary gas heater temperature increased α -MT signal, but considering the high α -MT concentrations measured in biological fluids from authentic cases [188,190], we favored the optimization of the other analytes, which were all more intense at 300°C. α -MT, α -ET, and NMT intensity was generally lower than that of the other analytes.

FullMS/ddMS² acquisition mode was used to scan and specifically fragment all extracted compounds from m/z 140–370 to allow for an easy update with new molecules without requiring a full validation, and the retrospective raw data analysis to look after potential metabolites or other tryptamines. A 70,000 resolution in full-scan HRMS combined to a 17,500 resolution in HRMS/MS was a compromise to acquire data with accurate mass capabilities while generating a sufficient number of scan per chromatographic peak in full-scan HRMS to achieve repeatable measures. A total of five data-dependent HRMS/MS scans were generated using the five most intense ions detected in the previous HRMS scan, with an inclusion list compiling the m/z values of the analytes' molecular ion to prioritize their fragmentation. Only one HRMS/MS scan around the apex of the chromatographic peak was necessary, and a dynamic exclusion of 2 s was therefore employed to avoid superfluous fragmentation.

3.1.3. Extraction Optimization

Tryptamines are prone to phase II conjugation, mainly *O*-glucuronidation [99,154,188], and sample hydrolysis is therefore a crucial step for the detection of tryptamines in biological fluids, especially in urine, to increase the detection capabilities of the parent and non-conjugated metabolites. A 90-min hydrolysis at 37°C with 5,000 units β -glucuronidase from limpets and ammonium acetate buffer at pH 5 for 500 µL urine proved suitable for the hydrolysis of α -MT glucuronides in previous experiments [188]. Due to the lack of standards for tryptamine conjugates and urine samples for cases of exposure, the hydrolysis procedure was not further optimized.

Diverse extraction procedures following glucuronide hydrolysis were evaluated in triplicates to assess analytical recovery and matrix effect before method validation. Protein precipitation and concentration achieved good analytical recoveries for all analytes, but also

high ion suppression, precluding their use. We therefore resorted to liquid-liquid extraction, which was mostly used in the scientific literature for the analysis of tryptamines, due to ease and speed of use in routine [116,125,191]. Due to their amine groups, alkaline conditions were necessary to extract the analytes, and ramping concentrations of sodium hydroxide were tested (0.05–1 mol/L), to finally opt for 1 mol/L. Ethyl acetate and dichloromethane, chloroform, diethyl ether, *tert*-butyl methyl ether, and hexane alone or in combination with ethyl acetate (75:5, 50:50, and 25:75; v/v) were tested as extraction solvents. However, dichloromethane, chloroform, and hexane generated substantial matrix effects with average to low recovery for the most polar compounds. A mix of ethyl acetate:diethyl ether (75:25, v/v) or ethyl acetate:*tert*-butyl methyl ether (75:25, v/v) proved to be the best options, but ethyl acetate:diethyl ether (75:25, v/v) was ultimately selected due to faster evaporation during sample extraction. Adding 0.25% HCl in methanol to the extraction solvent before evaporating decreased the tryptamines' volatility and increased analytical recoveries, as observed previously [116,125].

3.1.4. The Particular Case of Tryptamines with an Acetoxy Group

Tryptamines with an acetoxy group were completely cleaved during the extraction in alkaline conditions by nucleophilic attack. 4-AcO-DiPT and 4-AcO-DMT were therefore detected as 4-OH-DiPT and 4-OH-DMT, respectively. However, due to the acetoxy group proneness to metabolization in tryptamines, as observed with 4-AcO-DiPT in hepatocyte incubations [157], the detection of tryptamines or metabolites with an acetoxy group is unlikely in urine. 4-AcO-DiPT recovery and matrix effect could not be properly evaluated in the present experiments, as 4-OH-DiPT was not produced in set B) and C) (Section 2.5.6.).

3.2. Human Hepatocyte Incubations

Incubation with 10-donor pooled human hepatocytes proved to effectively predict major metabolite biomarkers of NPS consumption in urine [21,139,152,172,174] and 4-AcO-DiPT, 4-OH-MPT, and α -MT major *in vitro* metabolites were therefore added to the method [157,188,189]. Although all major metabolites were detected after extraction and analysis, it cannot be definitely assumed that these molecules will be extracted in a different matrix, i.e., urine.

3.3. Proof of Method

The method was applied to a real sample from a fatal drug intoxication involving α -MT. α -MT urinary concentration was higher than 50 $\mu\text{g/mL}$, which is consistent with the previous external dosing by LC-MS/MS (> 5 $\mu\text{g/mL}$) [157]. Major metabolites biomarkers

α -MT M1 and M2 were detected in the sample diluted 50 times in blank urine, proving the method suitability to identify cases of α -MT exposure. These metabolites were previously detected in α -MT incubations with human hepatocytes, and no additional biomarker was added to the method after analyzing the sample [157].

3.4. General Considerations

Although the method was validated to quantify 15 psychoactive tryptamines, it can currently be applied to detect 25 analogues and metabolites in total. To the best of the authors' knowledge, this is the most inclusive method reported to date for the detection of tryptamines in human biological samples. Only few methods for quantifying one to four tryptamines in urine for specific applications were reported [114,129,192–194], many authors opting for detection only (up to 15 analogues) [116,120,123–125,127,191]. Although it is true that urinary concentrations have a limited interest in toxicology, the relative abundance of tryptamines and metabolites may be crucial to determine what analogue was taken, considering that many analogues produce common metabolites, which can also be themselves available on the drug market (e.g., 4-AcO-DiPT and 4-OH-DiPT [167]). To the best of the authors' knowledge, the present method is the first method reported to detect 4-OH-DET, 4-OH-MPT, 5-MeO-DPT, and DiPT in urine, and therefore the first method to quantify 4-OH-DET, 4-OH-MPT, and DiPT in urine.

4. Conclusion

We developed a method for the specific and accurate quantification of trace amounts of 15 tryptamines and the detection of 10 additional analogues and metabolites in human urine for clinical and forensic applications. This is the most comprehensive quantification method for tryptamines in biological fluids reported to date, and it can be easily updated to cope with the never-ending emergence of new analogues onto the illicit drug market. This method will help toxicologists identify cases of recreational consumption and intoxication to treat patients, address drug use disorders, and support law enforcement in nipping the tryptamine trend in the bud.

Several tryptamines available on the drug market can also be produced through the metabolism of other analogues, and many tryptamines may share the same metabolites, making challenging the interpretation of urinary findings. However, the metabolism of tryptamines is still poorly understood. New metabolite identification studies and pharmacokinetic studies should be conducted to identify optimal metabolite biomarkers of exposure to the most popular and the most harmful analogues and update the method.

Conclusions

The human metabolic fate of three tryptamines was assessed in 10-donor-pooled human hepatocyte incubations and *postmortem* urine and blood, when available, using *in silico* metabolite predictions, LC-HRMS/MS, and software-assisted data mining. The HRMS/MS fragmentation patterns of newly identified metabolites were proposed to be included into online libraries mzCloud and HighResNPS.

Six 4-AcO-DiPT metabolites were identified following ester hydrolysis, *O*-glucuronidation, *O*-sulfation, *N*-oxidation, and *N*-dealkylation. 4-OH-DiPT, 4-OH-iPT, and 4-OH-DiPT-*N*-oxide are suggested as optimal biomarkers to identify 4-AcO-DiPT consumption. The study was recently published in *Metabolites*: **Malaca S**, Huestis MA, Lattanzio L, Marsella LT, Tagliabracci A, Carlier J*, and Busardò PB. Human hepatocyte 4-acetoxy-*N,N*-diisopropyltryptamine metabolite profiling by reversed-phase liquid chromatography coupled with high-resolution tandem mass spectrometry. *Metabolites*, 2022; 12 (8): 705 (DOI: 10.3390/metabo12080705).

Seven 4-OH-MPT metabolites were identified following *O*-glucuronidation, *O*-sulfation, *N*-oxidation, and *N*-dealkylation. 4-OH-MPT-*N*-oxide and 4-hydroxy-*N,N*-propyltryptamine (4-OH-PT) are suggested as optimal metabolite biomarkers of 4-OH-MPT consumption after glucuronide/sulfate hydrolysis in biological samples to improve the detection of 4-OH-MPT and phase I metabolites; 4-OH-MPT-glucuronide is suggested as an additional biomarker when hydrolysis is not performed. The study was recently published in *Expert Opinion on Drug Metabolism and Toxicology*: Carlier J, **Malaca S**, Huestis MA, Tagliabracci A, Tini A*, and Busardò FP. Biomarkers of 4-hydroxy-*N,N*-methylpropyltryptamine (4-OH-MPT) intake identified from human hepatocyte incubations. *Expert Opin Drug Met Toxicol*, 2023; 18 (12): 831-840 (DOI: 10.1080/17425255.2022.2166826).

Nine α -MT metabolites were identified *in vitro* and eight additional metabolites were found in urine; five metabolites were found in blood. The findings in hepatocyte incubations and *postmortem* samples were consistent, proving the *in vitro* model suitability. Metabolic transformations were hydroxylation, *O*-sulfation, *O*-glucuronidation, *N*-glucuronidation, and *N*-acetylation. α -MT, hydroxy- α -MT glucuronide, and two hydroxy- α -MT sulfates are suggested as biomarkers of α -MT use in non-hydrolyzed urine; α -MT, two hydroxy- α -MT sulfates and *N*-acetyl- α -MT are suggested as biomarkers of α -MT use in blood. The study was recently published in *Metabolites*: **Malaca S**, Bottinelli C, Fanton L, Cartiser N, Carlier J*, and Busardò FP. α -Methyltryptamine (α -MT) metabolite profiling in human hepatocyte incubations and postmortem urine and blood. *Metabolites*, 2023; 13 (1): 92 (DOI: 10.3390/metabo13010092).

These findings underscore how challenging it is to predict NPS metabolism, and demonstrate the value of experimental data. The *in vitro* model studied offers preliminary findings about tryptamines' human metabolism; however, these findings should be

confirmed using samples from authentic positive cases. Further studies on this NPS class in clinical and forensic caseworks with different doses and routes of administration are necessary to better explore tryptamines' metabolism. Additionally, further studies on these substances with different doses and routes of administration are necessary to explore their metabolism. These results provide important data to orientate analytical standard manufacturers' synthesis effort and will help toxicologists identify new cases to generate biological samples to refine the present results.

Proper analytical method for detecting tryptamines and metabolite biomarkers of consumption in biological matrices are essential to identify positive cases in forensic and clinical toxicology. We proposed a method for quantifying 15 tryptamines and detecting 10 additional analogues and metabolites in human urine for clinical and forensic applications. This is the most comprehensive quantification method for tryptamines in biological fluids reported to date, and it can be easily updated to cope with the never-ending emergence of new analogues onto the illicit drug market. Toxicologists will use this method to identify cases of recreational consumption and intoxication in order to treat patients, address drug use disorders, and assist law enforcement in halting the tryptamine trend. Several tryptamines available on the drug market can also be produced by the metabolism of other analogues, and many tryptamines may share the same metabolites, making urinary findings difficult to interpret. However, the metabolism of tryptamines remains poorly comprehended. New metabolite identification and pharmacokinetic studies should be carried out to identify optimal metabolite biomarkers of exposure to the most common and dangerous analogues, and update the present method. The study is currently under consideration for publication in *Talanta*: **Malaca S**, Bottinelli C, Fanton L, Cartiser N, Busardò FP*, and Carlier J. Inclusive screening for the quantification of 15 psychoactive tryptamines and detection of 10 additional analogues and metabolites in human urine by LC-HRMS/MS. *Talanta*, 2023; Submitted.

References

- [1] United Nations Office on Drugs and Crime (UNODC), What are NPS?, (n.d.). <https://www.unodc.org/LSS/Page/NPS> (accessed October 3, 2022).
- [2] United Nations Office on Drugs and Crime (UNODC), Cannabis and hallucinogens, *World Drug Rep.* 2019. (2019) 1–73. doi:10.18356/5b5a0f55-en.
- [3] R.A. Glennon, M. Titeler, J.D. McKenney, Evidence for 5-HT₂ involvement in the mechanism of action of hallucinogenic agents, *Life Sci.* 35 (1984) 2505–2511. doi:10.1016/0024-3205(84)90436-3.
- [4] D.E. Nichols, Hallucinogens, *Pharmacol. Ther.* 101 (2004) 131–181. doi:10.1016/j.pharmthera.2003.11.002.
- [5] M. Titeler, R.A. Lyon, R.A. Glennon, Radioligand binding evidence implicates the brain 5-HT₂ receptor as a site of action for LSD and phenylisopropylamine hallucinogens, *Psychopharmacology (Berl.)* 94 (1988) 213–216. doi:10.1007/BF00176847.
- [6] F.X. Vollenweider, M.F.I. Vollenweider-Scherpenhuyzen, A. Bähler, H. Vogel, D. Hell, Psilocybin induces schizophrenia-like psychosis in humans via a serotonin-2 agonist action, *Neuroreport.* 9 (1998) 3897–3902. doi:10.1097/00001756-199812010-00024.
- [7] A. Rickli, O.D. Moning, M.C. Hoener, M.E. Liechti, Receptor interaction profiles of novel psychoactive tryptamines compared with classic hallucinogens, *Eur. Neuropsychopharmacol.* 26 (2016) 1327–1337. doi:10.1016/J.EURONEURO.2016.05.001.
- [8] D. Baumeister, G. Barnes, G. Giaroli, D. Tracy, Classical hallucinogens as antidepressants? A review of pharmacodynamics and putative clinical roles, *Ther. Adv. Psychopharmacol.* 4 (2014) 156–169. doi:10.1177/2045125314527985/ASSET/IMAGES/LARGE/10.1177_2045125314527985-FIG1.JPEG.
- [9] J.R. Bunzow, M.S. Sonders, S. Arttamangkul, L.M. Harrison, G. Zhang, D.I. Quigley, T. Darland, K.L. Suchland, S. Pasumamula, J.L. Kennedy, S.B. Olson, R.E. Magenis, S.G. Amara, D.K. Grandy, Amphetamine, 3,4-Methylenedioxymethamphetamine, Lysergic Acid Diethylamide, and Metabolites of the Catecholamine Neurotransmitters Are Agonists of a Rat Trace Amine Receptor, *Mol. Pharmacol.* 60 (2001) 1181–1188. doi:10.1124/MOL.60.6.1181.
- [10] N. V. Cozzi, A. Gopalakrishnan, L.L. Anderson, J.T. Feih, A.T. Shulgin, P.F. Daley, A.E. Ruoho, Dimethyltryptamine and other hallucinogenic tryptamines exhibit substrate behavior at the serotonin uptake transporter and the vesicle monoamine transporter, *J. Neural Transm.* 116 (2009) 1591–1599. doi:10.1007/S00702-009-

0308-8/FIGURES/4.

- [11] W.E. Fantegrossi, A.W. Harrington, C.L. Kiessel, J.R. Eckler, R.A. Rabin, J.C. Winter, A. Coop, K.C. Rice, J.H. Woods, Hallucinogen-like actions of 5-methoxy-N,N-diisopropyltryptamine in mice and rats, *Pharmacol. Biochem. Behav.* 83 (2006) 122–129. doi:10.1016/J.PBB.2005.12.015.
- [12] D.J. Mckenna, D.B. Repke, L. Lo, S.J. Peroutka, Differential interactions of indolealkylamines with 5-hydroxytryptamine receptor subtypes, *Neuropharmacology.* 29 (1990) 193–198. doi:10.1016/0028-3908(90)90001-8.
- [13] D. Luethi, M.E. Liechti, Monoamine Transporter and Receptor Interaction Profiles *in Vitro* Predict Reported Human Doses of Novel Psychoactive Stimulants and Psychedelics, *Int. J. Neuropsychopharmacol.* 21 (2018) 926–931. doi:10.1093/IJNP/PYY047.
- [14] R.G. dos Santos, J.E.C. Hallak, Therapeutic use of serotonergic hallucinogens: A review of the evidence and of the biological and psychological mechanisms, *Neurosci. Biobehav. Rev.* 108 (2020) 423–434. doi:10.1016/J.NEUBIOREV.2019.12.001.
- [15] T.S. Ray, Psychedelics and the human receptorome, *PLoS One.* 5 (2010). doi:10.1371/JOURNAL.PONE.0009019.
- [16] Global Drug Survey (GDS), GDS Key Finding 2019, (n.d.). https://issuu.com/globaldrugsurvey/docs/gds2019_key_findings_report_may_16_?utm_medium=referral&utm_source=www.globaldrugsurvey.com (accessed February 20, 2023).
- [17] A.R. Winstock, Global Drug Survey, n.d. www.globaldrugsurvey.com (accessed February 20, 2023).
- [18] E. Marchei, S. Malaca, S. Graziano, M. Gottardi, S. Pichini, F.P. Busardò, Stability and degradation pathways of different psychoactive drugs in neat and in buffered oral fluid, *J. Anal. Toxicol.* 44 (2020) 570–579. doi:10.1093/JAT/BKZ114.
- [19] E. Marchei, R. Pacifici, G. Mannocchi, E. Marinelli, F.P. Busardò, S. Pichini, New synthetic opioids in biological and non-biological matrices: A review of current analytical methods, *TrAC - Trends Anal. Chem.* 102 (2018) 1–15. doi:10.1016/J.TRAC.2018.01.007.
- [20] A.F. Lo Faro, A. Di Trana, N. La Maida, A. Tagliabracci, R. Giorgetti, F.P. Busardò, Biomedical analysis of New Psychoactive Substances (NPS) of natural origin, *J. Pharm. Biomed. Anal.* 179 (2020). doi:10.1016/J.JPBA.2019.112945.
- [21] F.P. Busardò, A.F. Lo Faro, A. Sirignano, R. Giorgetti, J. Carlier, *In silico*, *in vitro*, and *in vivo* human metabolism of acetazolamide, a carbonic anhydrase inhibitor and common “diuretic and masking agent” in doping, *Arch. Toxicol.* 96 (2022) 1989–2001. doi:10.1007/S00204-022-03289-Z/FIGURES/4.

- [22] A. Giorgetti, F.P. Busardò, R. Tittarelli, V. Auwärter, R. Giorgetti, Post-Mortem Toxicology: A Systematic Review of Death Cases Involving Synthetic Cannabinoid Receptor Agonists, *Front. Psychiatry*. 11 (2020) 1–22. doi:10.3389/FPSYT.2020.00464.
- [23] M. Wilde, S. Pichini, R. Pacifici, A. Tagliabracci, F.P. Busardò, V. Auwärter, R. Solimini, Metabolic Pathways and Potencies of New Fentanyl Analogs, *Front. Pharmacol.* 10 (2019). doi:10.3389/FPHAR.2019.00238.
- [24] F.P. Busardò, J. Carlier, R. Giorgetti, A. Tagliabracci, R. Pacifici, M. Gottardi, S. Pichini, Ultra-High-Performance Liquid Chromatography-Tandem Mass Spectrometry Assay for Quantifying Fentanyl and 22 Analogs and Metabolites in Whole Blood, Urine, and Hair, *Front. Chem.* 7 (2019). doi:10.3389/FCHEM.2019.00184.
- [25] R. Tittarelli, G. Mannocchi, F. Pantano, F. Romolo, Recreational use, analysis and toxicity of tryptamines, *Curr. Neuropharmacol.* 13 (2015) 26–46. doi:10.2174/1570159X13666141210222409.
- [26] A.M. Araújo, F. Carvalho, M. de L. Bastos, P. Guedes de Pinho, M. Carvalho, The hallucinogenic world of tryptamines: an updated review, *Arch. Toxicol.* 89 (2015) 1151–1173. doi:10.1007/s00204-015-1513-x.
- [27] S.J. Murch, S.S.B. Campbell, P.K. Saxena, The role of serotonin and melatonin in plant morphogenesis: Regulation of auxin-induced root organogenesis in *in vitro*-cultured explants of St. John's wort (*hypericum perforatum* L.), *Vitr. Cell. Dev. Biol. Plant.* 37 (2001) 786–793. doi:10.1079/IVP2001235.
- [28] D. McKenna, J. Riba, New World Tryptamine Hallucinogens and the Neuroscience of Ayahuasca, *Curr. Top. Behav. Neurosci.* 36 (2018) 283–311. doi:10.1007/7854_2016_472.
- [29] S. Szára, DMT at fifty., *Neuropsychopharmacol. Hung.* 9 (2007) 201–205.
- [30] R.J. Strassman, C.R. Qualls, Dose-response study of N,N-dimethyltryptamine in humans. I. Neuroendocrine, autonomic, and cardiovascular effects, *Arch. Gen. Psychiatry.* 51 (1994) 85–97. doi:10.1001/ARCHPSYC.1994.03950020009001.
- [31] V. Erspamer, Observations on the fate of indolalkylamines in the organism, *J. Physiol.* 127 (1955) 118–133. doi:10.1113/JPHYSIOL.1955.SP005242.
- [32] S. Pichini, R. Pacifici, *Smart Drugs*, terza edizione, Dip. Del Farm. Ist. Super. Di Sanità. (2011).
- [33] K.W. Tupper, E. Wood, R. Yensen, M.W. Johnson, Psychedelic medicine: a re-emerging therapeutic paradigm, *CMAJ.* 187 (2015) 1054–1059. doi:10.1503/CMAJ.141124.
- [34] G. Słonina, K. Janczura, New psychoactive substances in Poland : An overview of

- psychodysleptics (lysergamides and tryptamines), *World Psychiatry*. 109 (2018) 245–262.
- [35] R.W. Bussmann, *Anadenanthera*. Visionary Plant of Ancient South America, *Econ. Bot.* 60 (2006) 302–302. doi:10.1663/0013-0001(2006)60[302:avpoas]2.0.co;2.
- [36] N.E. Paterson, W.C. Darby, P.S. Sandhu, N,N-Dimethyltryptamine-Induced Psychosis, *Clin. Neuropharmacol.* 38 (2015) 141–143. doi:10.1097/WNF.0000000000000078.
- [37] M.H. Bilhimer, R.F. Schult, K. V. Higgs, T.J. Wiegand, R.M. Gorodetsky, N.M. Acquistio, Acute Intoxication following Dimethyltryptamine Ingestion, *Case Rep. Emerg. Med.* 2018 (2018) 1–3. doi:10.1155/2018/3452691.
- [38] European Monitoring Centre for Drugs and Drug Addiction (EMCCDA), Hallucinogenic mushrooms drug profile, (n.d.). https://www.emcdda.europa.eu/publications/drug-profiles/hallucinogenic-mushrooms_en (accessed February 20, 2023).
- [39] A. Hofmann, R. Heim, A. Brack, H. Kobel, [Psilocybin, a psychotropic substance from the Mexican mushroom *Psilocybe mexicana* Heim], *Experientia*. 14 (1958) 107–109. doi:10.1007/BF02159243.
- [40] M. Pellegrini, M.C. Rotolo, E. Marchei, R. Pacifici, F. Saggio, S. Pichini, Magic truffles or Philosopher’s stones: a legal way to sell psilocybin?, *Drug Test. Anal.* 5 (2013) 182–185. doi:10.1002/DTA.1400.
- [41] D.E. Nichols, M.W. Johnson, C.D. Nichols, Psychedelics as Medicines: An Emerging New Paradigm, *Clin. Pharmacol. Ther.* 101 (2017) 209–219. doi:10.1002/CPT.557.
- [42] L.P. Cameron, A. Nazarian, D.E. Olson, Psychedelic Microdosing: Prevalence and Subjective Effects, *J. Psychoactive Drugs.* 52 (2020) 113–122. doi:10.1080/02791072.2020.1718250.
- [43] E. Honyiglo, A. Franchi, N. Cartiser, C. Bottinelli, A.S. Advenier, F. Bévalot, L. Fanton, Unpredictable Behavior Under the Influence of “Magic Mushrooms”: A Case Report and Review of the Literature, *J. Forensic Sci.* 64 (2019) 1266–1270. doi:10.1111/1556-4029.13982.
- [44] R.L. Carhart-Harris, M. Bolstridge, J. Rucker, C.M.J. Day, D. Erritzoe, M. Kaelen, M. Bloomfield, J.A. Rickard, B. Forbes, A. Feilding, D. Taylor, S. Pilling, V.H. Curran, D.J. Nutt, Psilocybin with psychological support for treatment-resistant depression: an open-label feasibility study, *The Lancet. Psychiatry*. 3 (2016) 619–627. doi:10.1016/S2215-0366(16)30065-7.
- [45] R.R. Griffiths, M.W. Johnson, M.A. Carducci, A. Umbricht, W.A. Richards, B.D. Richards, M.P. Cosimano, M.A. Klinedinst, Psilocybin produces substantial and sustained decreases in depression and anxiety in patients with life-threatening

- cancer: A randomized double-blind trial, *J. Psychopharmacol.* 30 (2016) 1181–1197. doi:10.1177/0269881116675513.
- [46] C.S. Grob, A.L. Danforth, G.S. Chopra, M. Hagerty, C.R. McKay, A.L. Halberstad, G.R. Greer, Pilot study of psilocybin treatment for anxiety in patients with advanced-stage cancer, *Arch. Gen. Psychiatry.* 68 (2011) 71–78. doi:10.1001/ARCHGENPSYCHIATRY.2010.116.
- [47] R.L. Carhart-Harris, M. Bolstridge, C.M.J. Day, J. Rucker, R. Watts, D.E. Erritzoe, M. Kaelen, B. Giribaldi, M. Bloomfield, S. Pilling, J.A. Rickard, B. Forbes, A. Feilding, D. Taylor, H. V. Curran, D.J. Nutt, Psilocybin with psychological support for treatment-resistant depression: six-month follow-up, *Psychopharmacology (Berl).* 235 (2018) 399–408. doi:10.1007/s00213-017-4771-x.
- [48] S. Ross, A. Bossis, J. Guss, G. Agin-Liebes, T. Malone, B. Cohen, S.E. Mennenga, A. Belser, K. Kalliontzi, J. Babb, Z. Su, P. Corby, B.L. Schmidt, Rapid and sustained symptom reduction following psilocybin treatment for anxiety and depression in patients with life-threatening cancer: a randomized controlled trial, *J. Psychopharmacol.* 30 (2016) 1165–1180. doi:10.1177/0269881116675512.
- [49] M.W. Johnson, A. Garcia-Romeu, M.P. Cosimano, R.R. Griffiths, Pilot study of the 5-HT_{2A}R agonist psilocybin in the treatment of tobacco addiction, *J. Psychopharmacol.* 28 (2014) 983–992. doi:10.1177/0269881114548296.
- [50] M.P. Bogenschutz, A.A. Forcehimes, J.A. Pommy, C.E. Wilcox, P. Barbosa, R.J. Strassman, Psilocybin-assisted treatment for alcohol dependence: a proof-of-concept study, *J. Psychopharmacol.* 29 (2015) 289–299. doi:10.1177/0269881114565144.
- [51] A.K. Davis, J.P. Barsuglia, R. Lancelotta, R.M. Grant, E. Renn, The epidemiology of 5-methoxy- N, N-dimethyltryptamine (5-MeO-DMT) use: Benefits, consequences, patterns of use, subjective effects, and reasons for consumption, *J. Psychopharmacol.* 32 (2018) 779–792. doi:10.1177/0269881118769063.
- [52] H.-W. Shen, X.-L. Jiang, J. C. Winter, A.-M. Yu, Psychedelic 5-methoxy-N,N-dimethyltryptamine: metabolism, pharmacokinetics, drug interactions, and pharmacological actions, *Curr. Drug Metab.* 11 (2010) 659–666. doi:10.2174/138920010794233495.
- [53] B.R. Sitaram, W.R. McLeod, Observations on the metabolism of the psychotomimetic indolealkylamines: implications for future clinical studies, *Biol. Psychiatry.* 28 (1990) 841–848. doi:10.1016/0006-3223(90)90566-K.
- [54] B.R. Sitaram, L. Lockett, G.L. Blackman, W.R. McLeod, Urinary excretion of 5-methoxy-N,N-dimethyltryptamine, N,N-dimethyltryptamine and their N-oxides in the rat, *Biochem. Pharmacol.* 36 (1987) 2235–2237. doi:10.1016/0006-2952(87)90159-6.
- [55] J. Sklerov, B. Levine, K.A. Moore, T. King, D. Fowler, A fatal intoxication following the ingestion of 5-methoxy-N,N-dimethyltryptamine in an ayahuasca

- preparation, *J. Anal. Toxicol.* 29 (2005) 838–841. doi:10.1093/JAT/29.8.838.
- [56] Dipartimento Politiche Antidroga, Tryptamine, (2013) 809–832. https://www.politicheantidroga.gov.it/media/1286/36_triptamine.pdf (accessed November 9, 2022).
- [57] D.B. Rusterholz, J.P. Long, D.E. Nichols, Effect of alpha-methyltryptamine on spontaneous activity in mice, *Pharmacol. Biochem. Behav.* 10 (1979) 223–227. doi:10.1016/0091-3057(79)90091-1.
- [58] Ryan, Cooper, Tauer, WHO Expert Committee on Drug Dependence, *Pap. Knowl. Towar. a Media Hist. Doc.* (2013) 12–26.
- [59] J. Wilcox, Psychoactive properties of alpha-methyltryptamine: analysis from self reports of users, *J. Psychoactive Drugs.* 44 (2012) 274–276. doi:10.1080/02791072.2012.704592.
- [60] H. Long, L.S. Nelson, R.S. Hoffman, Alpha-methyltryptamine revisited via easy Internet access - PubMed, *Vet. Hum. Toxicol.* 3 (2003) 149. <https://pubmed.ncbi.nlm.nih.gov/12776793/> (accessed November 10, 2022).
- [61] D.M. Boland, W. Andollo, G.W. Hime, W. Lee Hearn, Fatality Due to Acute 0 Methyltryptamine Intoxication, *J. Anal. Toxicol.* 29 (n.d.). <https://academic.oup.com/jat/article/29/5/394/730696> (accessed November 9, 2022).
- [62] T. Kanamori, K. Kuwayama, K. Tsujikawa, H. Miyaguchi, Y.T. Iwata, H. Inoue, *In vivo* metabolism of alpha-methyltryptamine in rats: identification of urinary metabolites, *Xenobiotica.* 38 (2008) 1476–1486. doi:10.1080/00498250802491654.
- [63] European Monitoring Centre for Drugs and Drug Addiction (EMCDDA), *European Drug Report*, (2018). https://www.emcdda.europa.eu/system/files/publications/8585/20181816_TDAT18001ENN_PDF.pdf (accessed November 10, 2022).
- [64] R.A. Glennon, T. Bondareva, R. Young, alpha-Ethyltryptamine (alpha-ET) as a discriminative stimulus in rats, *Pharmacol. Biochem. Behav.* 85 (2006) 448–453. doi:10.1016/J.PBB.2006.09.014.
- [65] T. Daldrup, C. Heller, U. Matthiesen, S. Honus, A. Bresges, K. Haarhoff, Etryptamine, a new designer drug with a fatal effect, *Z. Rechtsmed.* 97 (1986) 61–68. doi:10.1007/BF00200960.
- [66] Drug Enforcement Administration Toxicology Testing Program (DEA TOX), *Drugs of Abuse, A DEA resource guide*, (n.d.).
- [67] X. Huang, M.P. Johnson, D.E. Nichols, Reduction in brain serotonin markers by alpha-ethyltryptamine (Monase), *Eur. J. Pharmacol.* 200 (1991) 187–190. doi:10.1016/0014-2999(91)90686-K.
- [68] S. Malaca, A.F. Lo Faro, A. Tamborra, S. Pichini, F.P. Busardò, M.A. Huestis,

- Toxicology and Analysis of Psychoactive Tryptamines, *Int. J. Mol. Sci.* 21 (2020) 1–38. doi:10.3390/IJMS21239279.
- [69] E.J. Massaro, *Handbook of Neurotoxicology*, Humana Press: Totowa, NJ, USA, 2002.
- [70] European Monitoring Centre for Drugs and Drug Addiction (EMCDDA), *New psychoactive substances in Europe*, 2018.
- [71] K.M. Krebs, M.A. Geyer, Behavioral characterization of alpha-ethyltryptamine, a tryptamine derivative with MDMA-like properties in rats, *Psychopharmacology (Berl)*. 113 (1993) 284–287. doi:10.1007/BF02245712.
- [72] Diethyltryptamine, (n.d.). <https://www.chemurope.com/en/encyclopedia/Diethyltryptamine.html> (accessed February 20, 2023).
- [73] Drug bank, Diethyltryptamine: Uses, Interactions, Mechanism of Action, (n.d.). <https://go.drugbank.com/drugs/DB01460> (accessed February 20, 2023).
- [74] S. Szara, L.H. Rockland, D. Rosenthal, J.H. Handlon, Psychological effects and metabolism of N,N-diethyltryptamine in man, *Arch. Gen. Psychiatry*. 15 (1966) 320–329. doi:10.1001/ARCHPSYC.1966.01730150096014.
- [75] R.R. Laing, *Hallucinogens : a forensic drug handbook*, (2003) 290.
- [76] S.A. Barker, J. Borjigin, I. Lomnicka, R. Strassman, LC/MS/MS analysis of the endogenous dimethyltryptamine hallucinogens, their precursors, and major metabolites in rat pineal gland microdialysate, *Biomed. Chromatogr.* 27 (2013) 1690–1700. doi:10.1002/BMC.2981.
- [77] S. Grof, R.A. Soskin, W.A. Richards, A.A. Kurland, DPT as an adjunct in psychotherapy of alcoholics, *Int. Pharmacopsychiatry*. 8 (1973) 104–115. doi:10.1159/000467979.
- [78] Eurowid, Erowid Search Results for DPT, (n.d.). <https://www.erowid.org/search.php?exclude=&q=DPT&x=0&y=0> (accessed February 20, 2023).
- [79] H. V. Thiagaraj, E.B. Russo, A. Burnett, E. Goldstein, C.M. Thompson, K.K. Parker, Binding properties of dipropyltryptamine at the human 5-HT_{1a} receptor, *Pharmacology*. 74 (2005) 193–199. doi:10.1159/000085649.
- [80] W.E. Fantegrossi, C.J. Reissig, E.B. Katz, H.L. Yarosh, K.C. Rice, J.C. Winter, Hallucinogen-like effects of N,N-dipropyltryptamine (DPT): possible mediation by serotonin 5-HT_{1A} and 5-HT_{2A} receptors in rodents, *Pharmacol. Biochem. Behav.* 88 (2008) 358–365. doi:10.1016/J.PBB.2007.09.007.
- [81] J.M. Dailey, R.M.; Nelson, L.D.; Scaglione, Tachycardia and rhabdomyolysis after intentional ingestion of N,N-Dipropyltryptamine, *J. Toxicol. Clin. Toxicol.* 41

(2003) 742–743.

- [82] M.B. Gatch, M.J. Forster, A. Janowsky, A.J. Eshleman, Abuse liability profile of three substituted tryptamines, *J. Pharmacol. Exp. Ther.* 338 (2011) 280–289. doi:10.1124/JPET.111.179705.
- [83] A. Shulgin, A.; Shulgin, *Tryptamines that I Have Known and Loved (TiHKAL): The Continuation*, first, 1997.
- [84] D.B. Repke, W.J. Ferguson, D.K. Bates, Psilocin analogs II. Synthesis of 3-[2-(dialkylamino)ethyl]-, 3-[2-(N-methyl-N-alkylamino)ethyl]-, and 3-[2-(cycloalkylamino)ethyl]indol-4-ols, *J. Heterocycl. Chem.* 18 (1981) 175–179. doi:10.1002/JHET.5570180131.
- [85] Eurowid, 4-HO-DPT & 4-AcO-DALT - “A Report on 6-Carbon Tryptamines,” (n.d.). <https://erowid.org/experiences/exp.php?ID=101510> (accessed February 22, 2023).
- [86] Eurowid, *A Mirror to the Mind*, (n.d.). <https://erowid.org/experiences/exp.php?ID=94380>.
- [87] J.M. Sciani, C.B. Angeli, M.M. Antoniazzi, C. Jared, D.C. Pimenta, Differences and similarities among parotoid macrogland secretions in South American toads: a preliminary biochemical delineation, *ScientificWorldJournal*. 2013 (2013). doi:10.1155/2013/937407.
- [88] Britannica, *Bufotenine, Definition, Uses, Effects, and Facts*, (n.d.). <https://www.britannica.com/science/bufotenine> (accessed February 22, 2023).
- [89] M. Dobbs, *Clinical Neurotoxicology Syndromes, Substances, Environments*, first, Saunders: Philadelphia, PA, USA, 2009.
- [90] P. Keomany, S.; Mayxay, M.; Souvannasing, P.; Vilayhong, C.; Stuart, B.L.; Srour, L.; Newton, *Toad poisoning in Laos*, *Am. J. Trop. Med. Hyg.* 77 (2007) 850–853.
- [91] A.T. Weil, W. Davis, *Bufo alvarius: a potent hallucinogen of animal origin*, *J. Ethnopharmacol.* 41 (1994) 1–8. doi:10.1016/0378-8741(94)90051-5.
- [92] J. Ott, *Pharmañopo—Psychonautics: Human intranasal, sublingual, intrarectal, pulmonary and oral pharmacology of bufotenine*, *J. Psychoactive Drugs.* 33 (2001) 273–281. doi:10.1080/02791072.2001.10400574.
- [93] T.L. Postma, *Neurotoxic animal poisons and venoms*, *Clin. Neurotoxicol. Syndr. Subst. Env.* (2009) 463–489.
- [94] *Alpha-methyltryptamine revisited via easy Internet access*, (n.d.). <https://pubmed.ncbi.nlm.nih.gov/12776793/> (accessed February 20, 2023).
- [95] D.E.A. (DEA), *Methoxy-N,N-Diisopropyltryptamine (Street Names: Foxy, or Foxy Methoxy)*, (n.d.). http://www.deadiversion.usdoj.gov/drug_chem_info/5meodipt.pdf.

- [96] K. Noworyta-Sokołowska, K. Kamińska, G. Kreiner, Z. Rogóż, K. Gołombiowska, Neurotoxic Effects of 5-MeO-DIPT: A Psychoactive Tryptamine Derivative in Rats, *Neurotox. Res.* 30 (2016) 606–619. doi:10.1007/S12640-016-9654-0.
- [97] M.F. Shulgin, A.T.; Carter, N,N-Diisopropyltryptamine (DIPT) and 5-methoxy-N,N-diisopropyltryptamine (5-MeO-DIPT). Two Orally Active Tryptamine Analogs With CNS Activity, *Commun. Psychopharmacol.* 4 (1980) 363–369.
- [98] H.W. Shen, X.L. Jiang, A.M. Yu, Nonlinear pharmacokinetics of 5-methoxy-N,N-dimethyltryptamine in mice, *Drug Metab. Dispos.* 39 (2011) 1227–1234. doi:10.1124/DMD.111.039107.
- [99] T. Kamata, M. Katagi, H.T. Kamata, A. Miki, N. Shima, K. Zaitso, M. Nishikawa, E. Tanaka, K. Honda, H. Tsuchihashi, Metabolism of the psychotomimetic tryptamine derivative 5-methoxy-N,N-diisopropyltryptamine in humans: identification and quantification of its urinary metabolites, *Drug Metab. Dispos.* 34 (2006) 281–287. doi:10.1124/DMD.105.005835.
- [100] J.M. Wilson, F. McGeorge, S. Smolinske, R. Meatherall, A foxy intoxication, *Forensic Sci. Int.* 148 (2005) 31–36. doi:10.1016/j.forsciint.2004.04.017.
- [101] S.C. Smolinske, R. Rastogi, S. Schenkel, Foxy methoxy: a new drug of abuse., *J. Med. Toxicol.* 1 (2005) 23–25. doi:10.1007/bf03160901.
- [102] R. Meatherall, P. Sharma, Foxy, a designer tryptamine hallucinogen, *J. Anal. Toxicol.* 27 (2003) 313–317. doi:10.1093/JAT/27.5.313.
- [103] J.M. Corkery, E. Durkin, S. Elliott, F. Schifano, A.H. Ghodse, The recreational tryptamine 5-MeO-DALT (N,N-diallyl-5-methoxytryptamine): a brief review, *Prog. Neuropsychopharmacol. Biol. Psychiatry.* 39 (2012) 259–262. doi:10.1016/J.PNPBP.2012.05.022.
- [104] J.A. Michely, A.G. Helfer, S.D. Brandt, M.R. Meyer, H.H. Maurer, Metabolism of the new psychoactive substances N,N-diallyltryptamine (DALT) and 5-methoxy-DALT and their detectability in urine by GC-MS, LC-MSn, and LC-HR-MS-MS, *Anal. Bioanal. Chem.* 407 (2015). doi:10.1007/S00216-015-8955-0.
- [105] Erowid 5-MeO-MIPT Vault : Dosage, (n.d.). https://www.erowid.org/chemicals/5meo_mipt/5meo_mipt_dose.shtml (accessed February 22, 2023).
- [106] D.B. Repke, D.B. Grotjahn, A.T. Shulgin, Psychotomimetic N-methyl-N-isopropyltryptamines. Effects of variation of aromatic oxygen substituents, *J. Med. Chem.* 28 (1985) 892–896. doi:10.1021/JM00145A007.
- [107] Cayman Chemical, Product Information for 5-Methoxy DET (5-MeO DET, 5-methoxy-N,N-Diethyltryptamine), (n.d.). <https://www.caymanchem.com/pdfs/17300.pdf>.

- [108] K.E. Grafinger, M. Hädener, S. König, W. Weinmann, Study of the *in vitro* and *in vivo* metabolism of the tryptamine 5-MeO-MiPT using human liver microsomes and real case samples, *Drug Test. Anal.* 10 (2018) 562–574. doi:10.1002/DTA.2245.
- [109] E. Shimizu, H. Watanabe, T. Kojima, H. Hagiwara, M. Fujisaki, R. Miyatake, K. Hashimoto, M. Iyo, Combined intoxication with methylone and 5-MeO-MIPT, *Prog. Neuropsychopharmacol. Biol. Psychiatry.* 31 (2007) 288–291. doi:10.1016/J.PNPBP.2006.06.012.
- [110] Experiences - 5-MeO-MET | Drugs-Forum, (n.d.). <https://drugs-forum.com/threads/5-meo-met.40412/> (accessed February 22, 2023).
- [111] A. Wohlfarth, W. Weinmann, S. Dresen, LC-MS/MS screening method for designer amphetamines, tryptamines, and piperazines in serum, *Anal. Bioanal. Chem.* 396 (2010) 2403–2414. doi:10.1007/S00216-009-3394-4/TABLES/3.
- [112] C.D.R. Oliveira, G.G. Okai, J.L. Da Costa, R.M. De Almeida, D. Oliveira-Silva, M. Yonamine, Determination of dimethyltryptamine and β -carbolines (ayahuasca alkaloids) in plasma samples by LC–MS/MS, <Http://Dx.Doi.Org/10.4155/Bio.12.124>. 4 (2012) 1731–1738. doi:10.4155/BIO.12.124.
- [113] R. Martin, J. Schürenkamp, H. Pfeiffer, H. Köhler, A validated method for quantitation of psilocin in plasma by LC-MS/MS and study of stability, *Int. J. Legal Med.* 126 (2012) 845–849. doi:10.1007/S00414-011-0652-8/FIGURES/2.
- [114] R. Martin, J. Schürenkamp, A. Gasse, H. Pfeiffer, H. Köhler, Determination of psilocin, bufotenine, LSD and its metabolites in serum, plasma and urine by SPE-LC-MS/MS, *Int. J. Legal Med.* 127 (2013) 593–601. doi:10.1007/S00414-012-0796-1/TABLES/7.
- [115] L. Ambach, A. Hernández Redondo, S. König, W. Weinmann, Rapid and simple LC-MS/MS screening of 64 novel psychoactive substances using dried blood spots, *Drug Test. Anal.* 6 (2014) 367–375. doi:10.1002/DTA.1505.
- [116] L. Ambach, A. Hernández Redondo, S. König, V. Angerer, S. Schürch, W. Weinmann, Detection and quantification of 56 new psychoactive substances in whole blood and urine by LC-MS/MS, *Bioanalysis.* 7 (2015) 1119–1136. doi:10.4155/BIO.15.48.
- [117] S. Odoardi, M. Fisichella, F.S. Romolo, S. Strano-Rossi, High-throughput screening for new psychoactive substances (NPS) in whole blood by DLLME extraction and UHPLC–MS/MS analysis, *J. Chromatogr. B.* 1000 (2015) 57–68. doi:10.1016/J.JCHROMB.2015.07.007.
- [118] R. Martin, J. Schürenkamp, A. Gasse, H. Pfeiffer, H. Köhler, Analysis of Psilocin, Bufotenine and LSD in Hair, *J. Anal. Toxicol.* 39 (2015) 126–129. doi:10.1093/JAT/BKU141.

- [119] P. Adamowicz, B. Tokarczyk, Simple and rapid screening procedure for 143 new psychoactive substances by liquid chromatography-tandem mass spectrometry, *Drug Test. Anal.* 8 (2016) 652–667. doi:10.1002/DTA.1815.
- [120] S.D. Brandt, P. V. Kavanagh, G. Dowling, B. Talbot, F. Westphal, M.R. Meyer, H.H. Maurer, A.L. Halberstadt, Analytical characterization of N,N-diallyltryptamine (DALT) and 16 ring-substituted derivatives, *Drug Test. Anal.* 9 (2017) 115–126. doi:10.1002/dta.1974.
- [121] F. Vaiano, F.P. Busardò, D. Palumbo, C. Kyriakou, A. Fioravanti, V. Catalani, F. Mari, E. Bertol, A novel screening method for 64 new psychoactive substances and 5 amphetamines in blood by LC–MS/MS and application to real cases, *J. Pharm. Biomed. Anal.* 129 (2016) 441–449. doi:10.1016/J.JPBA.2016.07.009.
- [122] H. Gjerde, T. Nordfjærn, A.L. Bretteville-Jensen, M. Edland-Gryt, H. Furuhaugen, R. Karinen, E.L. Øiestad, Comparison of drugs used by nightclub patrons and criminal offenders in Oslo, Norway, *Forensic Sci. Int.* 265 (2016) 1–5. doi:10.1016/J.FORSCIINT.2015.12.029.
- [123] D. Fabregat-Safont, M. Barneo-Muñoz, F. Martinez-Garcia, J. V. Sancho, F. Hernández, M. Ibáñez, Proposal of 5-methoxy-N-methyl-N-isopropyltryptamine consumption biomarkers through identification of *in vivo* metabolites from mice, *J. Chromatogr. A.* 1508 (2017) 95–105. doi:10.1016/J.CHROMA.2017.06.010.
- [124] J.A. Michely, S.D. Brandt, M.R. Meyer, H.H. Maurer, Biotransformation and detectability of the new psychoactive substances N,N-diallyltryptamine (DALT) derivatives 5-fluoro-DALT, 7-methyl-DALT, and 5,6-methylenedioxy-DALT in urine using GC-MS, LC-MSn, and LC-HR-MS/MS, *Anal. Bioanal. Chem.* 409 (2017) 1681–1695. doi:10.1007/S00216-016-0117-5.
- [125] M. Fagiola, T. Hahn, J. Avella, Screening of Novel Psychoactive Substances in Postmortem Matrices by Liquid Chromatography-Tandem Mass Spectrometry (LC-MS-MS), *J. Anal. Toxicol.* 42 (2018) 562–569. doi:10.1093/JAT/BKY050.
- [126] R. Wang, P. Xiang, Z. Yu, Y. Shi, Application of hair analysis to document illegal 5-methoxy-N,N-dissopropyltrptamine (5-MeO-DIPT) use, *Forensic Sci. Int.* 304 (2019) 109972. doi:10.1016/J.FORSCIINT.2019.109972.
- [127] J.D. Pope, K.W. Choy, O.H. Drummer, H.G. Schneider, Harmala Alkaloids Identify Ayahuasca Intoxication in a Urine Drug Screen, *J. Anal. Toxicol.* 43 (2019) e23–e27. doi:10.1093/JAT/BKY105.
- [128] X. Yan, P. Xiang, Y. Zhao, Z. Yu, H. Yan, Determination of 5-MeO-DIPT in Human Urine Using Gas Chromatography Coupled with High-Resolution Orbitrap Mass Spectrometry, *J. Anal. Toxicol.* 44 (2020) 461–469. doi:10.1093/JAT/BKAA005.
- [129] X. Yan, S. Yuan, Z. Yu, Y. Zhao, S. Zhang, H. Wu, H. Yan, P. Xiang, Development of an LC-MS/MS method for determining 5-MeO-DIPT in dried urine spots and

application to forensic cases, *J. Forensic Leg. Med.* 72 (2020).
doi:10.1016/J.JFLM.2020.101963.

- [130] Y. Shi, R. Wang, S. Yuan, H. Qiang, M. Shen, B. Shen, O.H. Drummer, Z. Yu, Y. Zhao, P. Xiang, UHPLC-MS/MS method for simultaneously detecting 16 tryptamines and their metabolites in human hair and applications to real forensics cases, *J. Chromatogr. B Anal. Technol. Biomed. Life Sci.* 1159 (2020) 122392. doi:10.1016/j.jchromb.2020.122392.
- [131] F.K. Nzekoue, M. Agostini, M. Verboni, C. Renzoni, L. Alfieri, S. Barocci, M. Ricciutelli, G. Caprioli, S. Lucarini, A comprehensive UHPLC-MS/MS screening method for the analysis of 98 New Psychoactive Substances and related compounds in human hair, *J. Pharm. Biomed. Anal.* 205 (2021). doi:10.1016/J.JPBA.2021.114310.
- [132] D. Luethi, K.E. Kolaczynska, S.B. Vogt, L. Ley, L. Erne, M.E. Liechti, U. Duthaler, Liquid chromatography-tandem mass spectrometry method for the bioanalysis of N,N-dimethyltryptamine (DMT) and its metabolites DMT-N-oxide and indole-3-acetic acid in human plasma, *J. Chromatogr. B. Analyt. Technol. Biomed. Life Sci.* 1213 (2022). doi:10.1016/J.JCHROMB.2022.123534.
- [133] E. Eckernäs, A. Bendrioua, C. Cancellarini, C. Timmermann, R. Carhart-Harris, K.J. Hoffmann, M. Ashton, Development and application of a highly sensitive LC-MS/MS method for simultaneous quantification of N,N-dimethyltryptamine and two of its metabolites in human plasma, *J. Pharm. Biomed. Anal.* 212 (2022). doi:10.1016/J.JPBA.2022.114642.
- [134] M. Fagiola, T. Hahn, J. Avella, Screening of Novel Psychoactive Substances in Postmortem Matrices by Liquid Chromatography–Tandem Mass Spectrometry (LC–MS–MS), *J. Anal. Toxicol.* 42 (2018) 562–569. doi:10.1093/JAT/BKY050.
- [135] Eurowid, Erowid 4-Acetoxy-DiPT Vault : Legal Status, (n.d.). https://erowid.org/chemicals/4_acetoxy_dipt/4_acetoxy_dipt_law.shtml (accessed February 22, 2023).
- [136] C. Stork, G. Embruch, M. Šícho, C. De Bruyn Kops, Y. Chen, D. Svozil, J. Kirchmair, NERDD: a web portal providing access to *in silico* tools for drug discovery, *Bioinformatics.* 36 (2020) 1291–1292. doi:10.1093/BIOINFORMATICS/BTZ695.
- [137] A. Di Trana, P. Brunetti, R. Giorgetti, E. Marinelli, S. Zaami, F.P. Busardò, J. Carlier, *In silico* prediction, LC-HRMS/MS analysis, and targeted/untargeted data-mining workflow for the profiling of phenylfentanyl *in vitro* metabolites., *Talanta.* 235 (2021) 122740. doi:10.1016/j.talanta.2021.122740.
- [138] Y. Zhang, B. Yuan, N. Takagi, H. Wang, Y. Zhou, N. Si, J. Yang, X. Wei, H. Zhao, B. Bian, Comparative Analysis of Hydrophilic Ingredients in Toad Skin and Toad Venom Using the UHPLC-HR-MS/MS and UPLC-QqQ-MS/MS Methods Together with the Anti-Inflammatory Evaluation of Indolealkylamines, *Mol.* 2019, Vol. 24,

- [139] J. Carlier, X. Diao, M.A. Huestis, Synthetic cannabinoid BB-22 (QUCHIC): Human hepatocytes metabolism with liquid chromatography-high resolution mass spectrometry detection, *J. Pharm. Biomed. Anal.* 157 (2018) 27–35. doi:10.1016/J.JPBA.2018.05.007.
- [140] X. Diao, K.B. Scheidweiler, A. Wohlfarth, S. Pang, R. Kronstrand, M.A. Huestis, *In Vitro* and *In Vivo* Human Metabolism of Synthetic Cannabinoids FDU-PB-22 and FUB-PB-22, *AAPS J.* 18 (2016) 455–464. doi:10.1208/S12248-016-9867-4/FIGURES/5.
- [141] P.S. Bruni, K.E. Grafinger, S. Nussbaumer, S. König, S. Schürch, W. Weinmann, Study of the *in vitro* and *in vivo* metabolism of 4-HO-MET, *Forensic Sci. Int.* 290 (2018) 103–110. doi:10.1016/J.FORSCIINT.2018.06.037.
- [142] S.K. Manier, C. Felske, J. Zapp, N. Eckstein, M.R. Meyer, Studies on the *In Vitro* and *In Vivo* Metabolic Fate of the New Psychoactive Substance N-Ethyl-N-Propyltryptamine for Analytical Purposes, *J Anal Toxicol.* 45 (2021) 195–202. doi:10.1093/jat/bkaa060.
- [143] C. De Bruyn Kops, M. Šícho, A. Mazzolari, J. Kirchmair, GLORYx: Prediction of the Metabolites Resulting from Phase 1 and Phase 2 Biotransformations of Xenobiotics, *Chem. Res. Toxicol.* 34 (2021) 286–299. doi:10.1021/ACS.CHEMRESTOX.0C00224.
- [144] E. Monitoring Centre for Drugs, D. Addiction, Trends and Developments, (n.d.). doi:10.2810/725386.
- [145] I. Khan, Convention on psychotropic substances, 1971, *Prog. Neuropsychopharmacol.* 3 (1979) 11–14. doi:10.1016/0364-7722(79)90064-x.
- [146] Eurowid forum, (1995). <https://www.eurowid.org>.
- [147] M. Schulz, A. Schmoltdt, H. Andresen-Streichert, S. Iwersen-Bergmann, Revisited: Therapeutic and toxic blood concentrations of more than 1100 drugs and other xenobiotics, *Crit. Care.* 24 (2020) 195. doi:10.1186/S13054-020-02915-5.
- [148] M.S. Castaneto, A. Wohlfarth, S. Pang, M. Zhu, K.B. Scheidweiler, R. Kronstrand, M.A. Huestis, Identification of AB-FUBINACA metabolites in human hepatocytes and urine using high-resolution mass spectrometry, *Forensic Toxicol.* 2 (2015) 295–310. doi:10.1007/S11419-015-0275-8.
- [149] A. Wohlfarth, K.B. Scheidweiler, S. Pang, M. Zhu, M. Castaneto, R. Kronstrand, M.A. Huestis, Metabolic characterization of AH-7921, a synthetic opioid designerdrug: *in vitro* metabolic stability assessment and metabolite identification, evaluation of *in silico* prediction, and *in vivo* confirmation, *Drug Test. Anal.* 8 (2016) 779. doi:10.1002/DTA.1856.

- [150] M.J. Swortwood, J. Carlier, K.N. Ellefsen, A. Wohlfarth, X. Diao, M. Concheiro-Guisan, R. Kronstrand, M.A. Huestis, *In vitro*, *in vivo* and *in silico* metabolic profiling of α -pyrrolidinopentiothiophenone, a novel thiophene stimulant, [Http://Dx.Doi.Org/10.4155/Bio.15.237](http://dx.doi.org/10.4155/Bio.15.237). 8 (2015) 65–82. doi:10.4155/BIO.15.237.
- [151] X. Diao, M.A. Huestis, Approaches, Challenges, and Advances in Metabolism of New Synthetic Cannabinoids and Identification of Optimal Urinary Marker Metabolites, *Clin. Pharmacol. Ther.* 101 (2017) 239–253. doi:10.1002/CPT.534.
- [152] J. Carlier, X. Diao, R. Giorgetti, F.P. Busardò, M.A. Huestis, Pyrrolidinyl Synthetic Cathinones α -PHP and 4F- α -PVP Metabolite Profiling Using Human Hepatocyte Incubations, *Int. J. Mol. Sci. Artic.* (2020). doi:10.3390/ijms22010230.
- [153] M. Bortolato, K. Chen, J.C. Shih, The Degradation of Serotonin: Role of MAO, *Handb. Behav. Neurosci.* 21 (2010) 203–218. doi:10.1016/S1569-7339(10)70079-5.
- [154] R.J. Dinis-Oliveira, Metabolism of psilocybin and psilocin: clinical and forensic toxicological relevance, [Http://Dx.Doi.Org/10.1080/03602532.2016.1278228](http://dx.doi.org/10.1080/03602532.2016.1278228). 49 (2017) 84–91. doi:10.1080/03602532.2016.1278228.
- [155] A.T. Caspar, J.B. Gaab, J.A. Michely, S.D. Brandt, M.R. Meyer, H.H. Maurer, Metabolism of the tryptamine-derived new psychoactive substances 5-MeO-2-Me-DALT, 5-MeO-2-Me-ALCHT, and 5-MeO-2-Me-DIPT and their detectability in urine studied by GC–MS, LC–MSn, and LC-HR-MS/MS, *Drug Test. Anal.* 10 (2018) 184–195. doi:10.1002/DTA.2197.
- [156] L. Wagmann, S.K. Manier, M.R. Meyer, Can the Intake of a Synthetic Tryptamine be Detected Only by Blood Plasma Analysis? A Clinical Toxicology Case Involving 4-HO-MET, *J. Anal. Toxicol.* 46 (2022) 567–572. doi:10.1093/JAT/BKAB062.
- [157] S. Malaca, M.A. Huestis, L. Lattanzio, L.T. Marsella, A. Tagliabracci, J. Carlier, F.P. Busardò, Human Hepatocyte 4-Acetoxy-N,N-Diisopropyltryptamine Metabolite Profiling by Reversed-Phase Liquid Chromatography Coupled with High-Resolution Tandem Mass Spectrometry., *Metabolites.* 12 (2022) 705. doi:10.3390/metabo12080705.
- [158] B.O. Keller, J. Sui, A.B. Young, R.M. Whittal, Interferences and contaminants encountered in modern mass spectrometry, *Anal. Chim. Acta.* 627 (2008) 71–81. doi:10.1016/J.ACA.2008.04.043.
- [159] M. Schäfer, M. Drayß, A. Springer, P. Zacharias, K. Meerholz, Radical Cations in Electrospray Mass Spectrometry: Formation of Open-Shell Species, Examination of the Fragmentation Behaviour in ESI-MSn and Reaction Mechanism Studies by Detection of Transient Radical Cations, *European J. Org. Chem.* 2007 (2007) 5162–5174. doi:10.1002/EJOC.200700199.
- [160] S.K. Manier, L.H.J. Richter, J. Schäper, H.H. Maurer, M.R. Meyer, Different *in vitro* and *in vivo* tools for elucidating the human metabolism of alpha-cathinone-derived drugs of abuse, *Drug Test. Anal.* 10 (2018) 1119–1130. doi:10.1002/DTA.2355.

- [161] X. Diao, J. Carlier, M. Zhu, M.A. Huestis, Human Hepatocyte Metabolism of Novel Synthetic Cannabinoids MN-18 and Its 5-Fluoro Analog 5F-MN-18, *Clin. Chem.* 63 (2017) 1753–1763. doi:10.1373/CLINCHEM.2017.277152.
- [162] P. Brunetti, A.F. Lo Faro, A. Di Trana, A. Montana, G. Basile, J. Carlier, F.P. Busardò, β' -Phenylfentanyl Metabolism in Primary Human Hepatocyte Incubations: Identification of Potential Biomarkers of Exposure in Clinical and Forensic Toxicology, *J. Anal. Toxicol.* 46 (2023) e207–e217. doi:10.1093/JAT/BKAC065.
- [163] J. Carlier, D. Berardinelli, E. Montanari, A. Sirignano, A. Di Trana, F.P. Busardò, 3F- α -pyrroldinovalerophenone (3F- α -PVP) *in vitro* human metabolism: Multiple *in silico* predictions to assist in LC-HRMS/MS analysis and targeted/untargeted data mining, *J. Chromatogr. B.* 1193 (2022) 123162. doi:10.1016/J.JCHROMB.2022.123162.
- [164] S. Malaca, A.F. Lo Faro, A. Tamborra, S. Pichini, F.P. Busardò, M.A. Huestis, Toxicology and Analysis of Psychoactive Tryptamines, *Int. J. Mol. Sci.* 21 (2020) 1–38. doi:10.3390/IJMS21239279.
- [165] R.J. Dinis-Oliveira, Metabolism of psilocybin and psilocin: clinical and forensic toxicological relevance, *Drug Metab. Rev.* 49 (2017) 84–91. doi:10.1080/03602532.2016.1278228.
- [166] A.T. Caspar, J.B. Gaab, J.A. Michely, S.D. Brandt, M.R. Meyer, H.H. Maurer, Metabolism of the tryptamine-derived new psychoactive substances 5-MeO-2-Me-DALT, 5-MeO-2-Me-ALCHT, and 5-MeO-2-Me-DIPT and their detectability in urine studied by GC–MS, LC–MSn, and LC-HR-MS/MS, *Drug Test. Anal.* 10 (2018) 184–195. doi:10.1002/dta.2197.
- [167] S. Malaca, M.A. Huestis, L. Lattanzio, L.T. Marsella, A. Tagliabracci, J. Carlier, F.P. Busardò, Human Hepatocyte 4-Acetoxy-N,N-Diisopropyltryptamine Metabolite Profiling by Reversed-Phase Liquid Chromatography Coupled with High-Resolution Tandem Mass Spectrometry., *Metabolites.* 12 (2022). doi:10.3390/metabo12080705.
- [168] J. Wilcox, Psychoactive properties of alpha-methyltryptamine: analysis from self reports of users, *J. Psychoactive Drugs.* 44 (2012) 274–276. doi:10.1080/02791072.2012.704592.
- [169] Expert Committee On Drug Dependence (ECDD), Alpha-methyltryptamine (AMT) Critical Review Report Agenda item 4.20 Expert Committee on Drug Dependence Thirty-sixth Meeting, (2014).
- [170] S. Szara, 6-Hydroxylation: An important metabolic route for α -methyltryptamine, *Experientia.* 17 (1961) 76. doi:10.1007/BF02171429/METRICS.
- [171] T. Kanamori, K. Kuwayama, K. Tsujikawa, H. Miyaguchi, Y.T. Iwata, H. Inoue, *In vivo* metabolism of alpha-methyltryptamine in rats: identification of urinary metabolites, *Xenobiotica.* 38 (2008) 1476–1486. doi:10.1080/00498250802491654.

- [172] M. Grapp, C. Kaufmann, H.M. Schwelm, M.A. Neukamm, Toxicological Investigation of a Case Series Involving the Synthetic Cathinone α -Pyrrolidinohexiophenone (α -PHP) and Identification of Phase I and II Metabolites in Human Urine, *J. Anal. Toxicol.* (2022). doi:10.1093/JAT/BKAC057.
- [173] J. Carlier, X. Diao, C. Sempio, M.A. Huestis, Identification of New Synthetic Cannabinoid ADB-CHMINACA (MAB-CHMINACA) Metabolites in Human Hepatocytes, *AAPS J.* 19 (2017) 568–577. doi:10.1208/S12248-016-0037-5.
- [174] K. Hasegawa, K. Minakata, K. Gonmori, H. Nozawa, I. Yamagishi, K. Watanabe, O. Suzuki, Identification and quantification of predominant metabolites of synthetic cannabinoid MAB-CHMINACA in an authentic human urine specimen, *Drug Test. Anal.* 10 (2018) 365–371. doi:10.1002/DTA.2220.
- [175] Y. Djoumbou-Feunang, J. Fiamoncini, A. Gil-de-la-Fuente, R. Greiner, C. Manach, D.S. Wishart, BioTransformer: A comprehensive computational tool for small molecule metabolism prediction and metabolite identification, *J. Cheminform.* 11 (2019) 1–25. doi:10.1186/S13321-018-0324-5/FIGURES/9.
- [176] S. Malaca, M.A. Huestis, L. Lattanzio, L.T. Marsella, A. Tagliabracci, J. Carlier, F.P. Busardò, Human Hepatocyte 4-Acetoxy-N,N-Diisopropyltryptamine Metabolite Profiling by Reversed-Phase Liquid Chromatography Coupled with High-Resolution Tandem Mass Spectrometry., *Metabolites.* 12 (2022). doi:10.3390/metabo12080705.
- [177] S. Malaca, A.F. Lo Faro, A. Tamborra, S. Pichini, F.P. Busardò, M.A. Huestis, Toxicology and analysis of psychoactive tryptamines, *Int. J. Mol. Sci.* 21 (2020) 1–38. doi:10.3390/IJMS21239279.
- [178] D.X. Tan, R. Hardeland, K. Back, L.C. Manchester, M.A. Alatorre-Jimenez, R.J. Reiter, On the significance of an alternate pathway of melatonin synthesis via 5-methoxytryptamine: comparisons across species, *J. Pineal Res.* (2016) 27–40. doi:10.1111/JPI.12336.
- [179] BRENDA Enzyme Database, (n.d.). <https://www.brenda-enzymes.org/index.php> (accessed February 14, 2023).
- [180] A.M. Araújo, F. Carvalho, M. de L. Bastos, P. Guedes de Pinho, M. Carvalho, The hallucinogenic world of tryptamines: an updated review, *Arch. Toxicol.* 89 (2015) 1151–1173. doi:10.1007/S00204-015-1513-X.
- [181] D.E. Nichols, Hallucinogens, *Pharmacol. Ther.* 101 (2004) 131–181. doi:10.1016/J.PHARMTHERA.2003.11.002.
- [182] R. Carhart-Harris, B. Giribaldi, R. Watts, M. Baker-Jones, A. Murphy-Beiner, R. Murphy, J. Martell, A. Blemings, D. Erritzoe, D.J. Nutt, Trial of Psilocybin versus Escitalopram for Depression, *N. Engl. J. Med.* 384 (2021) 1402–1411. doi:10.1056/NEJMOA2032994.
- [183] R.E. Daws, C. Timmermann, B. Giribaldi, J.D. Sexton, M.B. Wall, D. Erritzoe, L.

- Roseman, D. Nutt, R. Carhart-Harris, Increased global integration in the brain after psilocybin therapy for depression, (n.d.). doi:10.1038/s41591-022-01744-z.
- [184] GDS Key Finding 2019 by globaldrugsurvey - Issuu, (n.d.). https://issuu.com/globaldrugsurvey/docs/gds2019_key_findings_report_may_16_?utm_medium=referral&utm_source=www.globaldrugsurvey.com (accessed February 20, 2023).
- [185] M. Schulz, A. Schmoltdt, H. Andresen-Streichert, S. Iwersen-Bergmann, *Critical Care*, (n.d.). doi:10.1186/s13054-020-02915-5.
- [186] Standard Practices for Method Validation in Forensic Toxicology, (n.d.). www.asbstandardsboard.org. (accessed February 20, 2023).
- [187] J. Van Looc, M. Elskens, C. Croux, H. Beernaert, Linearity of calibration curves: Use and misuse of the correlation coefficient, *Accredit. Qual. Assur.* 7 (2002) 281–285. doi:10.1007/s00769-002-0487-6.
- [188] S. Malaca, C. Bottinelli, L. Fanton, N. Cartiser, J. Carlier, F.P. Busardò, α -Methyltryptamine (α -MT) Metabolite Profiling in Human Hepatocyte Incubations and Postmortem Urine and Blood, *Metabolites*. 13 (2023) 92. doi:10.3390/METABO13010092.
- [189] J. Carlier, S. Malaca, M.A. Huestis, A. Tagliabracci, A. Tini, F.P. Busardò, Biomarkers of 4-hydroxy-N,N-methylpropyltryptamine (4-OH-MPT) intake identified from human hepatocyte incubations., *Expert Opin. Drug Metab. Toxicol.* 18 (2022) 831–840. doi:10.1080/17425255.2022.2166826.
- [190] D.M. Boland, W. Andollo, G.W. Hime, W.L. Hearn, Fatality due to acute alpha-methyltryptamine intoxication, *J. Anal. Toxicol.* 29 (2005) 394–397. doi:10.1093/JAT/29.5.394.
- [191] J.A. Michely, A.G. Helfer, S.D. Brandt, M.R. Meyer, H.H. Maurer, Metabolism of the new psychoactive substances N,N-diallyltryptamine (DALT) and 5-methoxy-DALT and their detectability in urine by GC–MS, LC–MSn, and LC–HR–MS–MS, *Anal. Bioanal. Chem.* 407 (2015) 7831–7842. doi:10.1007/S00216-015-8955-0/FIGURES/4.
- [192] S.P. Vorce, J.H. Sklerov, A general screening and confirmation approach to the analysis of designer tryptamines and phenethylamines in blood and urine using GC–EI–MS and HPLC–electrospray–MS, *J. Anal. Toxicol.* 28 (2004) 407–410. doi:10.1093/JAT/28.6.407.
- [193] T. Forsström, J. Tuominen, J. Kärkkäinen, Determination of potentially hallucinogenic N-dimethylated indoleamines in human urine by HPLC/ESI–MS–MS, *Scand. J. Clin. Lab. Invest.* 61 (2001) 547–556. doi:10.1080/003655101753218319.
- [194] R.A. Morano, C. Spies, F.B. Walker, S.M. Plank, Fatal intoxication involving etryptamine, *J. Forensic Sci.* 38 (1993) 13461J. doi:10.1520/jfs13461j.

Acknowledgements